

Density Model for Spinner Dolphin (*Stenella longirostris*) for the U.S. Gulf of Mexico: Supplementary Report

Duke University Marine Geospatial Ecology Lab*

Model Version 2.3 - 2015-09-29

Citation

When referencing our methodology or results generally, please cite our open-access article:

Roberts JJ, Best BD, Mannocci L, Fujioka E, Halpin PN, Palka DL, Garrison LP, Mullin KD, Cole TVN, Khan CB, McLellan WM, Pabst DA, Lockhart GG (2016) Habitat-based cetacean density models for the U.S. Atlantic and Gulf of Mexico. *Scientific Reports* 6: 22615. doi: [10.1038/srep22615](https://doi.org/10.1038/srep22615)

To reference this specific model or Supplementary Report, please cite:

Roberts JJ, Best BD, Mannocci L, Fujioka E, Halpin PN, Palka DL, Garrison LP, Mullin KD, Cole TVN, Khan CB, McLellan WM, Pabst DA, Lockhart GG (2015) Density Model for Spinner Dolphin (*Stenella longirostris*) for the U.S. Gulf of Mexico Version 2.3, 2015-09-29, and Supplementary Report. Marine Geospatial Ecology Lab, Duke University, Durham, North Carolina.

Copyright and License



This document and the accompanying results are © 2015 by the Duke University Marine Geospatial Ecology Laboratory and are licensed under a [Creative Commons Attribution 4.0 International License](https://creativecommons.org/licenses/by/4.0/).

Revision History

Version	Date	Description of changes
1	2014-11-24	Initial version.
2	2015-01-10	Added a missing sighting and refitted models.
2.1	2015-02-02	Updated the documentation. No changes to the model.
2.2	2015-05-14	Updated calculation of CVs. Switched density rasters to logarithmic breaks. No changes to the model.
2.3	2015-09-29	Updated the documentation. No changes to the model.

*For questions, or to offer feedback about this model or report, please contact Jason Roberts (jason.roberts@duke.edu)

Survey Data

Survey	Period	Length (1000 km)	Hours	Sightings
SEFSC GOMEX92-96 Aerial Surveys	1992-1996	27	152	0
SEFSC Gulf of Mexico Shipboard Surveys, 2003-2009	2003-2009	19	1156	15
SEFSC GulfCet I Aerial Surveys	1992-1994	50	257	4
SEFSC GulfCet II Aerial Surveys	1996-1998	22	124	7
SEFSC GulfSCAT 2007 Aerial Surveys	2007-2007	18	95	0
SEFSC Oceanic CetShip Surveys	1992-2001	49	3102	42
SEFSC Shelf CetShip Surveys	1994-2001	10	707	3
Total		195	5593	71

Table 2: Survey effort and sightings used in this model. Effort is tallied as the cumulative length of on-effort transects and hours the survey team was on effort. Sightings are the number of on-effort encounters of the modeled species for which a perpendicular sighting distance (PSD) was available. Off effort sightings and those without PSDs were omitted from the analysis.

Period	Length (1000 km)	Hours	Sightings
1992-2009	195	5592	71
1998-2009	62	2679	25
% Lost	68	52	65

Table 3: Survey effort and on-effort sightings having perpendicular sighting distances. % Lost shows the percentage of effort or sightings lost by restricting the analysis to surveys performed in 1998 and later, the era in which remotely-sensed chlorophyll and derived productivity estimates are available. See Figure 1 for more information.

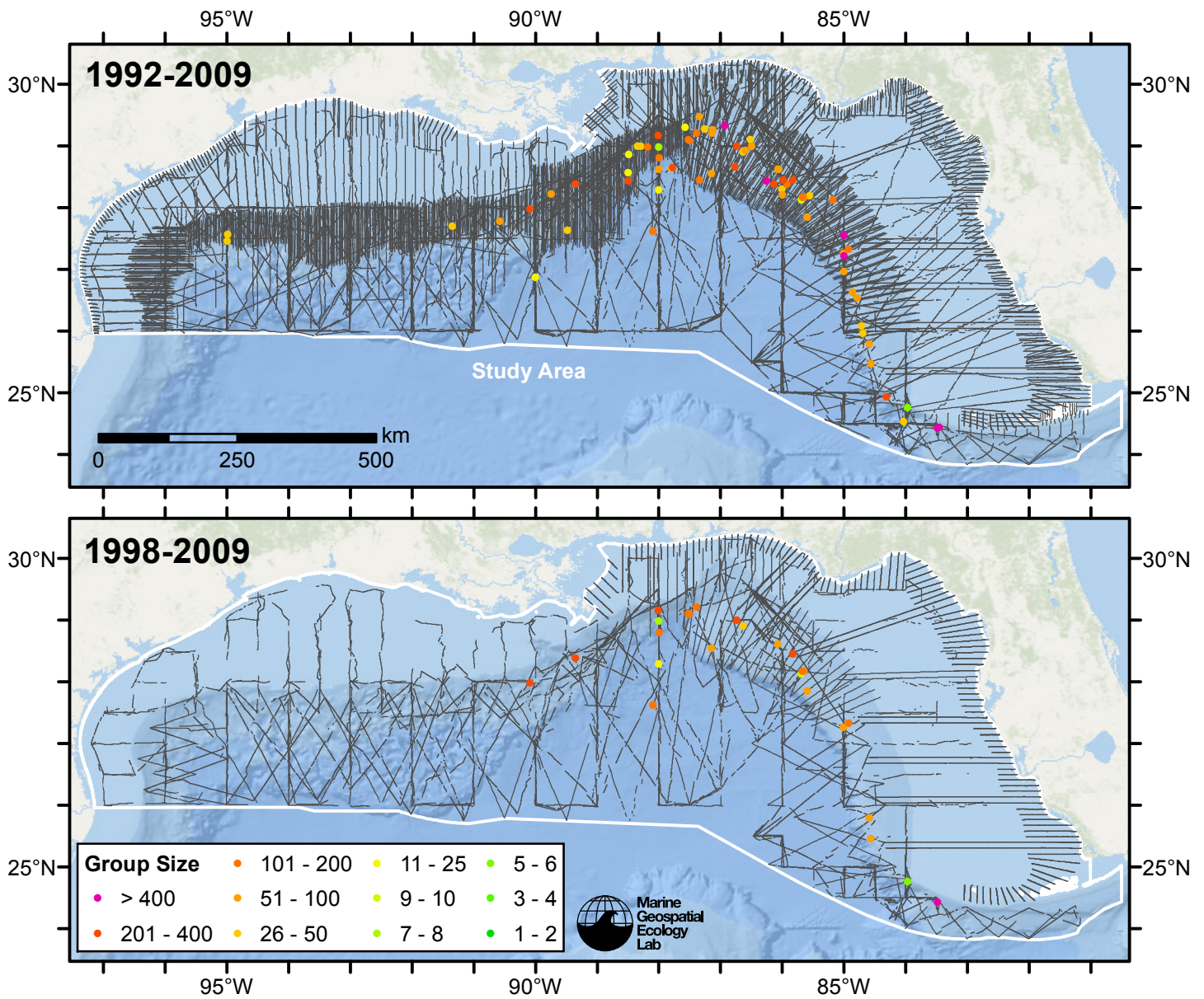


Figure 1: Spinner dolphin sightings and survey tracklines. The top map shows all surveys. The bottom map shows surveys performed in 1998 or later, the era in which remotely-sensed chlorophyll and derived productivity estimates are available. Models fitted to contemporaneous (day-of-sighting) estimates of those predictors only utilize these surveys. These maps illustrate the survey data lost in order to utilize those predictors. Models fitted to climatological estimates of those predictors do not suffer this data loss.

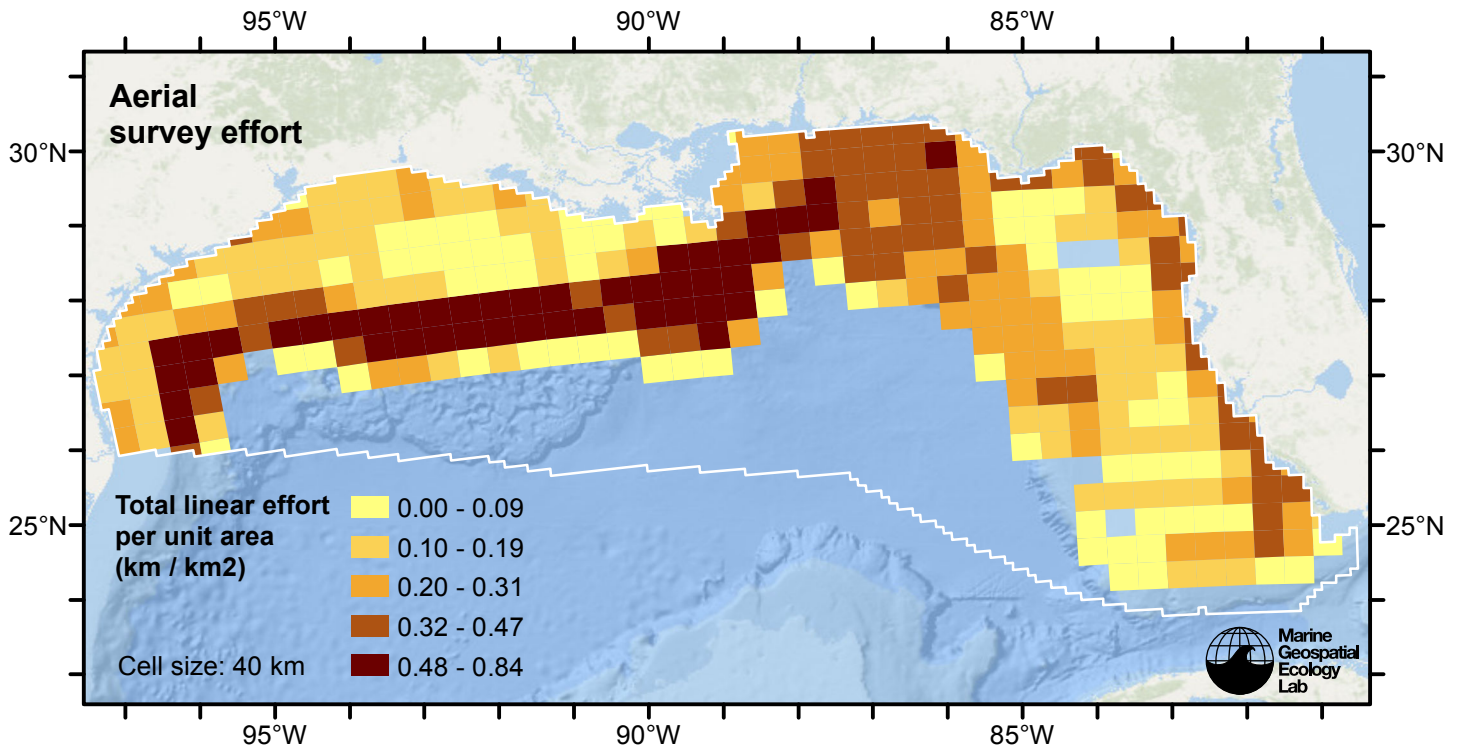


Figure 2: Aerial linear survey effort per unit area.

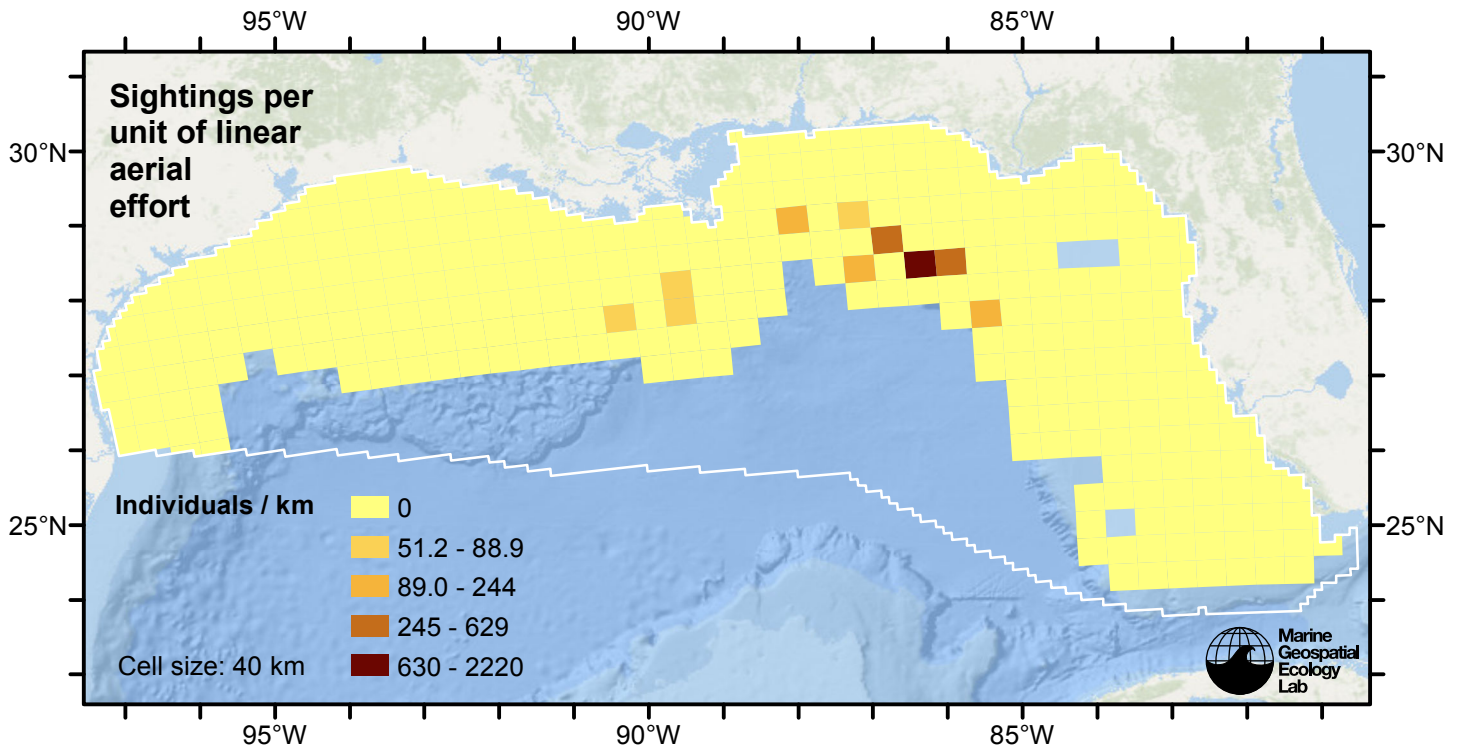


Figure 3: Spinner dolphin sightings per unit aerial linear survey effort.

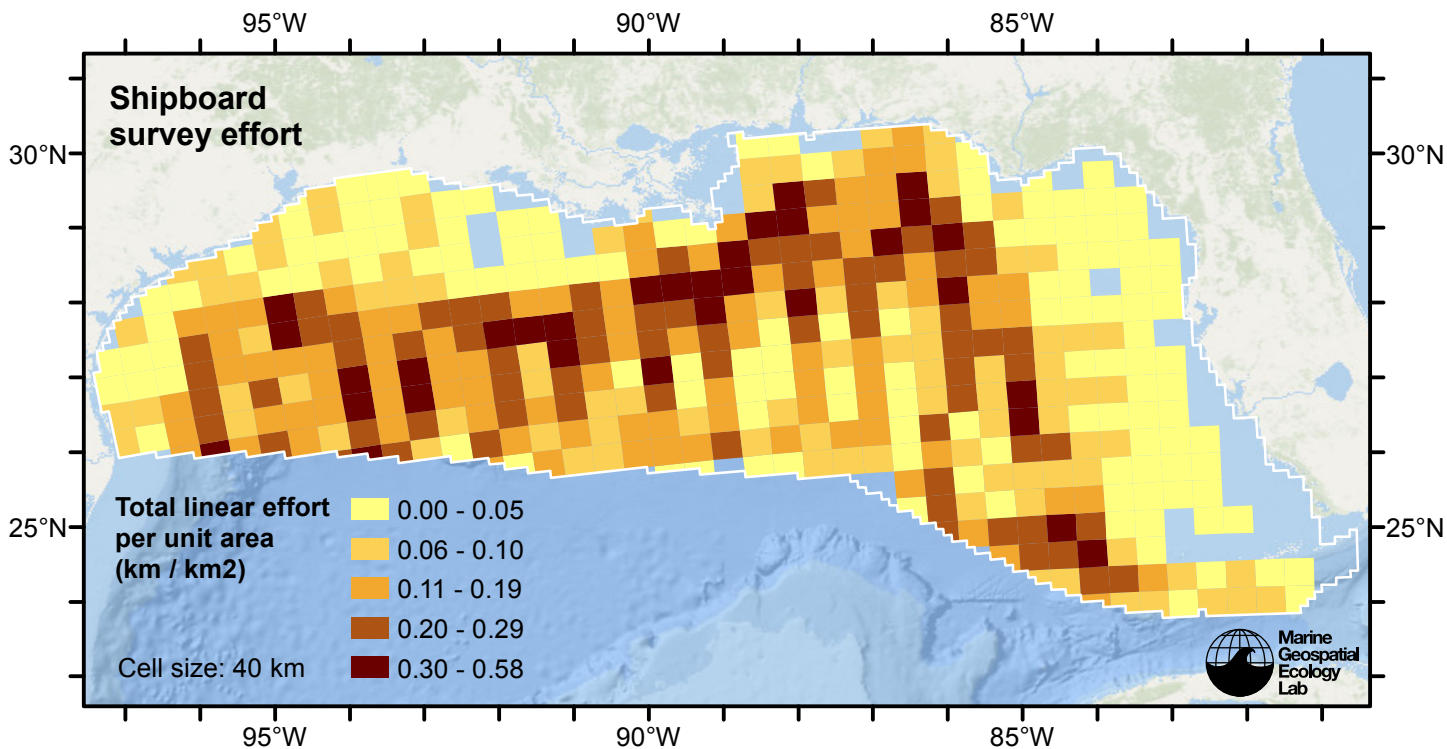


Figure 4: Shipboard linear survey effort per unit area.

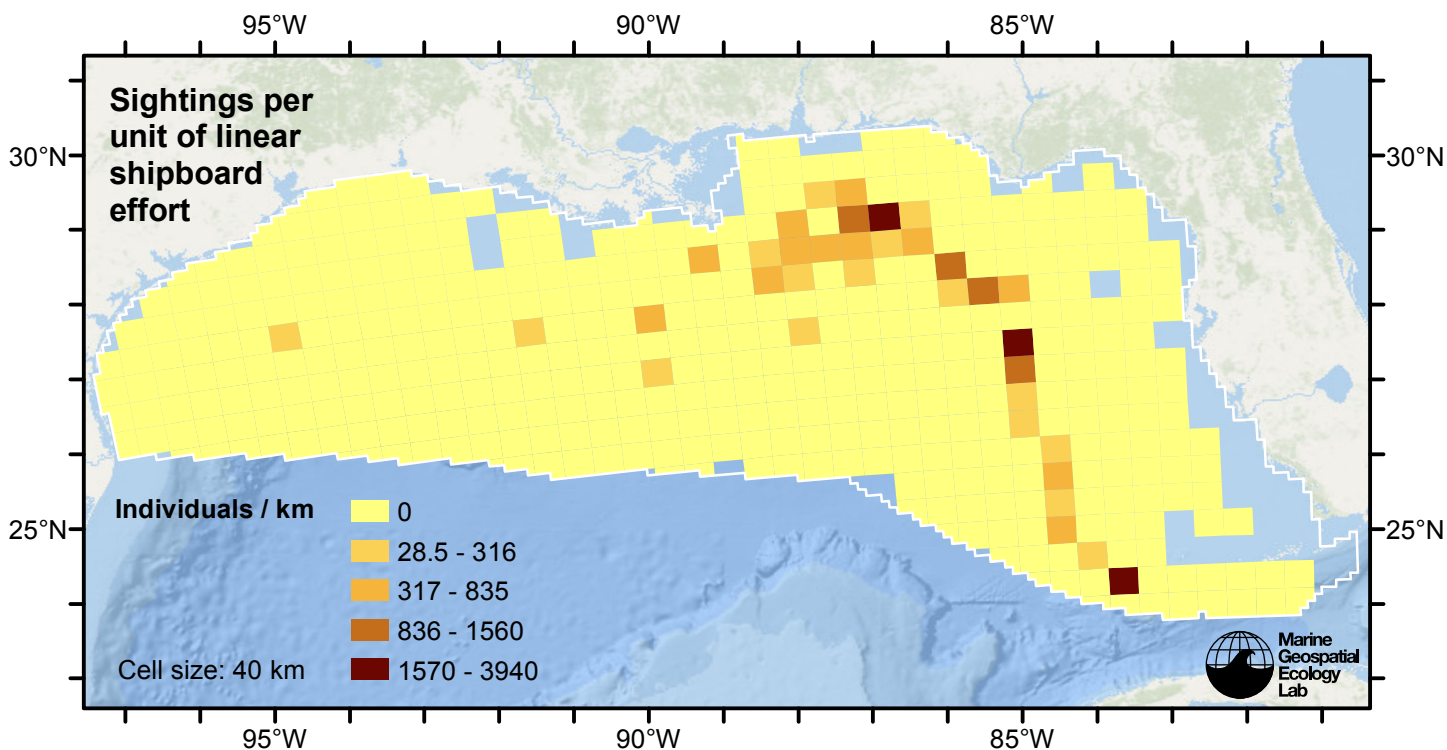


Figure 5: Spinner dolphin sightings per unit shipboard linear survey effort.

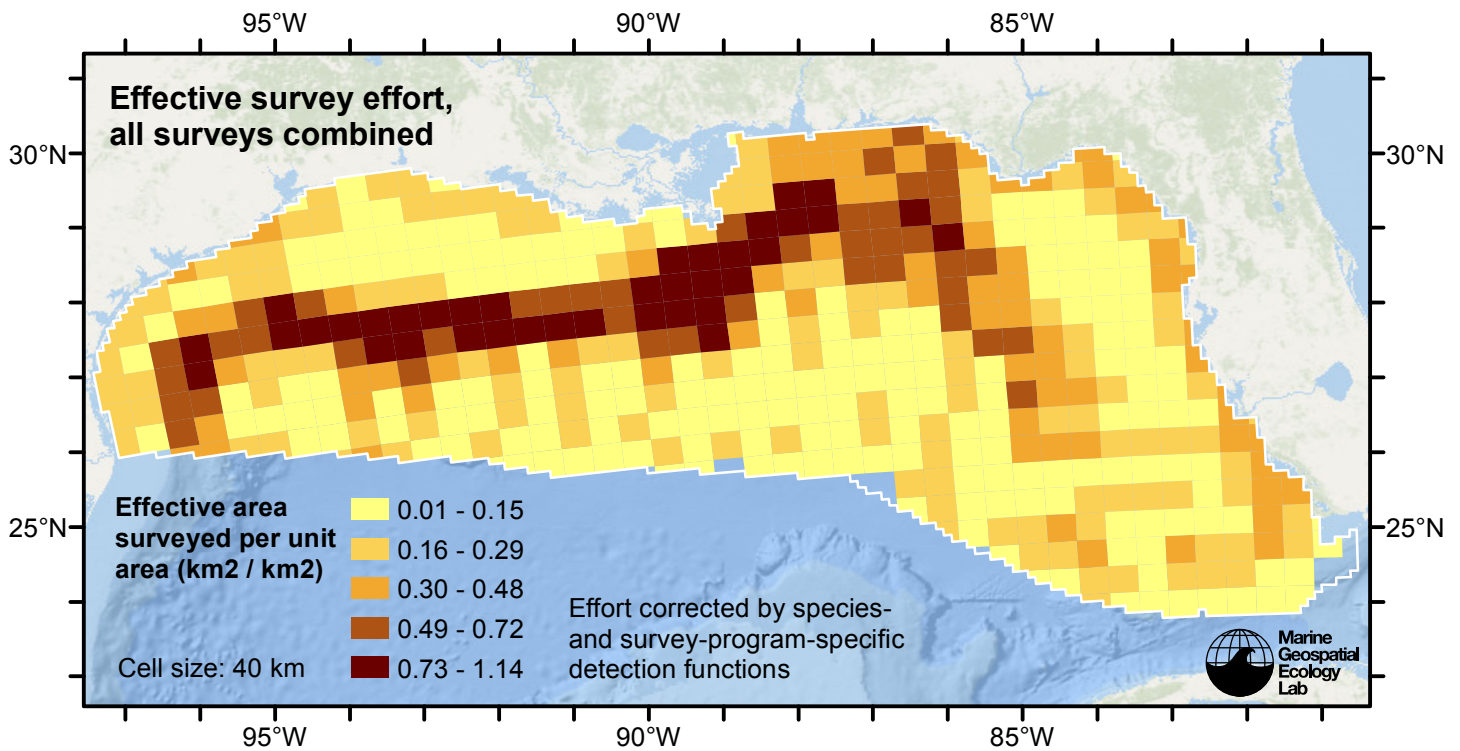


Figure 6: Effective survey effort per unit area, for all surveys combined. Here, effort is corrected by the species- and survey-program-specific detection functions used in fitting the density models.

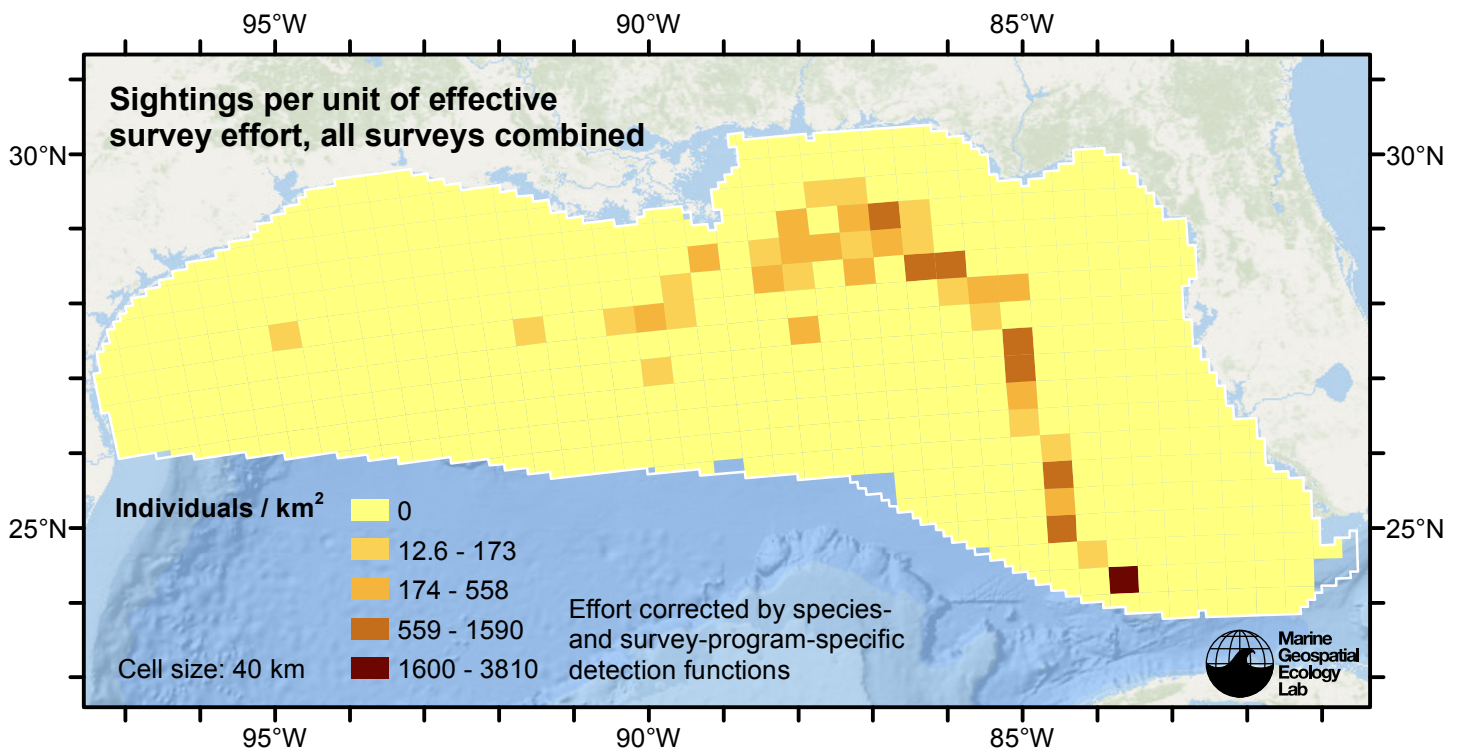


Figure 7: Spinner dolphin sightings per unit of effective survey effort, for all surveys combined. Here, effort is corrected by the species- and survey-program-specific detection functions used in fitting the density models.

Detection Functions

The detection hierarchy figures below show how sightings from multiple surveys were pooled to try to achieve Buckland et. al’s (2001) recommendation that at least 60-80 sightings be used to fit a detection function. Leaf nodes, on the right, usually represent individual surveys, while the hierarchy to the left shows how they have been grouped according to how similar we believed the surveys were to each other in their detection performance.

At each node, the red or green number indicates the total number of sightings below that node in the hierarchy, and is colored green if 70 or more sightings were available, and red otherwise. If a grouping node has zero sightings—i.e. all of the surveys within it had zero sightings—it may be collapsed and shown as a leaf to save space.

Each histogram in the figure indicates a node where a detection function was fitted. The actual detection functions do not appear in this figure; they are presented in subsequent sections. The histogram shows the frequency of sightings by perpendicular sighting distance for all surveys contained by that node. Each survey (leaf node) receives the detection function that is closest to it up the hierarchy. Thus, for common species, sufficient sightings may be available to fit detection functions deep in the hierarchy, with each function applying to only a few surveys, thereby allowing variability in detection performance between surveys to be addressed relatively finely. For rare species, so few sightings may be available that we have to pool many surveys together to try to meet Buckland’s recommendation, and fit only a few coarse detection functions high in the hierarchy.

A blue Proxy Species tag indicates that so few sightings were available that, rather than ascend higher in the hierarchy to a point that we would pool grossly-incompatible surveys together, (e.g. shipboard surveys that used big-eye binoculars with those that used only naked eyes) we pooled sightings of similar species together instead. The list of species pooled is given in following sections.

Shipboard Surveys

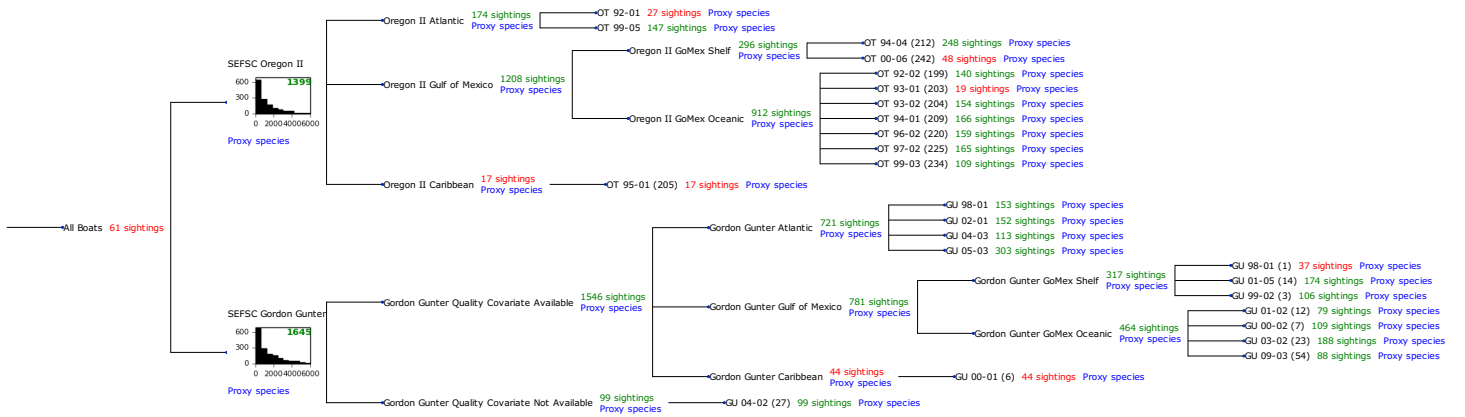


Figure 8: Detection hierarchy for shipboard surveys

SEFSC Oregon II

Because this taxon was sighted too infrequently to fit a detection function to its sightings alone, we fit a detection function to the pooled sightings of several other species that we believed would exhibit similar detectability. These “proxy species” are listed below.

Reported By Observer	Common Name	n
Delphinus capensis	Long-beaked common dolphin	0
Delphinus delphis	Short-beaked common dolphin	2
Delphinus delphis/Lagenorhynchus acutus	Short-beaked common or Atlantic white-sided dolphin	0
Delphinus delphis/Stenella	Short-beaked common dolphin or Stenella spp.	0
Delphinus delphis/Stenella coeruleoalba	Short-beaked common or striped dolphin	0

Grampus griseus	Risso’s dolphin	156
Grampus griseus/Tursiops truncatus	Risso’s or Bottlenose dolphin	0
Lagenodelphis hosei	Fraser’s dolphin	3
Lagenorhynchus acutus	Atlantic white-sided dolphin	0
Lagenorhynchus albirostris	White-beaked dolphin	0
Lagenorhynchus albirostris/Lagenorhynchus acutus	White-beaked or white-sided dolphin	0
Stenella	Unidentified Stenella	17
Stenella attenuata	Pantropical spotted dolphin	347
Stenella attenuata/frontalis	Pantropical or Atlantic spotted dolphin	0
Stenella clymene	Clymene dolphin	44
Stenella coeruleoalba	Striped dolphin	48
Stenella frontalis	Atlantic spotted dolphin	242
Stenella frontalis/Tursiops truncatus	Atlantic spotted or Bottlenose dolphin	0
Stenella longirostris	Spinner dolphin	38
Steno bredanensis	Rough-toothed dolphin	22
Steno bredanensis/Tursiops truncatus	Bottlenose or rough-toothed dolphin	0
Tursiops truncatus	Bottlenose dolphin	490
Total		1409

Table 4: Proxy species used to fit detection functions for SEFSC Oregon II. The number of sightings, n , is before truncation.

The sightings were right truncated at 4000m.

Covariate	Description
beaufort	Beaufort sea state.
quality	Survey-specific index of the quality of observation conditions, utilizing relevant factors other than Beaufort sea state (see methods).
size	Estimated size (number of individuals) of the sighted group.

Table 5: Covariates tested in candidate “multi-covariate distance sampling” (MCDS) detection functions.

Key	Adjustment	Order	Covariates	Succeeded	Δ AIC	Mean ESHW (m)
hr			beaufort, size	Yes	0.00	858
hr			size	Yes	50.03	748
hr			beaufort, quality	Yes	67.60	602
hr			quality	Yes	96.79	551
hr			beaufort	Yes	103.66	541
hr				Yes	139.18	480
hr	poly	4		Yes	140.62	488

hr	poly	2		Yes	141.16	478
hn	cos	2		Yes	352.56	1338
hn			beaufort, quality, size	Yes	417.28	1818
hn	cos	3		Yes	423.70	1297
hn			beaufort, size	Yes	446.32	1839
hn			quality, size	Yes	452.18	1818
hn			beaufort, quality	Yes	477.95	1794
hn			size	Yes	483.25	1835
hn			quality	Yes	498.37	1798
hn			beaufort	Yes	524.87	1799
hn				Yes	546.13	1802
hn	herm	4		No		
hr			quality, size	No		
hr			beaufort, quality, size	No		

Table 6: Candidate detection functions for SEFSC Oregon II. The first one listed was selected for the density model.

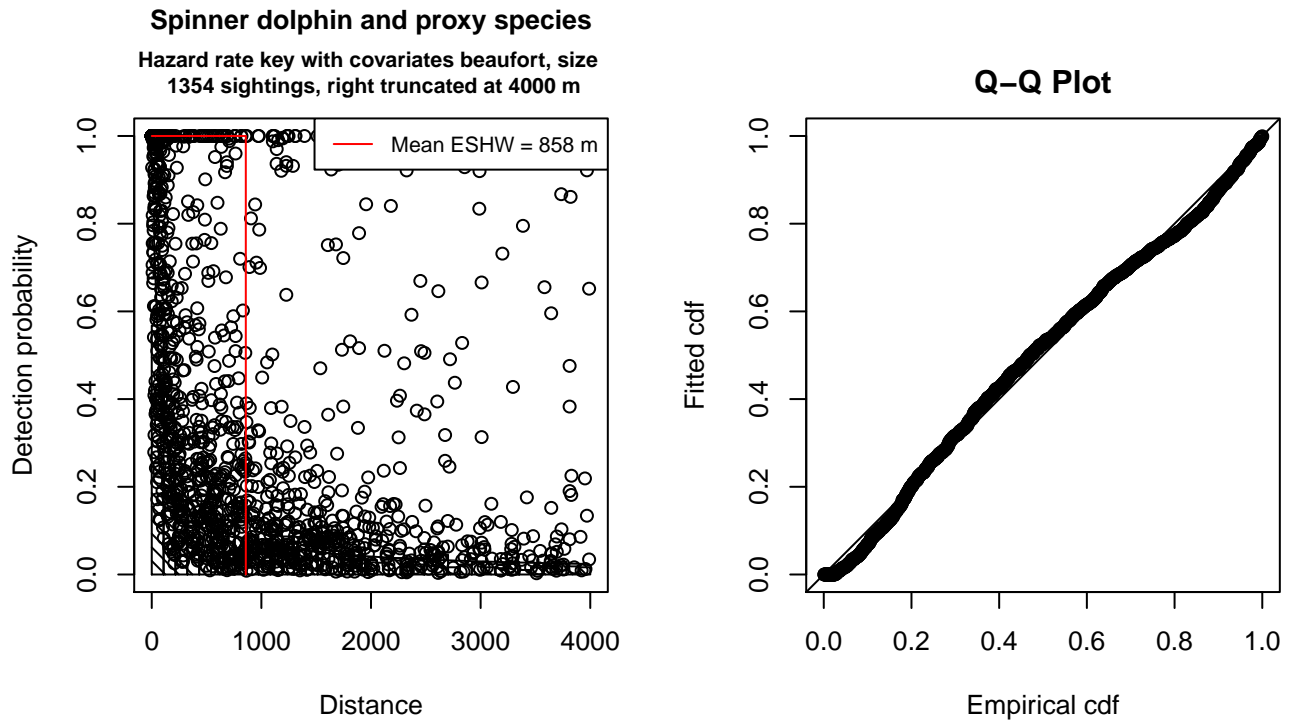


Figure 9: Detection function for SEFSC Oregon II that was selected for the density model

Statistical output for this detection function:

```
Summary for ds object
Number of observations : 1354
```

Distance range : 0 - 4000
 AIC : 21045.15

Detection function:
 Hazard-rate key function

Detection function parameters

Scale Coefficients:

	estimate	se
(Intercept)	5.3277865	0.21247442
beaufort	-0.6331561	0.06992127
size	2.8156065	0.27363496

Shape parameters:

	estimate	se
(Intercept)	0	0.03651385

	Estimate	SE	CV
Average p	7.551776e-02	8.294606e-03	0.1098365
N in covered region	1.792956e+04	2.032413e+03	0.1133554

Additional diagnostic plots:

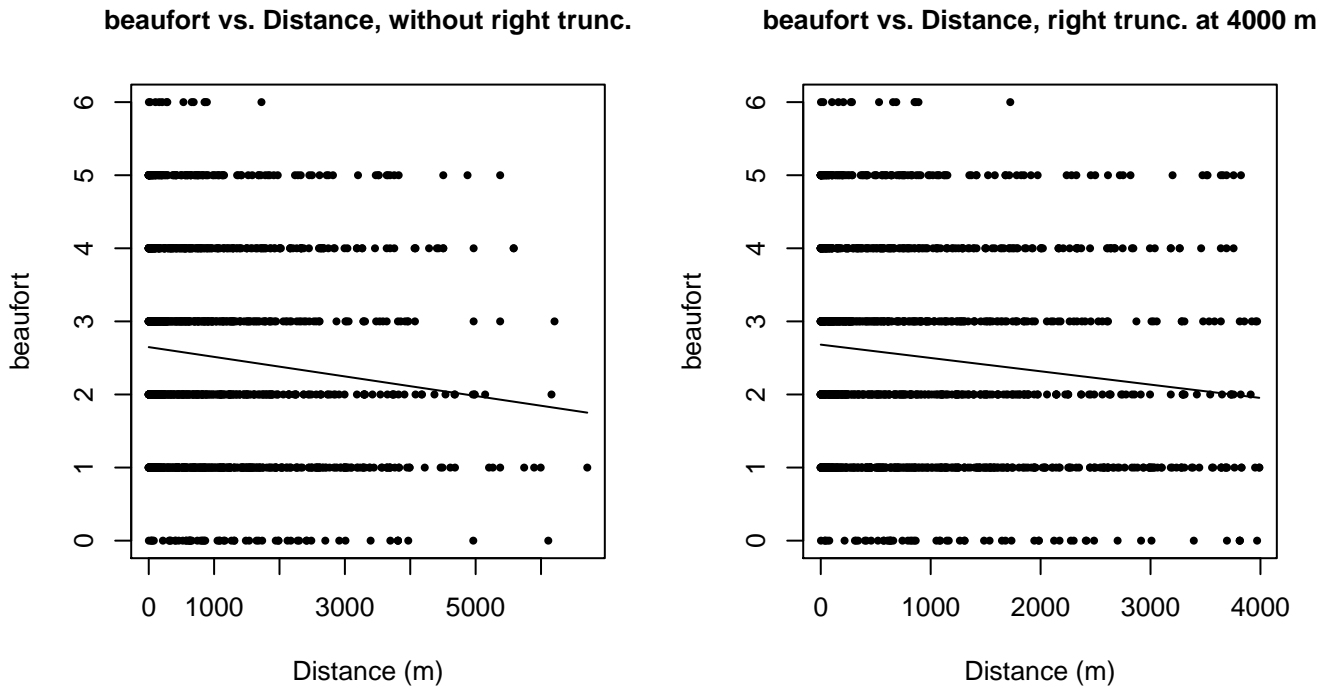
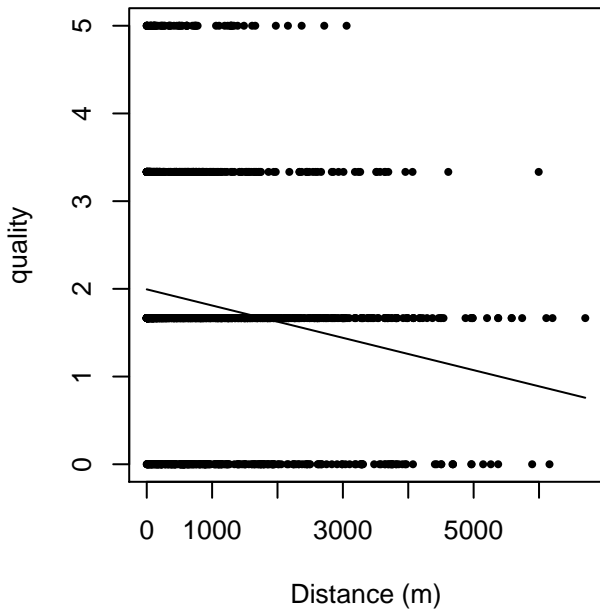


Figure 10: Scatterplots showing the relationship between Beaufort sea state and perpendicular sighting distance, for all sightings (left) and only those not right truncated (right). The line is a simple linear regression.

quality vs. Distance, without right trunc.



quality vs. Distance, right trunc. at 4000 m

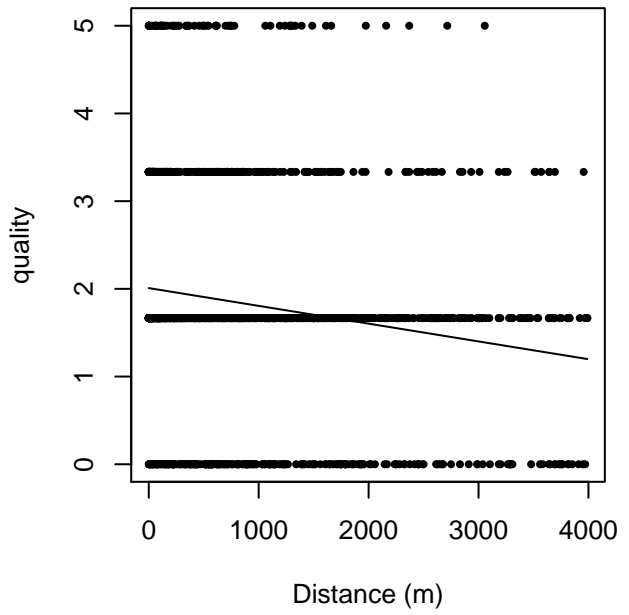
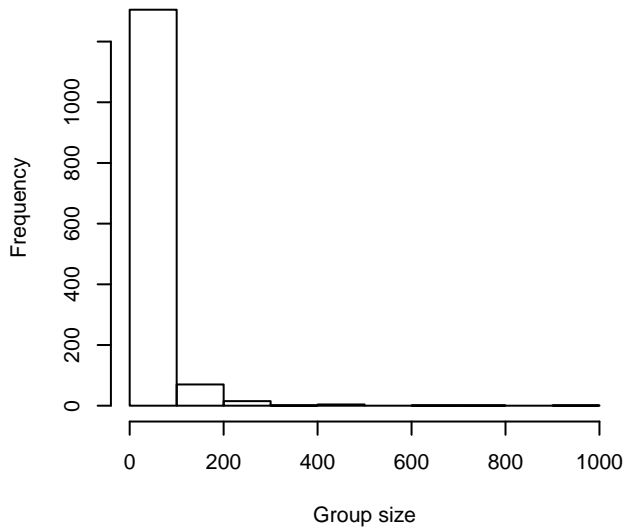
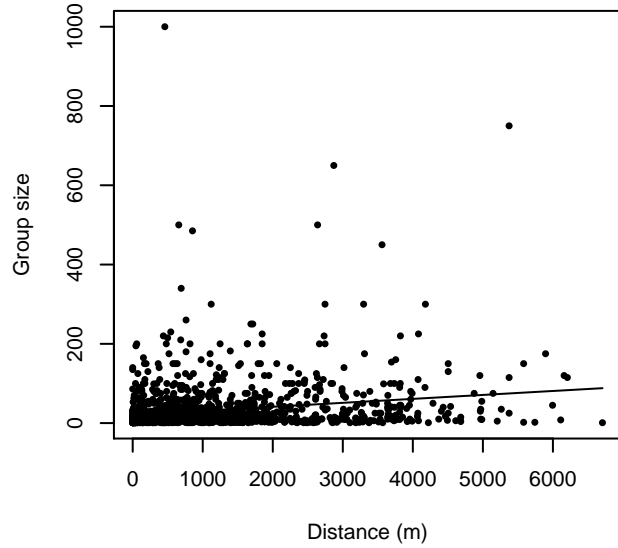


Figure 11: Scatterplots showing the relationship between the survey-specific index of the quality of observation conditions and perpendicular sighting distance, for all sightings (left) and only those not right truncated (right). Low values of the quality index correspond to better observation conditions. The line is a simple linear regression.

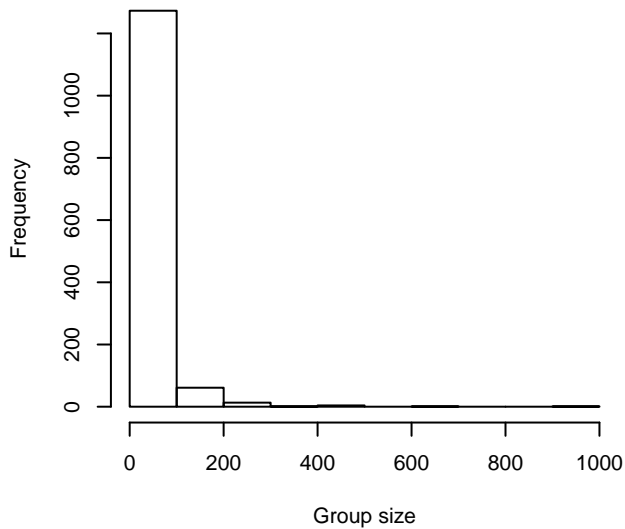
Group Size Frequency, without right trunc.



Group Size vs. Distance, without right trunc.



Group Size Frequency, right trunc. at 4000 m



Group Size vs. Distance, right trunc. at 4000 m

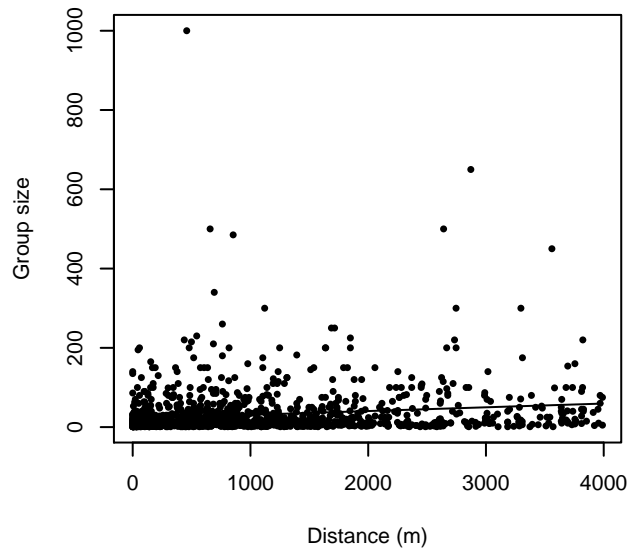


Figure 12: Histograms showing group size frequency and scatterplots showing the relationship between group size and perpendicular sighting distance, for all sightings (top row) and only those not right truncated (bottom row). In the scatterplot, the line is a simple linear regression.

SEFSC Gordon Gunter

Because this taxon was sighted too infrequently to fit a detection function to its sightings alone, we fit a detection function to the pooled sightings of several other species that we believed would exhibit similar detectability. These “proxy species” are listed below.

Reported By Observer	Common Name	n
Delphinus capensis	Long-beaked common dolphin	9
Delphinus delphis	Short-beaked common dolphin	35

Delphinus delphis/Lagenorhynchus acutus	Short-beaked common or Atlantic white-sided dolphin	0
Delphinus delphis/Stenella	Short-beaked common dolphin or Stenella spp.	0
Delphinus delphis/Stenella coeruleoalba	Short-beaked common or striped dolphin	0
Grampus griseus	Risso’s dolphin	129
Grampus griseus/Tursiops truncatus	Risso’s or Bottlenose dolphin	0
Lagenodelphis hosei	Fraser’s dolphin	1
Lagenorhynchus acutus	Atlantic white-sided dolphin	0
Lagenorhynchus albirostris	White-beaked dolphin	0
Lagenorhynchus albirostris/Lagenorhynchus acutus	White-beaked or white-sided dolphin	0
Stenella	Unidentified Stenella	30
Stenella attenuata	Pantropical spotted dolphin	303
Stenella attenuata/frontalis	Pantropical or Atlantic spotted dolphin	0
Stenella clymene	Clymene dolphin	29
Stenella coeruleoalba	Striped dolphin	78
Stenella frontalis	Atlantic spotted dolphin	376
Stenella frontalis/Tursiops truncatus	Atlantic spotted or Bottlenose dolphin	1
Stenella longirostris	Spinner dolphin	24
Steno bredanensis	Rough-toothed dolphin	24
Steno bredanensis/Tursiops truncatus	Bottlenose or rough-toothed dolphin	0
Tursiops truncatus	Bottlenose dolphin	606
Total		1645

Table 7: Proxy species used to fit detection functions for SEFSC Gordon Gunter. The number of sightings, n , is before truncation.

The sightings were right truncated at 5000m.

Covariate	Description
beaufort	Beaufort sea state.
size	Estimated size (number of individuals) of the sighted group.

Table 8: Covariates tested in candidate “multi-covariate distance sampling” (MCDS) detection functions.

Key	Adjustment	Order	Covariates	Succeeded	Δ AIC	Mean ESHW (m)
hr			beaufort	Yes	0.00	857
hr			size	Yes	50.37	859
hr	poly	4		Yes	141.17	661
hr	poly	2		Yes	146.67	660
hr				Yes	147.38	624
hn			beaufort, size	Yes	346.21	2229

hn	cos	2		Yes	368.32	1681
hn	cos	3		Yes	399.02	1559
hn			beaufort	Yes	442.65	2176
hn			size	Yes	486.38	2236
hn				Yes	553.05	2189
hn	herm	4		No		
hr			beaufort, size	No		

Table 9: Candidate detection functions for SEFSC Gordon Gunter. The first one listed was selected for the density model.

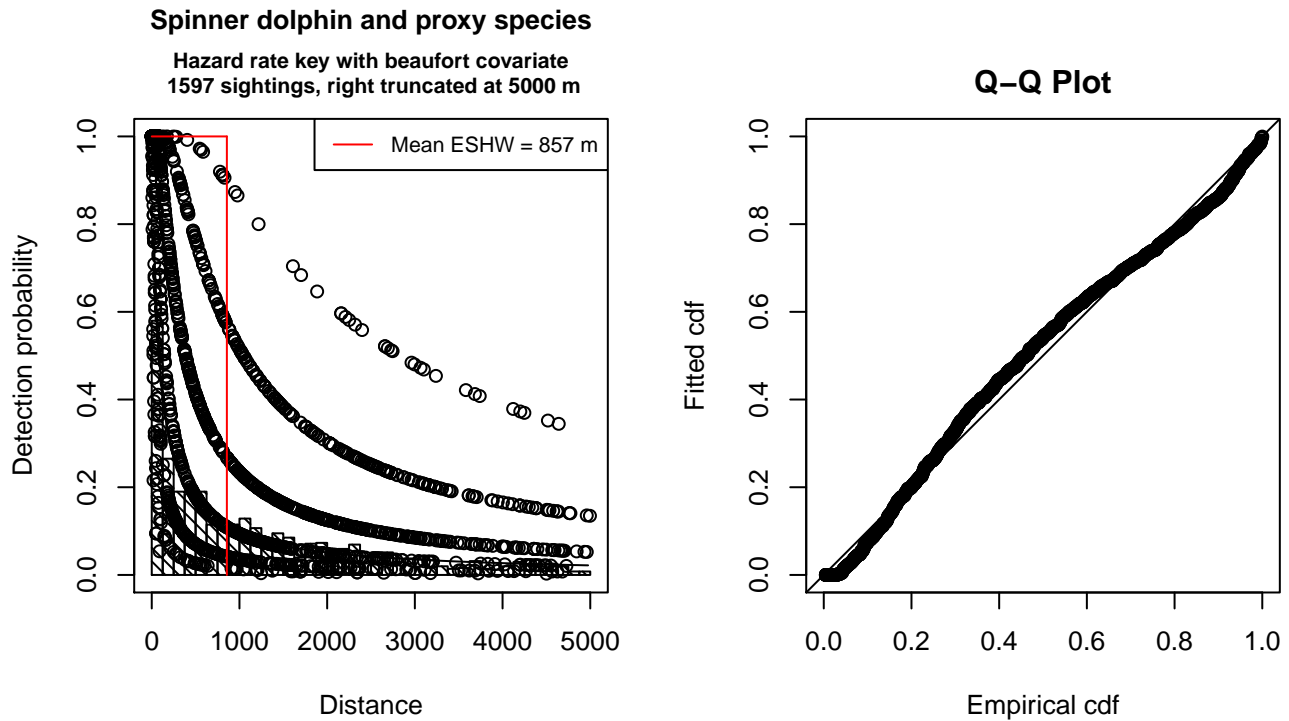


Figure 13: Detection function for SEFSC Gordon Gunter that was selected for the density model

Statistical output for this detection function:

```
Summary for ds object
Number of observations : 1597
Distance range       : 0 - 5000
AIC                  : 25548.72
```

```
Detection function:
Hazard-rate key function
```

```
Detection function parameters
Scale Coefficients:
      estimate      se
(Intercept) 7.5810508 0.1916869
beaufort    -0.9961196 0.0736659
```

Shape parameters:

	estimate	se
(Intercept)	0	0.03544042

	Estimate	SE	CV
Average p	7.898292e-02	8.260688e-03	0.1045883
N in covered region	2.021956e+04	2.175200e+03	0.1075790

Additional diagnostic plots:

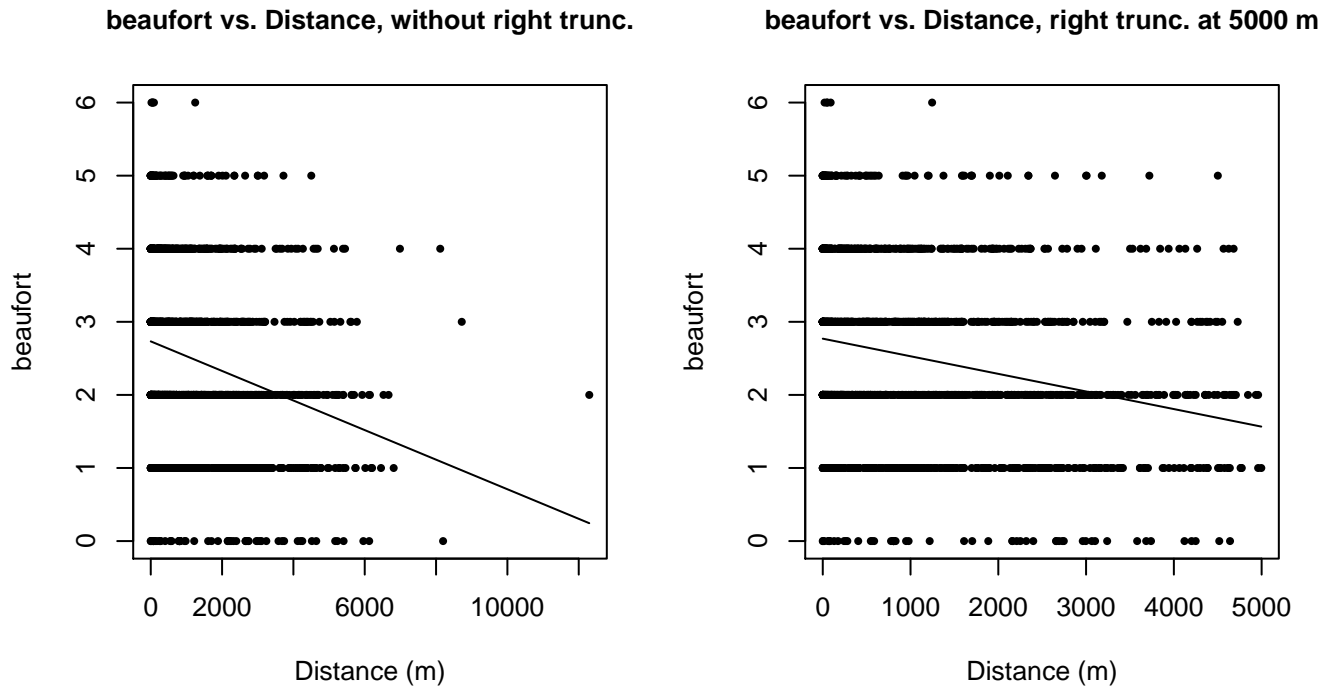
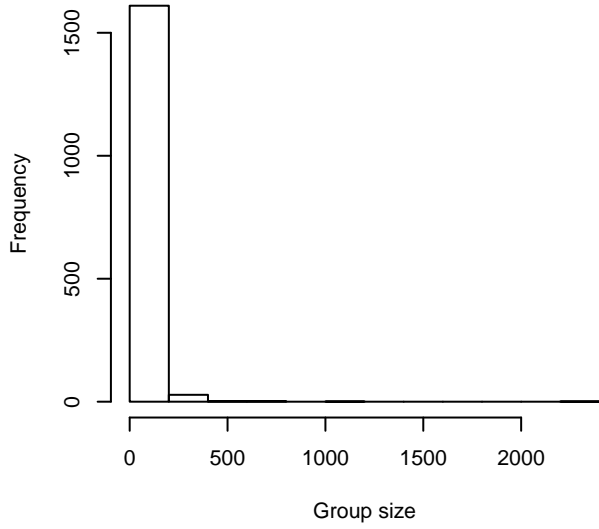
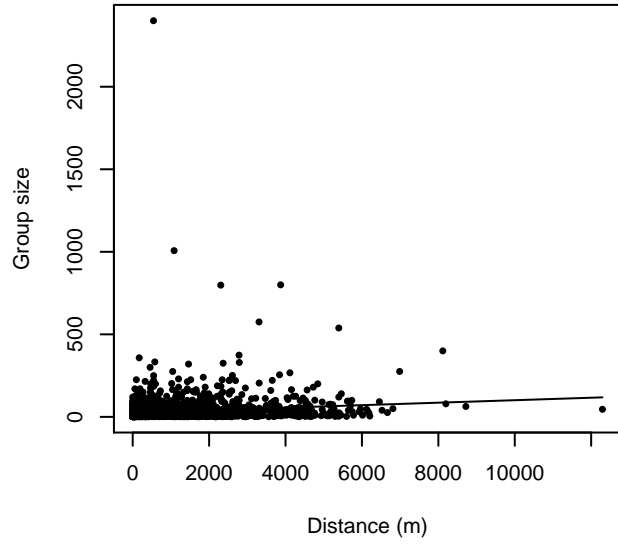


Figure 14: Scatterplots showing the relationship between Beaufort sea state and perpendicular sighting distance, for all sightings (left) and only those not right truncated (right). The line is a simple linear regression.

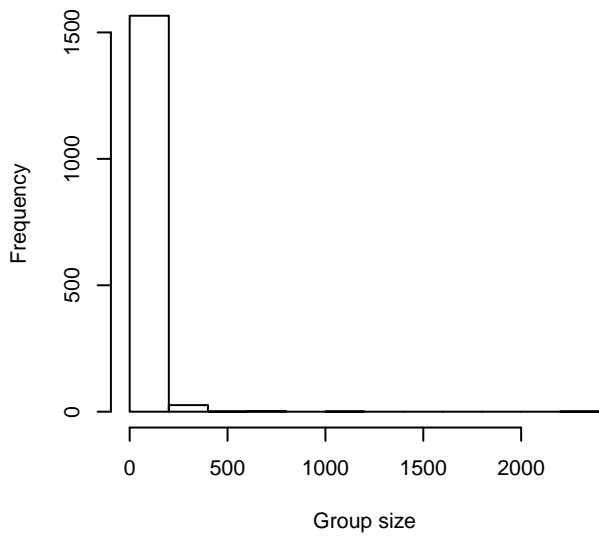
Group Size Frequency, without right trunc.



Group Size vs. Distance, without right trunc.



Group Size Frequency, right trunc. at 5000 m



Group Size vs. Distance, right trunc. at 5000 m

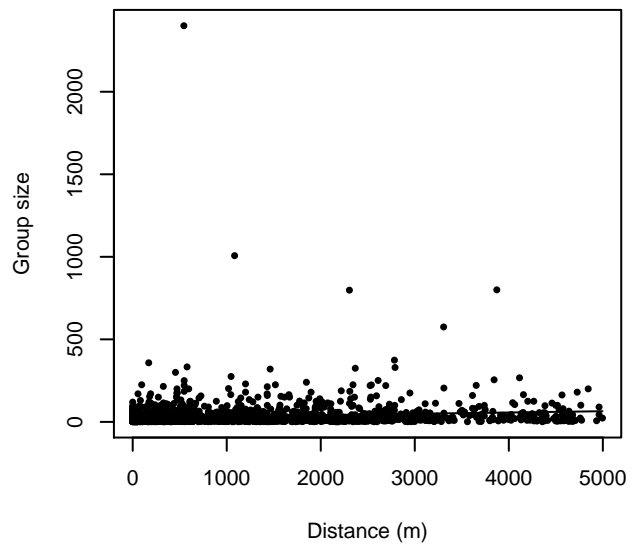


Figure 15: Histograms showing group size frequency and scatterplots showing the relationship between group size and perpendicular sighting distance, for all sightings (top row) and only those not right truncated (bottom row). In the scatterplot, the line is a simple linear regression.

Aerial Surveys

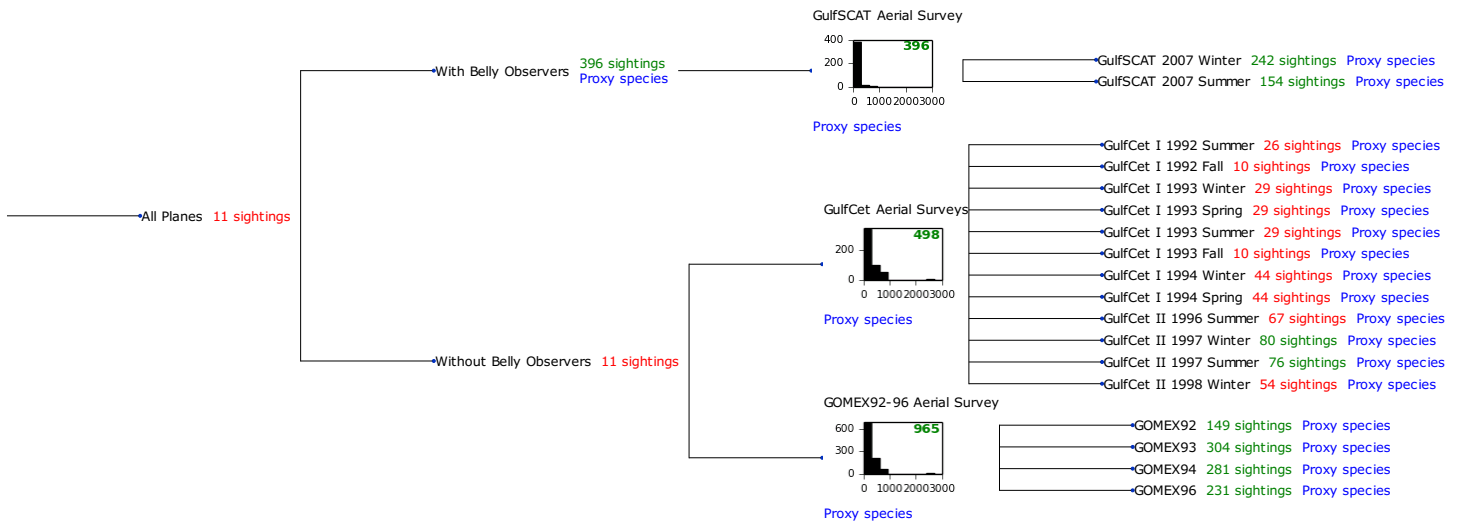


Figure 16: Detection hierarchy for aerial surveys

GulfSCAT Aerial Survey

Because this taxon was sighted too infrequently to fit a detection function to its sightings alone, we fit a detection function to the pooled sightings of several other species that we believed would exhibit similar detectability. These “proxy species” are listed below.

Reported By Observer	Common Name	n
<i>Delphinus capensis</i>	Long-beaked common dolphin	0
<i>Delphinus delphis</i>	Short-beaked common dolphin	0
<i>Delphinus delphis/Lagenorhynchus acutus</i>	Short-beaked common or Atlantic white-sided dolphin	0
<i>Delphinus delphis/Stenella</i>	Short-beaked common dolphin or <i>Stenella</i> spp.	0
<i>Delphinus delphis/Stenella coeruleoalba</i>	Short-beaked common or striped dolphin	0
<i>Grampus griseus</i>	Risso’s dolphin	0
<i>Grampus griseus/Tursiops truncatus</i>	Risso’s or Bottlenose dolphin	0
<i>Lagenodelphis hosei</i>	Fraser’s dolphin	0
<i>Lagenorhynchus acutus</i>	Atlantic white-sided dolphin	0
<i>Lagenorhynchus albirostris</i>	White-beaked dolphin	0
<i>Lagenorhynchus albirostris/Lagenorhynchus acutus</i>	White-beaked or white-sided dolphin	0
<i>Stenella</i>	Unidentified <i>Stenella</i>	0
<i>Stenella attenuata</i>	Pantropical spotted dolphin	0
<i>Stenella attenuata/frontalis</i>	Pantropical or Atlantic spotted dolphin	0
<i>Stenella clymene</i>	Clymene dolphin	0
<i>Stenella coeruleoalba</i>	Striped dolphin	0
<i>Stenella frontalis</i>	Atlantic spotted dolphin	15
<i>Stenella frontalis/Tursiops truncatus</i>	Atlantic spotted or Bottlenose dolphin	0
<i>Stenella longirostris</i>	Spinner dolphin	0

Steno bredanensis	Rough-toothed dolphin	0
Steno bredanensis/Tursiops truncatus	Bottlenose or rough-toothed dolphin	0
Tursiops truncatus	Bottlenose dolphin	381
Total		396

Table 10: Proxy species used to fit detection functions for GulfSCAT Aerial Survey. The number of sightings, n , is before truncation.

The sightings were right truncated at 400m.

Covariate	Description
beaufort	Beaufort sea state.
quality	Survey-specific index of the quality of observation conditions, utilizing relevant factors other than Beaufort sea state (see methods).
size	Estimated size (number of individuals) of the sighted group.

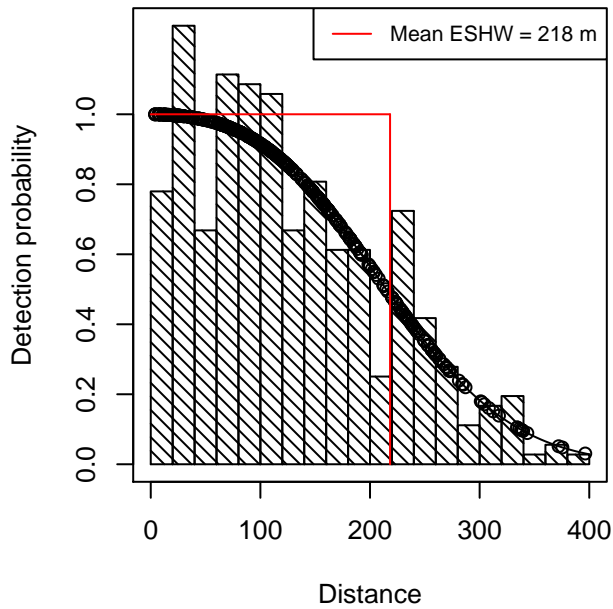
Table 11: Covariates tested in candidate “multi-covariate distance sampling” (MCDS) detection functions.

Key	Adjustment	Order	Covariates	Succeeded	Δ AIC	Mean ESHW (m)
hn	herm	4		Yes	0.00	218
hn	cos	2		Yes	0.09	221
hn				Yes	0.90	199
hn			size	Yes	2.21	199
hn	cos	3		Yes	2.37	209
hr	poly	2		Yes	2.39	218
hr	poly	4		Yes	2.47	223
hr				Yes	4.46	230
hr			size	Yes	5.04	232
hn			beaufort	No		
hr			beaufort	No		
hn			quality	No		
hr			quality	No		
hn			beaufort, quality	No		
hr			beaufort, quality	No		
hn			beaufort, size	No		
hr			beaufort, size	No		
hn			quality, size	No		
hr			quality, size	No		
hn			beaufort, quality, size	No		
hr			beaufort, quality, size	No		

Table 12: Candidate detection functions for GulfSCAT Aerial Survey. The first one listed was selected for the density model.

Spinner dolphin and proxy species

Half-normal key with 4th order Hermite polynomial adj.
392 sightings, right truncated at 400 m



Q-Q Plot

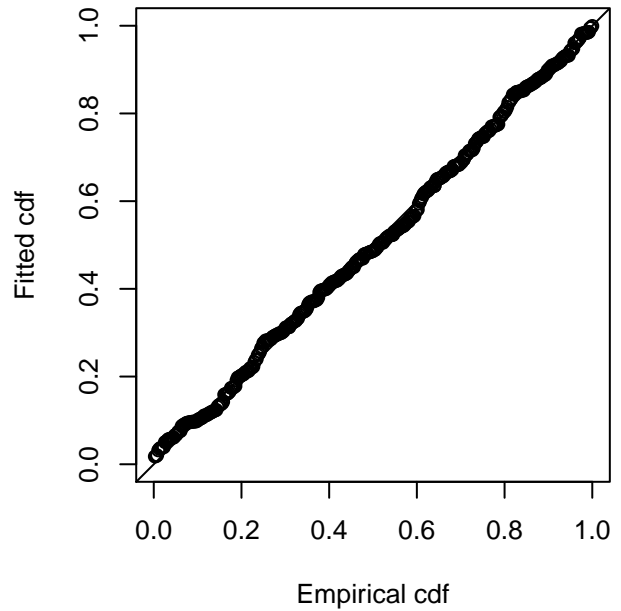


Figure 17: Detection function for GulfSCAT Aerial Survey that was selected for the density model

Statistical output for this detection function:

Summary for ds object

Number of observations : 392
Distance range : 0 - 400
AIC : 4505.917

Detection function:

Half-normal key function with Hermite polynomial adjustment term of order 4

Detection function parameters

Scale Coefficients:

	estimate	se
(Intercept)	4.855663	0.07416754

Adjustment term parameter(s):

	estimate	se
herm, order 4	-0.04125525	0.01270717

Monotonicity constraints were enforced.

	Estimate	SE	CV
Average p	0.5457496	0.04201246	0.07698119
N in covered region	718.2781288	60.45882396	0.08417188

Monotonicity constraints were enforced.

Additional diagnostic plots:

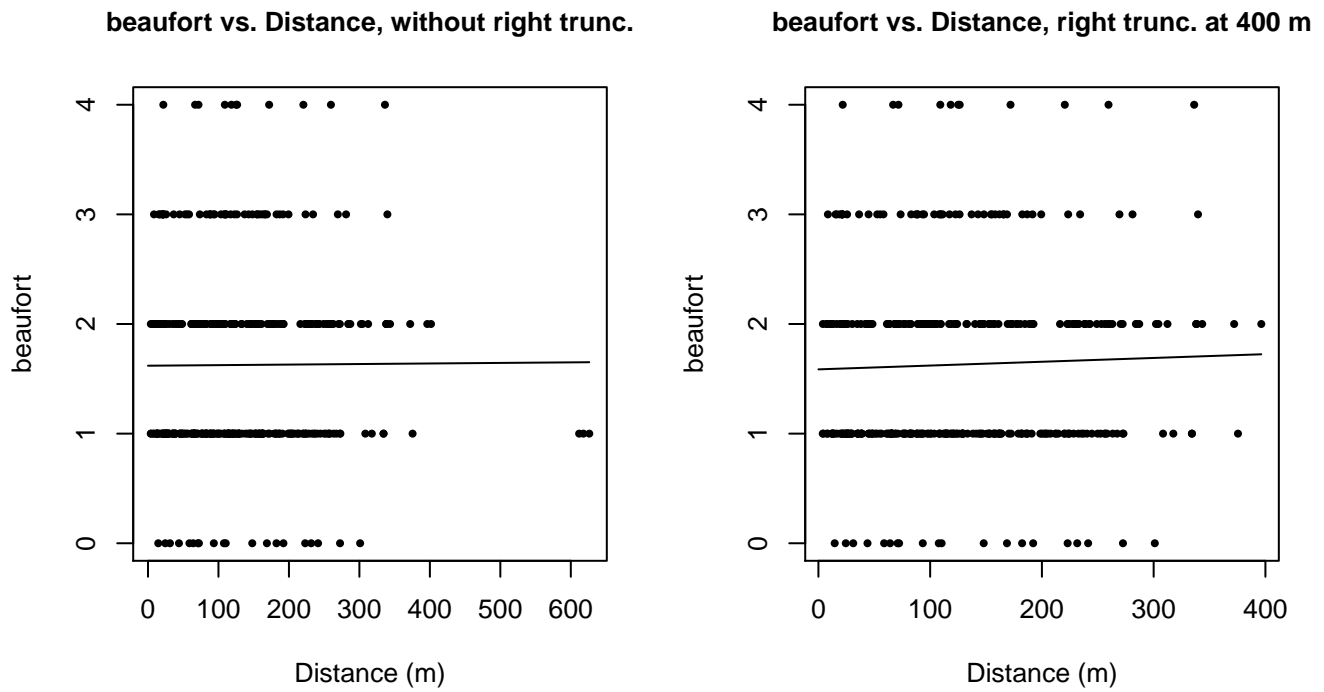


Figure 18: Scatterplots showing the relationship between Beaufort sea state and perpendicular sighting distance, for all sightings (left) and only those not right truncated (right). The line is a simple linear regression.

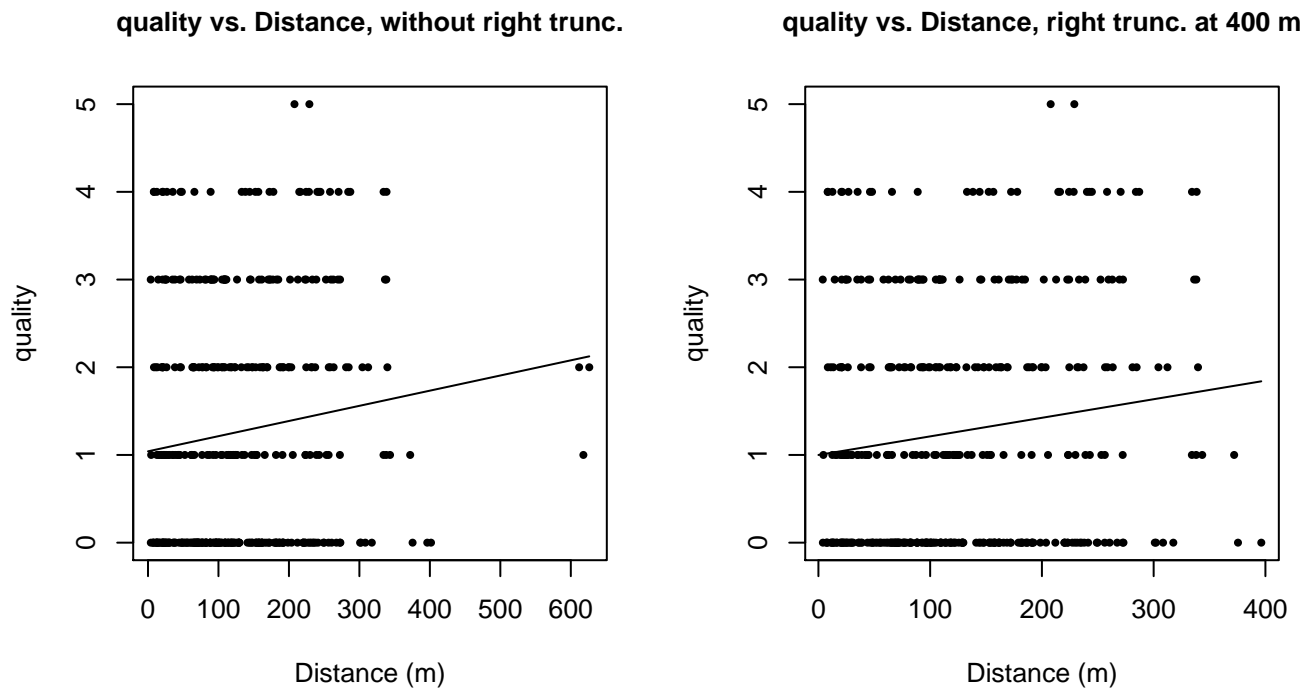


Figure 19: Scatterplots showing the relationship between the survey-specific index of the quality of observation conditions and perpendicular sighting distance, for all sightings (left) and only those not right truncated (right). Low values of the quality index correspond to better observation conditions. The line is a simple linear regression.

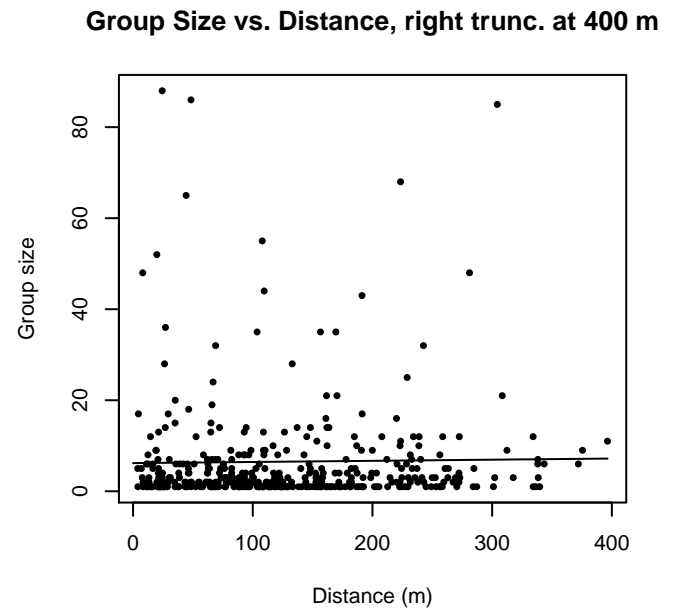
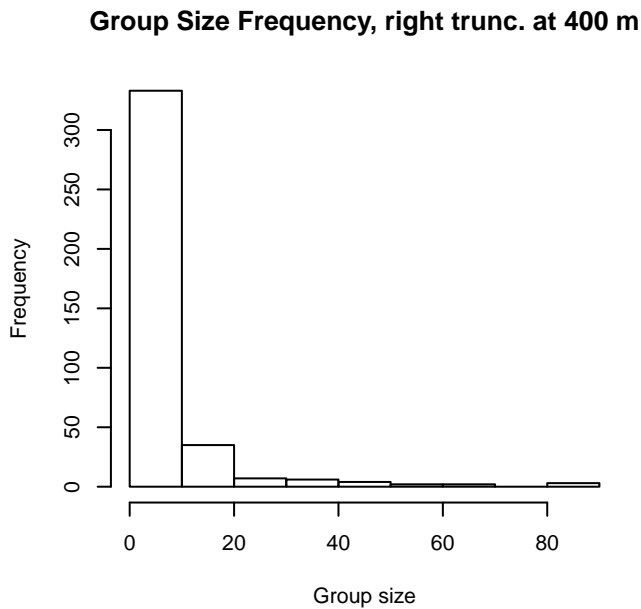
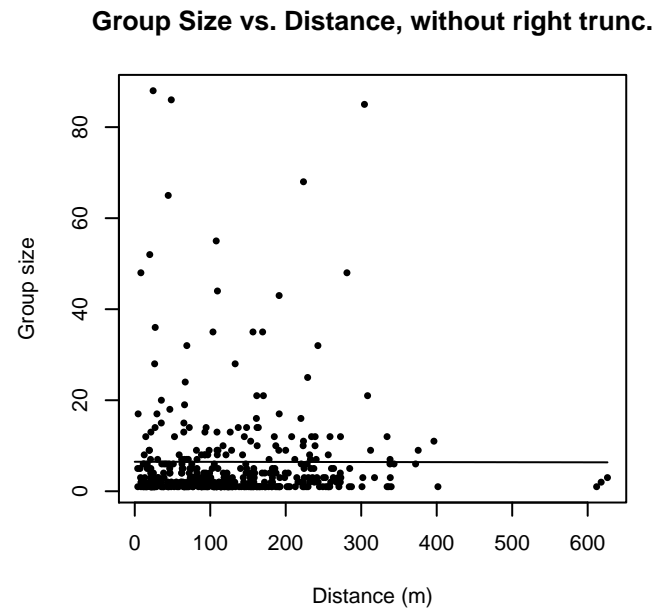
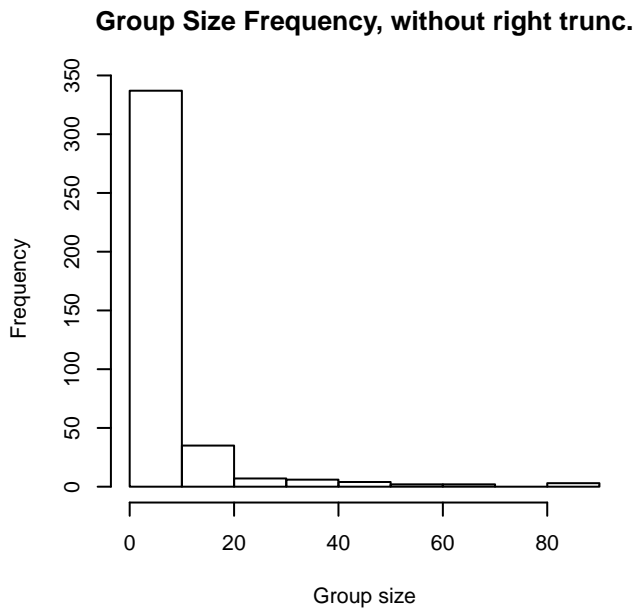


Figure 20: Histograms showing group size frequency and scatterplots showing the relationship between group size and perpendicular sighting distance, for all sightings (top row) and only those not right truncated (bottom row). In the scatterplot, the line is a simple linear regression.

GulfCet Aerial Surveys

Because this taxon was sighted too infrequently to fit a detection function to its sightings alone, we fit a detection function to the pooled sightings of several other species that we believed would exhibit similar detectability. These “proxy species” are listed below.

Reported By Observer	Common Name	n
Delphinus capensis	Long-beaked common dolphin	0
Delphinus delphis	Short-beaked common dolphin	0

Delphinus delphis/Lagenorhynchus acutus	Short-beaked common or Atlantic white-sided dolphin	0
Delphinus delphis/Stenella	Short-beaked common dolphin or Stenella spp.	0
Delphinus delphis/Stenella coeruleoalba	Short-beaked common or striped dolphin	0
Grampus griseus	Risso’s dolphin	71
Grampus griseus/Tursiops truncatus	Risso’s or Bottlenose dolphin	0
Lagenodelphis hosei	Fraser’s dolphin	2
Lagenorhynchus acutus	Atlantic white-sided dolphin	0
Lagenorhynchus albirostris	White-beaked dolphin	0
Lagenorhynchus albirostris/Lagenorhynchus acutus	White-beaked or white-sided dolphin	0
Stenella	Unidentified Stenella	10
Stenella attenuata	Pantropical spotted dolphin	94
Stenella attenuata/frontalis	Pantropical or Atlantic spotted dolphin	0
Stenella clymene	Clymene dolphin	12
Stenella coeruleoalba	Striped dolphin	16
Stenella frontalis	Atlantic spotted dolphin	36
Stenella frontalis/Tursiops truncatus	Atlantic spotted or Bottlenose dolphin	0
Stenella longirostris	Spinner dolphin	11
Steno bredanensis	Rough-toothed dolphin	9
Steno bredanensis/Tursiops truncatus	Bottlenose or rough-toothed dolphin	0
Tursiops truncatus	Bottlenose dolphin	237
Total		498

Table 13: Proxy species used to fit detection functions for GulfCet Aerial Surveys. The number of sightings, n , is before truncation.

The sightings were right truncated at 1296m. The vertical sighting angles were heaped at 10 degree increments, so the candidate detection functions were fitted using linear bins scaled accordingly.

Covariate	Description
beaufort	Beaufort sea state.
quality	Survey-specific index of the quality of observation conditions, utilizing relevant factors other than Beaufort sea state (see methods).
size	Estimated size (number of individuals) of the sighted group.

Table 14: Covariates tested in candidate “multi-covariate distance sampling” (MCDS) detection functions.

Key	Adjustment	Order	Covariates	Succeeded	Δ AIC	Mean ESHW (m)
hr			size	Yes	0.00	402
hr				Yes	1.41	394
hr	poly	2		Yes	3.41	394

hr	poly	4		Yes	3.41	394
hn	cos	2		Yes	4.97	368
hn	cos	3		Yes	10.69	340
hn			size	Yes	31.42	441
hn				Yes	34.80	439
hn	herm	4		Yes	36.57	439
hn			beaufort	No		
hr			beaufort	No		
hn			quality	No		
hr			quality	No		
hn			beaufort, quality	No		
hr			beaufort, quality	No		
hn			beaufort, size	No		
hr			beaufort, size	No		
hn			quality, size	No		
hr			quality, size	No		
hn			beaufort, quality, size	No		
hr			beaufort, quality, size	No		

Table 15: Candidate detection functions for GulfCet Aerial Surveys. The first one listed was selected for the density model.

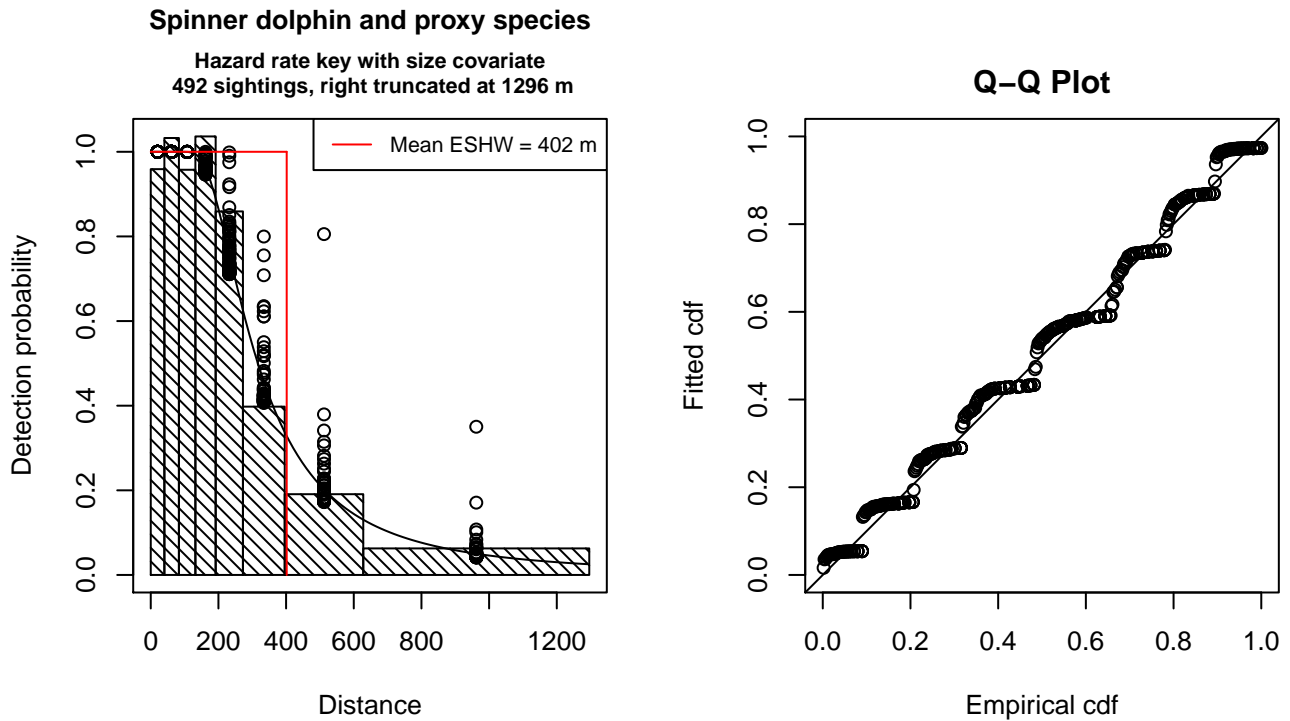


Figure 21: Detection function for GulfCet Aerial Surveys that was selected for the density model

Statistical output for this detection function:

Summary for ds object

Number of observations : 492
Distance range : 0 - 1296
AIC : 2031.84

Detection function:

Hazard-rate key function

Detection function parameters

Scale Coefficients:

	estimate	se
(Intercept)	5.535347	0.09109734
size	0.139986	0.06272901

Shape parameters:

	estimate	se
(Intercept)	0.866934	0.08296851

	Estimate	SE	CV
Average p	0.3057269	0.0166754	0.05454346
N in covered region	1609.2795060	106.6843878	0.06629326

Additional diagnostic plots:

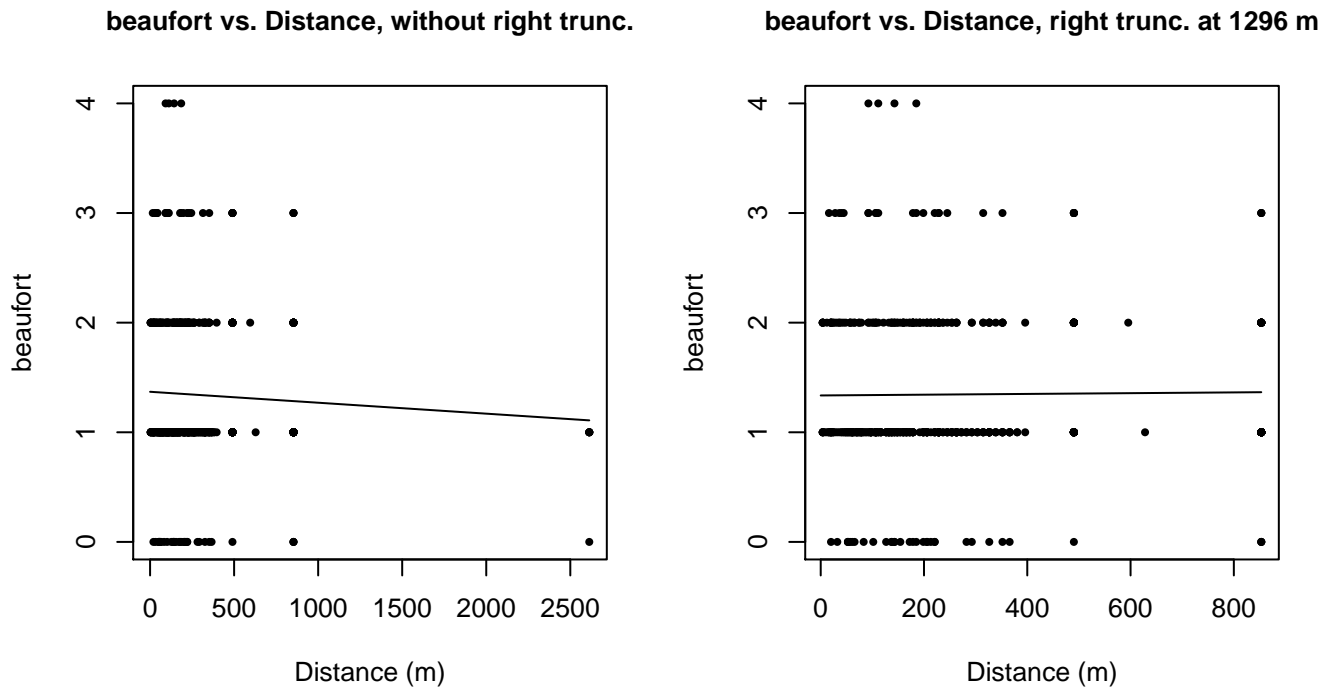
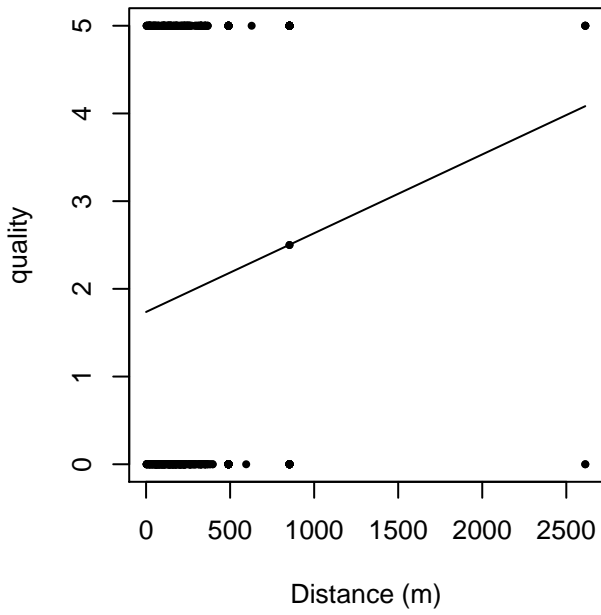


Figure 22: Scatterplots showing the relationship between Beaufort sea state and perpendicular sighting distance, for all sightings (left) and only those not right truncated (right). The line is a simple linear regression.

quality vs. Distance, without right trunc.



quality vs. Distance, right trunc. at 1296 m

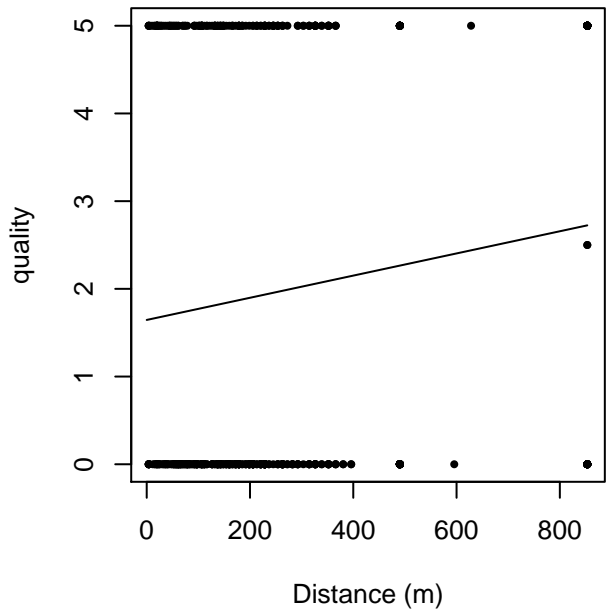
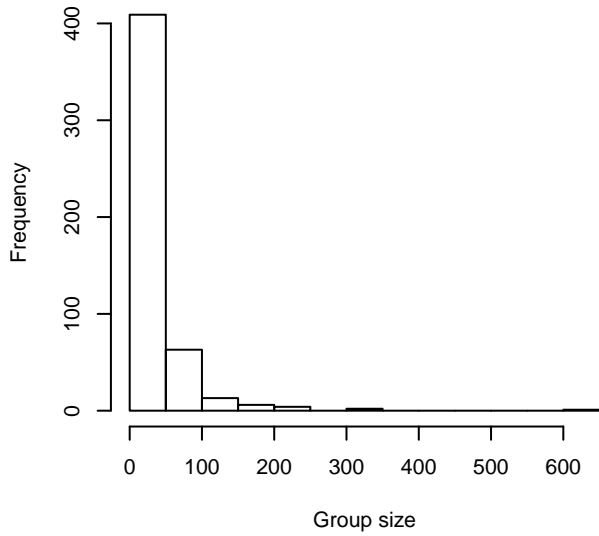
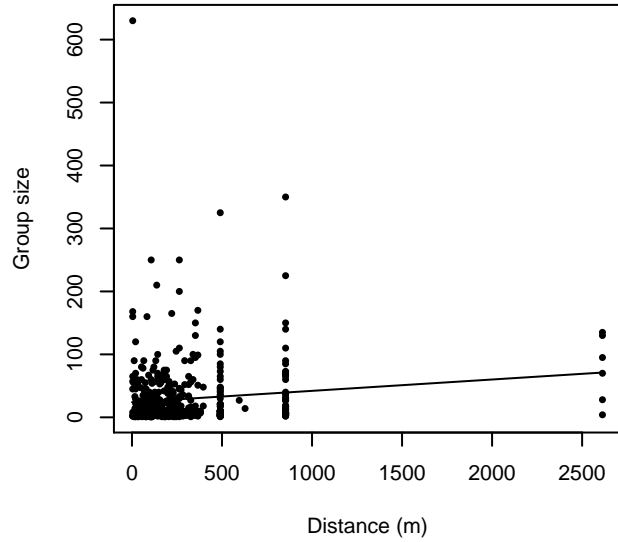


Figure 23: Scatterplots showing the relationship between the survey-specific index of the quality of observation conditions and perpendicular sighting distance, for all sightings (left) and only those not right truncated (right). Low values of the quality index correspond to better observation conditions. The line is a simple linear regression.

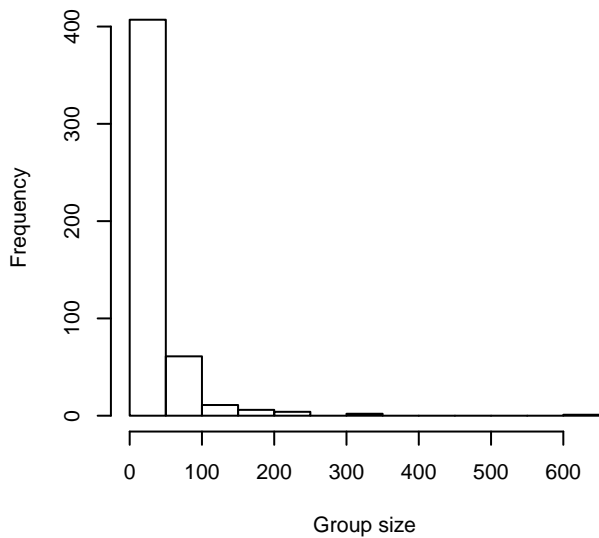
Group Size Frequency, without right trunc.



Group Size vs. Distance, without right trunc.



Group Size Frequency, right trunc. at 1296 m



Group Size vs. Distance, right trunc. at 1296 m

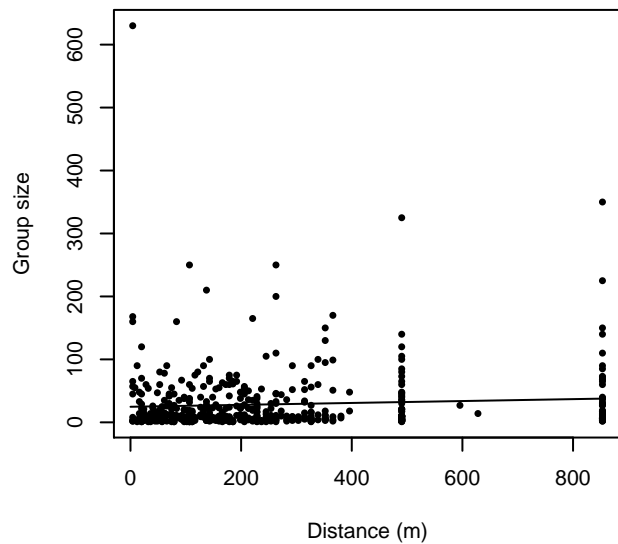


Figure 24: Histograms showing group size frequency and scatterplots showing the relationship between group size and perpendicular sighting distance, for all sightings (top row) and only those not right truncated (bottom row). In the scatterplot, the line is a simple linear regression.

GOMEX92-96 Aerial Survey

Because this taxon was sighted too infrequently to fit a detection function to its sightings alone, we fit a detection function to the pooled sightings of several other species that we believed would exhibit similar detectability. These “proxy species” are listed below.

Reported By Observer	Common Name	n
Delphinus capensis	Long-beaked common dolphin	0
Delphinus delphis	Short-beaked common dolphin	0

Delphinus delphis/Lagenorhynchus acutus	Short-beaked common or Atlantic white-sided dolphin	0
Delphinus delphis/Stenella	Short-beaked common dolphin or Stenella spp.	0
Delphinus delphis/Stenella coeruleoalba	Short-beaked common or striped dolphin	0
Grampus griseus	Risso’s dolphin	4
Grampus griseus/Tursiops truncatus	Risso’s or Bottlenose dolphin	0
Lagenodelphis hosei	Fraser’s dolphin	0
Lagenorhynchus acutus	Atlantic white-sided dolphin	0
Lagenorhynchus albirostris	White-beaked dolphin	0
Lagenorhynchus albirostris/Lagenorhynchus acutus	White-beaked or white-sided dolphin	0
Stenella	Unidentified Stenella	1
Stenella attenuata	Pantropical spotted dolphin	0
Stenella attenuata/frontalis	Pantropical or Atlantic spotted dolphin	0
Stenella clymene	Clymene dolphin	0
Stenella coeruleoalba	Striped dolphin	0
Stenella frontalis	Atlantic spotted dolphin	24
Stenella frontalis/Tursiops truncatus	Atlantic spotted or Bottlenose dolphin	0
Stenella longirostris	Spinner dolphin	0
Steno bredanensis	Rough-toothed dolphin	0
Steno bredanensis/Tursiops truncatus	Bottlenose or rough-toothed dolphin	0
Tursiops truncatus	Bottlenose dolphin	936
Total		965

Table 16: Proxy species used to fit detection functions for GOMEX92-96 Aerial Survey. The number of sightings, n , is before truncation.

The sightings were right truncated at 1296m. Due to a reduced frequency of sightings close to the trackline that plausibly resulted from the behavior of the observers and/or the configuration of the survey platform, the sightings were left truncated as well. Sightings closer than 83 m to the trackline were omitted from the analysis, and it was assumed that the area closer to the trackline than this was not surveyed. This distance was estimated by inspecting histograms of perpendicular sighting distances. The vertical sighting angles were heaped at 10 degree increments, so the candidate detection functions were fitted using linear bins scaled accordingly.

Covariate	Description
beaufort	Beaufort sea state.
quality	Survey-specific index of the quality of observation conditions, utilizing relevant factors other than Beaufort sea state (see methods).
size	Estimated size (number of individuals) of the sighted group.

Table 17: Covariates tested in candidate “multi-covariate distance sampling” (MCDS) detection functions.

Key	Adjustment	Order	Covariates	Succeeded	Δ AIC	Mean ESHW (m)
-----	------------	-------	------------	-----------	--------------	---------------

hr			size	Yes	0.00	281
hr	poly	4		Yes	4.73	273
hn	cos	3		Yes	4.85	220
hr				Yes	4.90	278
hr	poly	2		Yes	5.13	269
hn	cos	2		Yes	12.07	259
hn			size	Yes	39.53	304
hn				Yes	41.94	304
hn	herm	4		Yes	43.71	304
hn			beaufort	No		
hr			beaufort	No		
hn			quality	No		
hr			quality	No		
hn			beaufort, quality	No		
hr			beaufort, quality	No		
hn			beaufort, size	No		
hr			beaufort, size	No		
hn			quality, size	No		
hr			quality, size	No		
hn			beaufort, quality, size	No		
hr			beaufort, quality, size	No		

Table 18: Candidate detection functions for GOMEX92-96 Aerial Survey. The first one listed was selected for the density model.

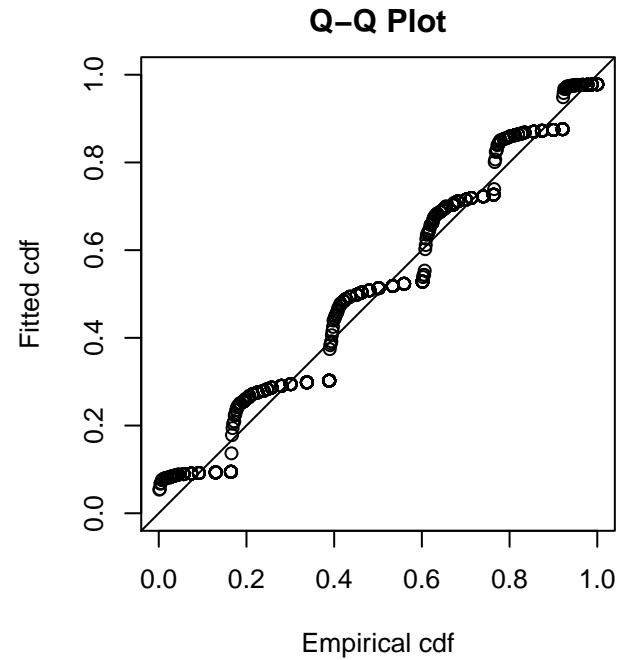
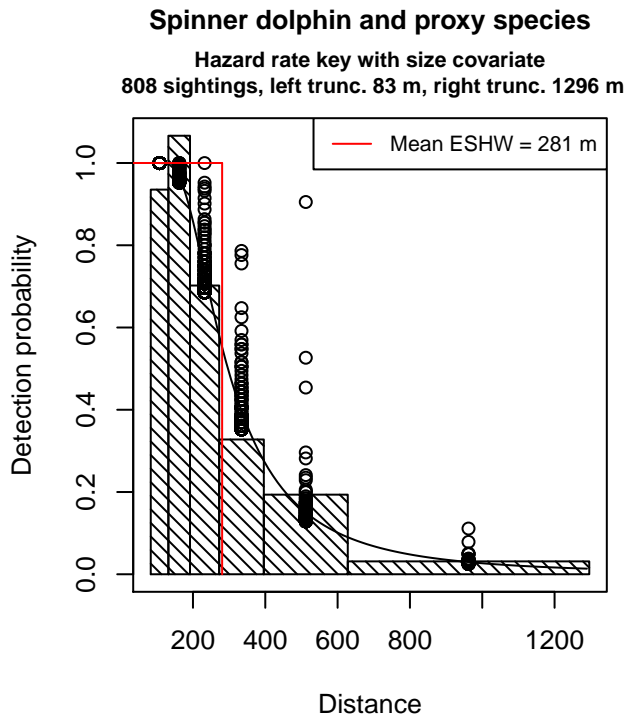


Figure 25: Detection function for GOMEX92-96 Aerial Survey that was selected for the density model

Statistical output for this detection function:

Summary for ds object

Number of observations : 808
 Distance range : 83.2036 - 1296
 AIC : 2832.217

Detection function:
 Hazard-rate key function

Detection function parameters

Scale Coefficients:

	estimate	se
(Intercept)	5.49007390	0.06761203
size	0.09577309	0.04016336

Shape parameters:

	estimate	se
(Intercept)	0.9893445	0.05859387

	Estimate	SE	CV
Average p	0.2138621	0.01146898	0.05362795
N in covered region	3778.1360570	234.49525749	0.06206639

Additional diagnostic plots:

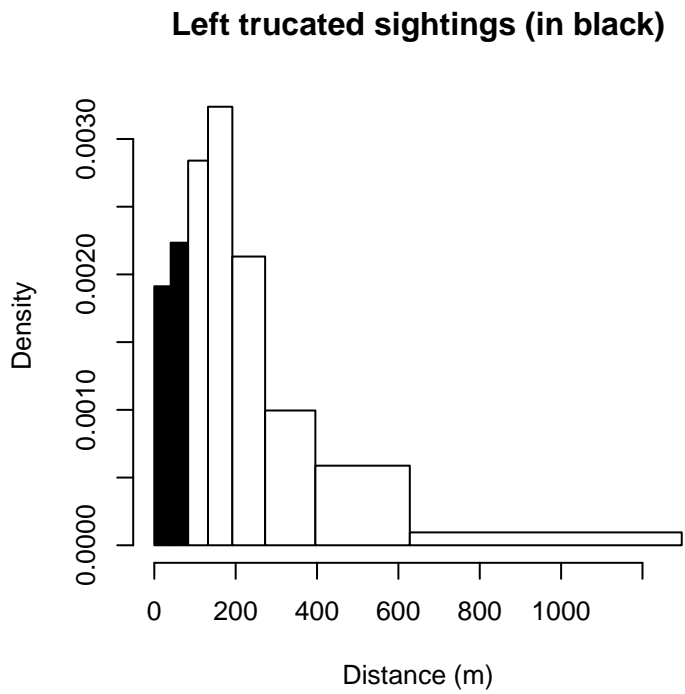


Figure 26: Density of sightings by perpendicular distance for GOMEX92-96 Aerial Survey. Black bars on the left show sightings that were left truncated.

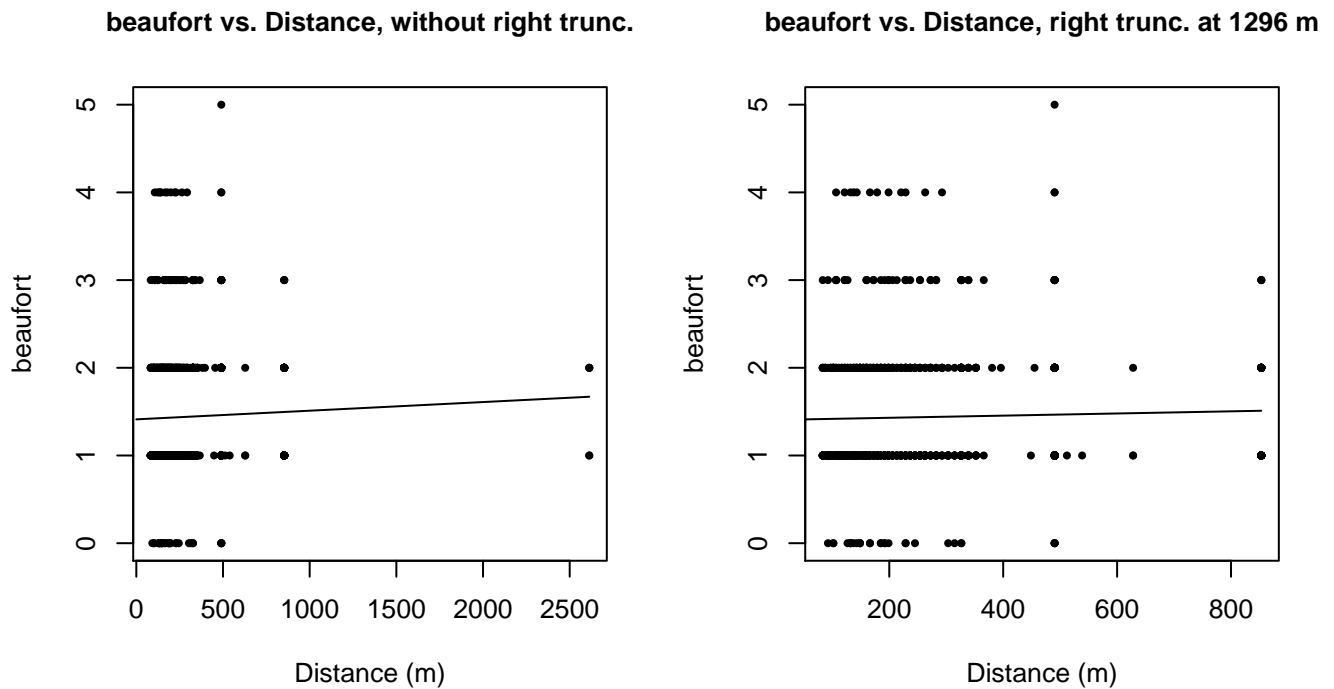
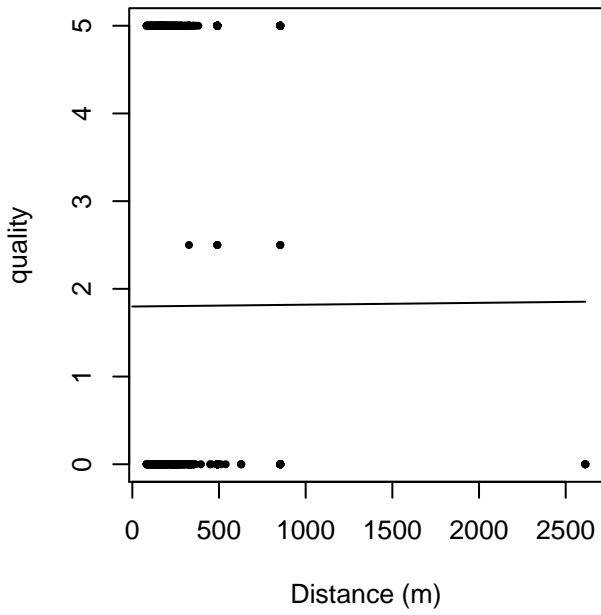


Figure 27: Scatterplots showing the relationship between Beaufort sea state and perpendicular sighting distance, for all sightings (left) and only those not right truncated (right). The line is a simple linear regression.

quality vs. Distance, without right trunc.



quality vs. Distance, right trunc. at 1296 m

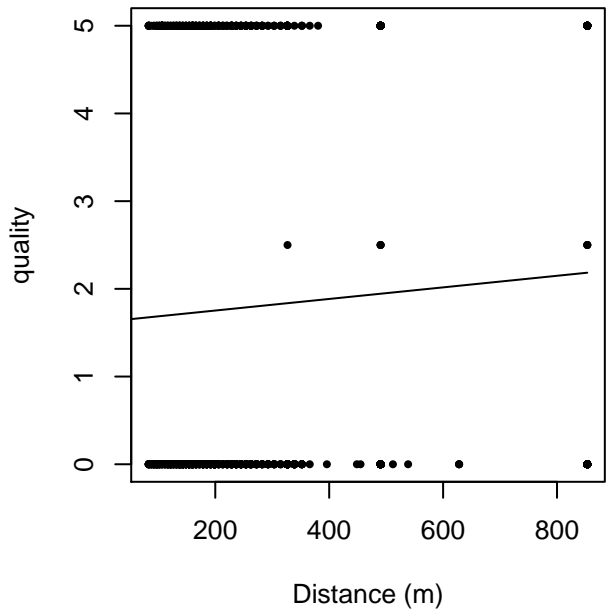
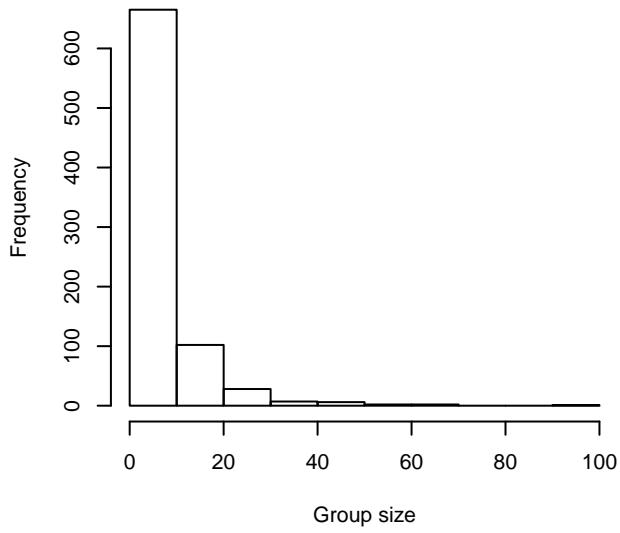
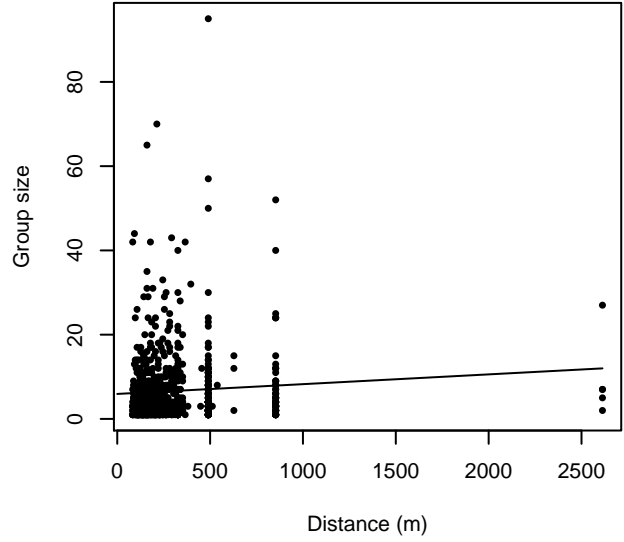


Figure 28: Scatterplots showing the relationship between the survey-specific index of the quality of observation conditions and perpendicular sighting distance, for all sightings (left) and only those not right truncated (right). Low values of the quality index correspond to better observation conditions. The line is a simple linear regression.

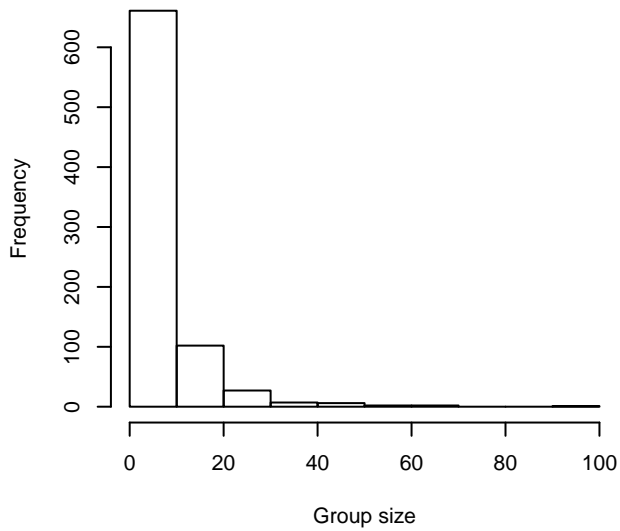
Group Size Frequency, without right trunc.



Group Size vs. Distance, without right trunc.



Group Size Frequency, right trunc. at 1296 m



Group Size vs. Distance, right trunc. at 1296 m

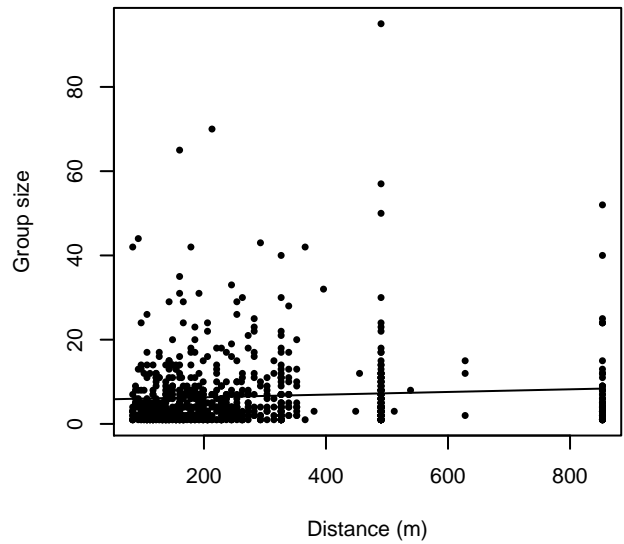


Figure 29: Histograms showing group size frequency and scatterplots showing the relationship between group size and perpendicular sighting distance, for all sightings (top row) and only those not right truncated (bottom row). In the scatterplot, the line is a simple linear regression.

$g(0)$ Estimates

Platform	Surveys	Group Size	$g(0)$	Biases Addressed	Source
Shipboard	All	1-20	0.856	Perception	Barlow and Forney (2007)
		>20	0.970	Perception	Barlow and Forney (2007)
Aerial	All	1-5	0.43	Both	Palka (2006)
		>5	0.960	Both	Carretta et al. (2000)

Table 19: Estimates of $g(0)$ used in this density model.

No $g(0)$ estimates were published for any of the shipboard surveys available to us from this region. Instead, we utilized Barlow and Forney’s (2007) estimates for delphinids, produced from several years of dual-team surveys that used bigeye binoculars and similar protocols to the surveys in our study. This study provided separate estimates for small and large groups, but pooled sightings of several species together to provide a generic estimate for all delphinids, due to sample-size limitations. To our knowledge, there is no species-specific shipboard $g(0)$ estimate that treats small and large groups separately, so we believe Barlow and Forney (2007) provide the best general-purpose alternative. Their estimate accounted for perception bias but not availability bias; dive times for dolphins are short enough that availability bias is not expected to be significant for dolphins observed from shipboard surveys.

For aerial surveys, we were unable to locate species-specific $g(0)$ estimates in the literature. For small groups, defined here as 1-5 individuals, we used Palka’s (2006) estimate of $g(0)$ for groups of 1-5 small cetaceans, estimated from two years of aerial surveys using the Hiby (1999) circle-back method. This estimate accounted for both availability and perception bias, but pooled sightings of several species together to provide a generic estimate for all delphinids, due to sample-size limitations. For large groups, defined here as greater than 5 individuals, Palka (2006) assumed that $g(0)$ was 1. When we discussed this with NOAA SWFSC reviewers, they agreed that it was safe to assume that the availability bias component of $g(0)$ was 1 but insisted that perception bias should be slightly less than 1, because it was possible to miss large groups. We agreed to take a conservative approach and obtained our $g(0)$ for large groups from Carretta et al. (2000), who estimated $g(0)$ for both small and large groups of delphinids. We used Carretta et al.’s $g(0)$ estimate for groups of 1-25 individuals (0.960), rather than their larger one for more than 25 individuals (0.994), to account for the fact that we were using Palka’s definition of large groups as those with more than 5 individuals.

Density Models

Worldwide, the spinner dolphin occurs in both oceanic and coastal tropical waters but is presumed to be an offshore, deep-water species (Waring et al. 2014). In the Gulf of Mexico, the surveys in our database reported 71 sightings, all beyond the continental shelf edge, at depths ranging from about 250 to 2600m. Most of these occurred in the northeast Gulf of Mexico along the continental slope, between 250-1000m. We found no definitive descriptions in the literature of seasonal movements by spinner dolphins in the Gulf of Mexico. Accordingly we fitted a year-round model to off-shelf waters, defined here as those deeper than the 100m isobath.

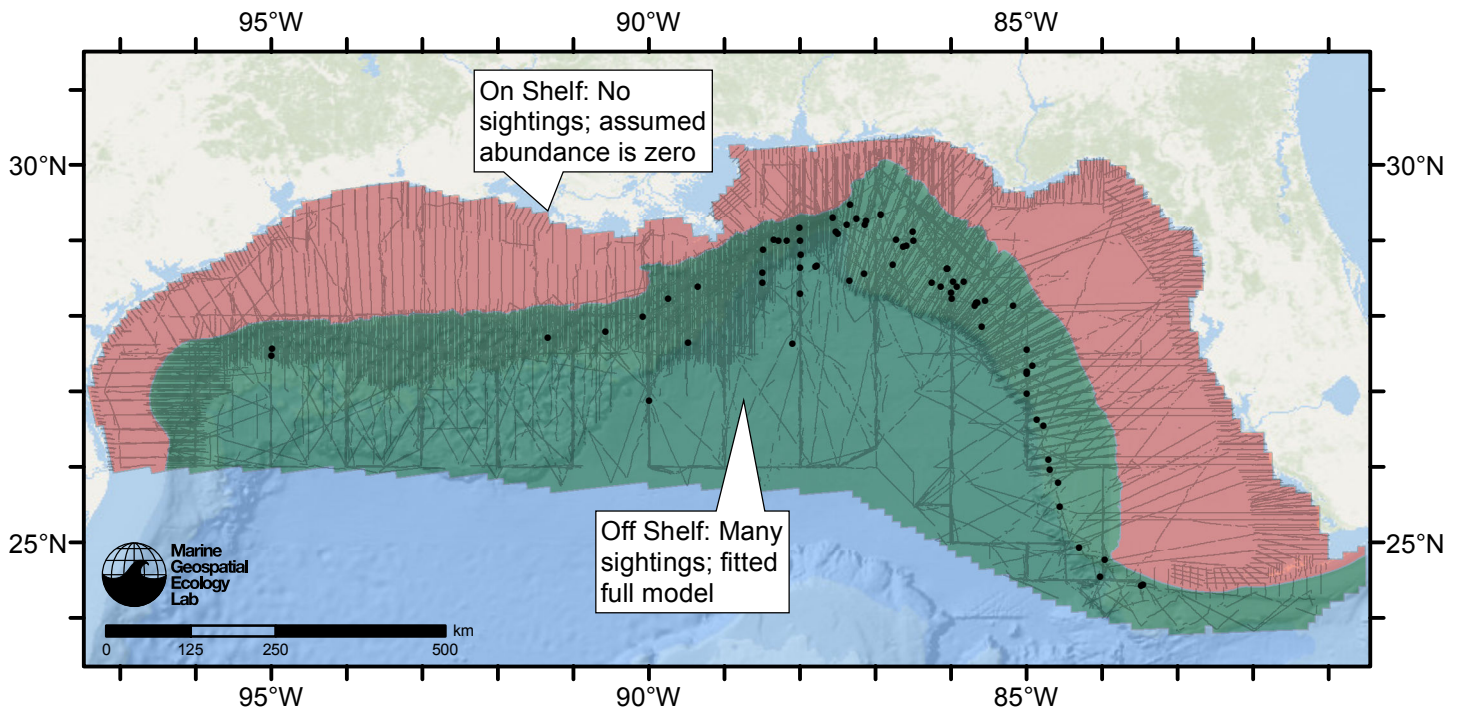


Figure 30: Spinner dolphin density model schematic. All on-effort sightings are shown, including those that were truncated when detection functions were fitted.

Climatological Model

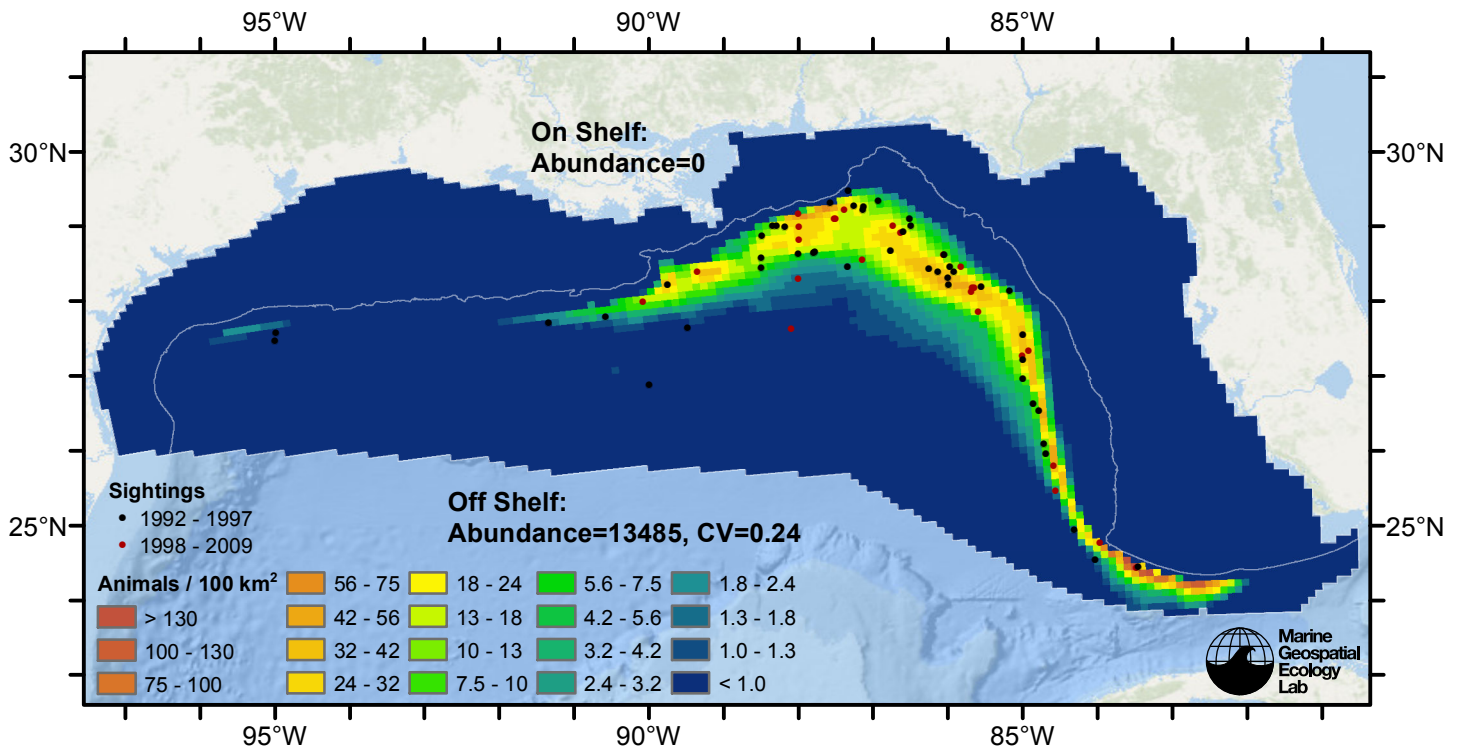


Figure 31: Spinner dolphin density predicted by the climatological model that explained the most deviance. Pixels are 10x10 km. The legend gives the estimated individuals per pixel; breaks are logarithmic. Abundance for each region was computed by summing the density cells occurring in that region.

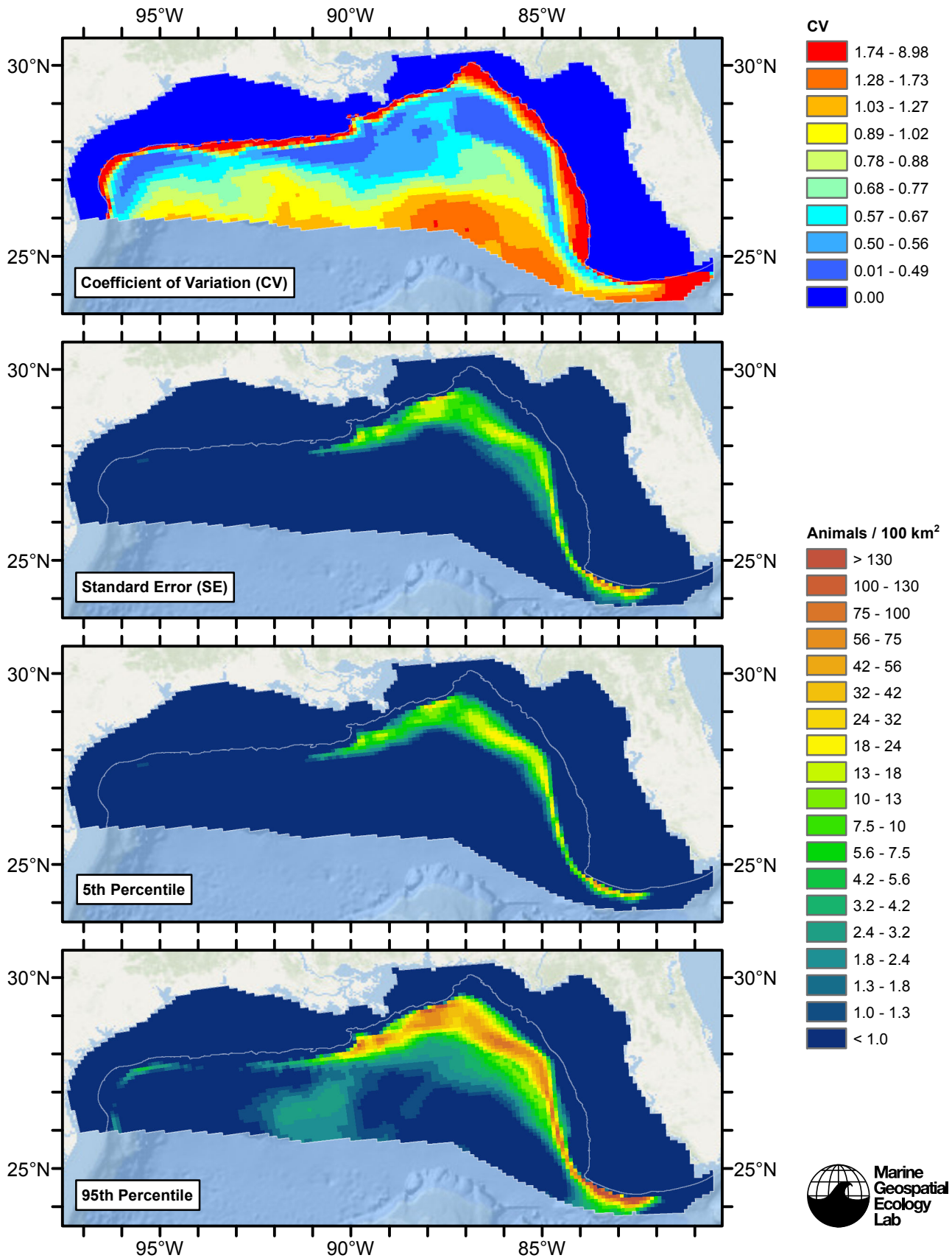


Figure 32: Estimated uncertainty for the climatological model that explained the most deviance. These estimates only incorporate the statistical uncertainty estimated for the spatial model (by the R mgcv package). They do not incorporate uncertainty in the detection functions, $g(0)$ estimates, predictor variables, and so on.

Off Shelf

Statistical output

Rscript.exe: This is mgcv 1.8-3. For overview type 'help("mgcv-package")'.

Family: Tweedie(p=1.44)

Link function: log

Formula:

```
abundance ~ offset(log(area_km2)) + s(log10(Depth), bs = "ts",
  k = 5) + s(ClimSST, bs = "ts", k = 5) + s(pmin(I(ClimDistToFront1/1000),
  250), bs = "ts", k = 5) + s(log10(pmax(ClimTKE, 0.001)),
  bs = "ts", k = 5) + s(pmin(I(ClimDistToEddy9/1000), 700),
  bs = "ts", k = 5) + s(log10(ClimCumVGPM45), bs = "ts", k = 5)
```

Parametric coefficients:

```
Estimate Std. Error t value Pr(>|t|)
(Intercept) -6.7021 0.4678 -14.33 <2e-16 ***
```

Signif. codes: 0 '***' 0.001 '**' 0.01 '*' 0.05 '.' 0.1 ' ' 1

Approximate significance of smooth terms:

	edf	Ref.df	F	p-value	
s(log10(Depth))	3.546	4	7.522	1.03e-06	***
s(ClimSST)	1.092	4	8.753	1.09e-09	***
s(pmin(I(ClimDistToFront1/1000), 250))	1.045	4	7.930	1.99e-09	***
s(log10(pmax(ClimTKE, 0.001)))	3.234	4	7.079	8.93e-07	***
s(pmin(I(ClimDistToEddy9/1000), 700))	3.601	4	13.641	3.46e-12	***
s(log10(ClimCumVGPM45))	3.270	4	7.490	5.52e-07	***

Signif. codes: 0 '***' 0.001 '**' 0.01 '*' 0.05 '.' 0.1 ' ' 1

R-sq.(adj) = 0.0178 Deviance explained = 52.3%

-REML = 890.67 Scale est. = 391.02 n = 14455

All predictors were significant. This is the final model.

Creating term plots.

Diagnostic output from gam.check():

Method: REML Optimizer: outer newton

full convergence after 11 iterations.

Gradient range [-5.437467e-05,4.218622e-06]

(score 890.6712 & scale 391.0197).

Hessian positive definite, eigenvalue range [0.4746274,152.0107].

Model rank = 25 / 25

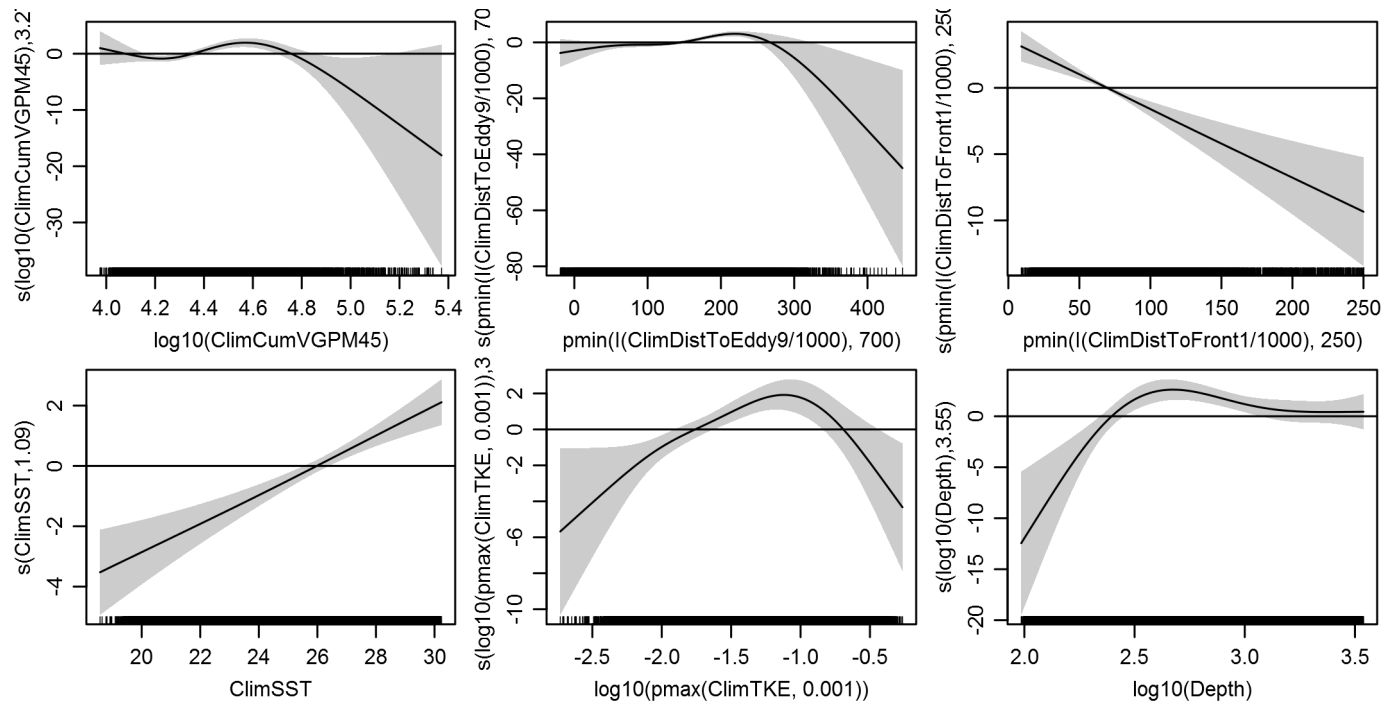
Basis dimension (k) checking results. Low p-value (k-index<1) may indicate that k is too low, especially if edf is close to k'.

	k'	edf	k-index	p-value
s(log10(Depth))	4.000	3.546	0.625	0.00
s(ClimSST)	4.000	1.092	0.670	0.02
s(pmin(I(ClimDistToFront1/1000), 250))	4.000	1.045	0.679	0.02
s(log10(pmax(ClimTKE, 0.001)))	4.000	3.234	0.692	0.08
s(pmin(I(ClimDistToEddy9/1000), 700))	4.000	3.601	0.666	0.01
s(log10(ClimCumVGPM45))	4.000	3.270	0.619	0.00

Predictors retained during the model selection procedure: Depth, ClimSST, ClimDistToFront1, ClimTKE, ClimDistToEddy9, ClimCumVGPM45

Predictors dropped during the model selection procedure: Slope, DistTo300m

Model term plots



Diagnostic plots

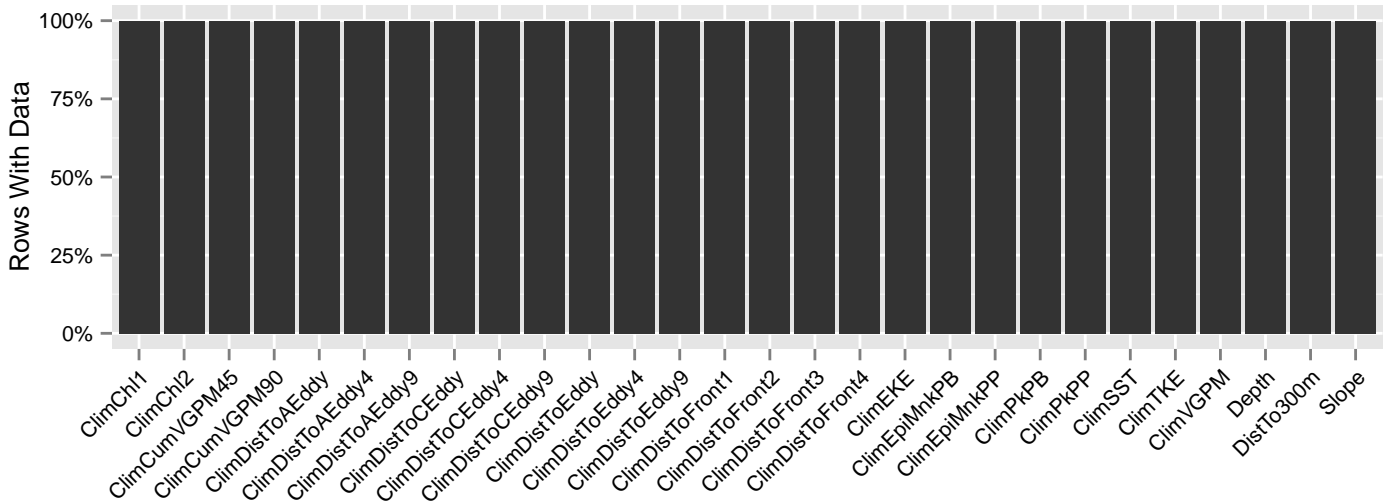


Figure 33: Segments with predictor values for the Spinner dolphin Climatological model, Off Shelf. This plot is used to assess how many segments would be lost by including a given predictor in a model.

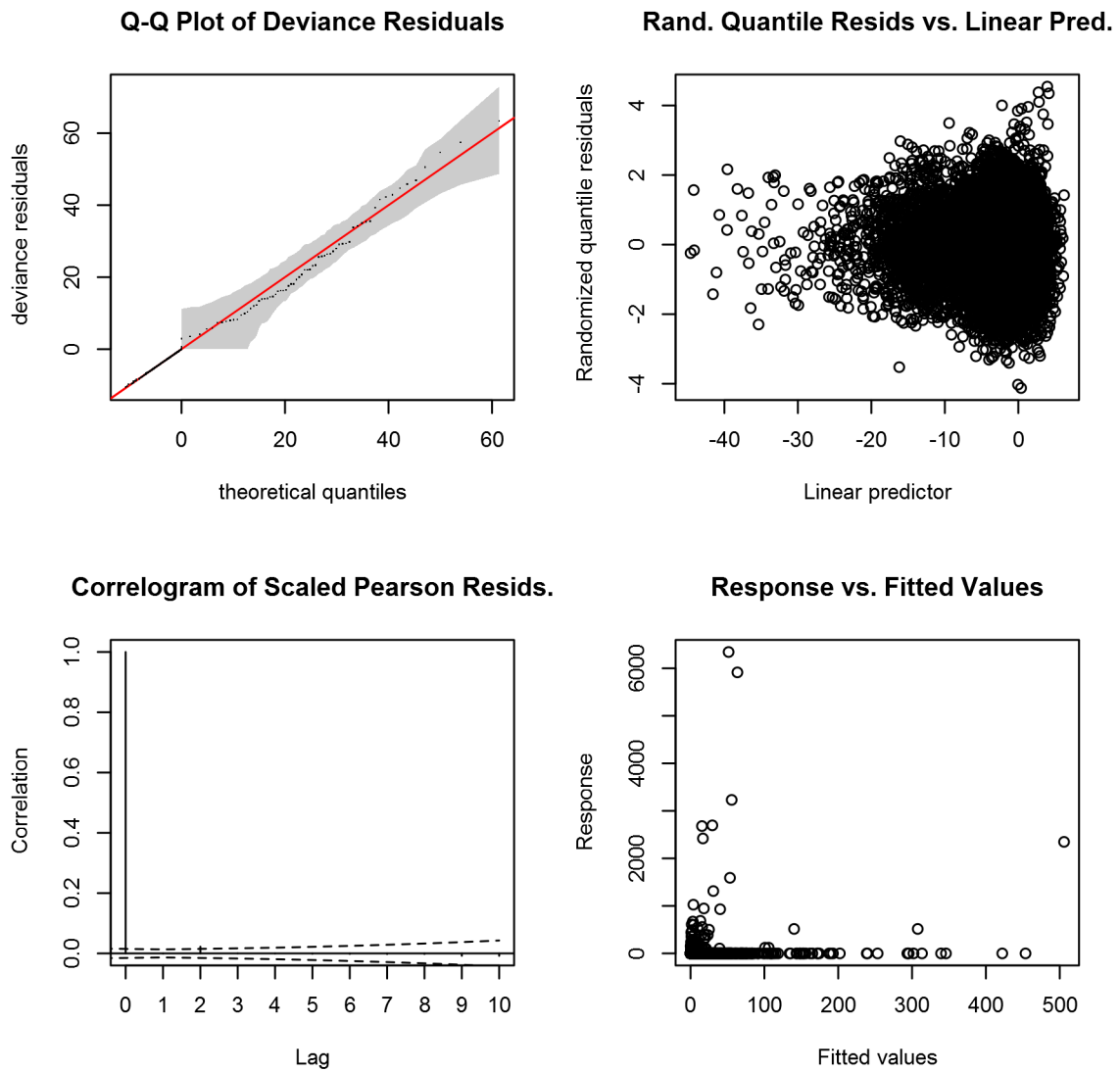


Figure 34: Statistical diagnostic plots for the Spinner dolphin Climatological model, Off Shelf.

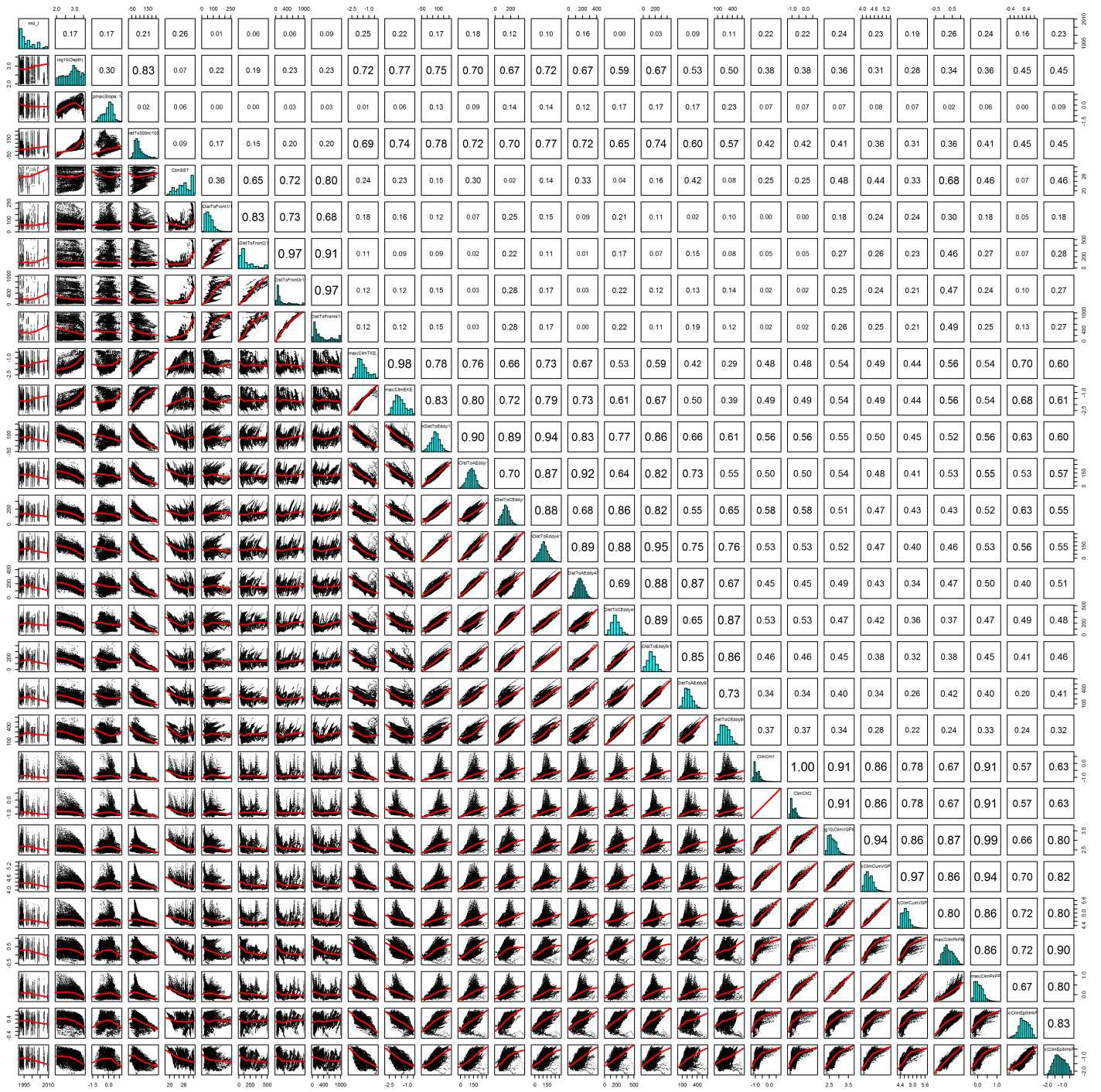


Figure 35: Scatterplot matrix for the Spinner dolphin Climatological model, Off Shelf. This plot is used to inspect the distribution of predictors (via histograms along the diagonal), simple correlation between predictors (via pairwise Pearson coefficients above the diagonal), and linearity of predictor correlations (via scatterplots below the diagonal). This plot is best viewed at high magnification.

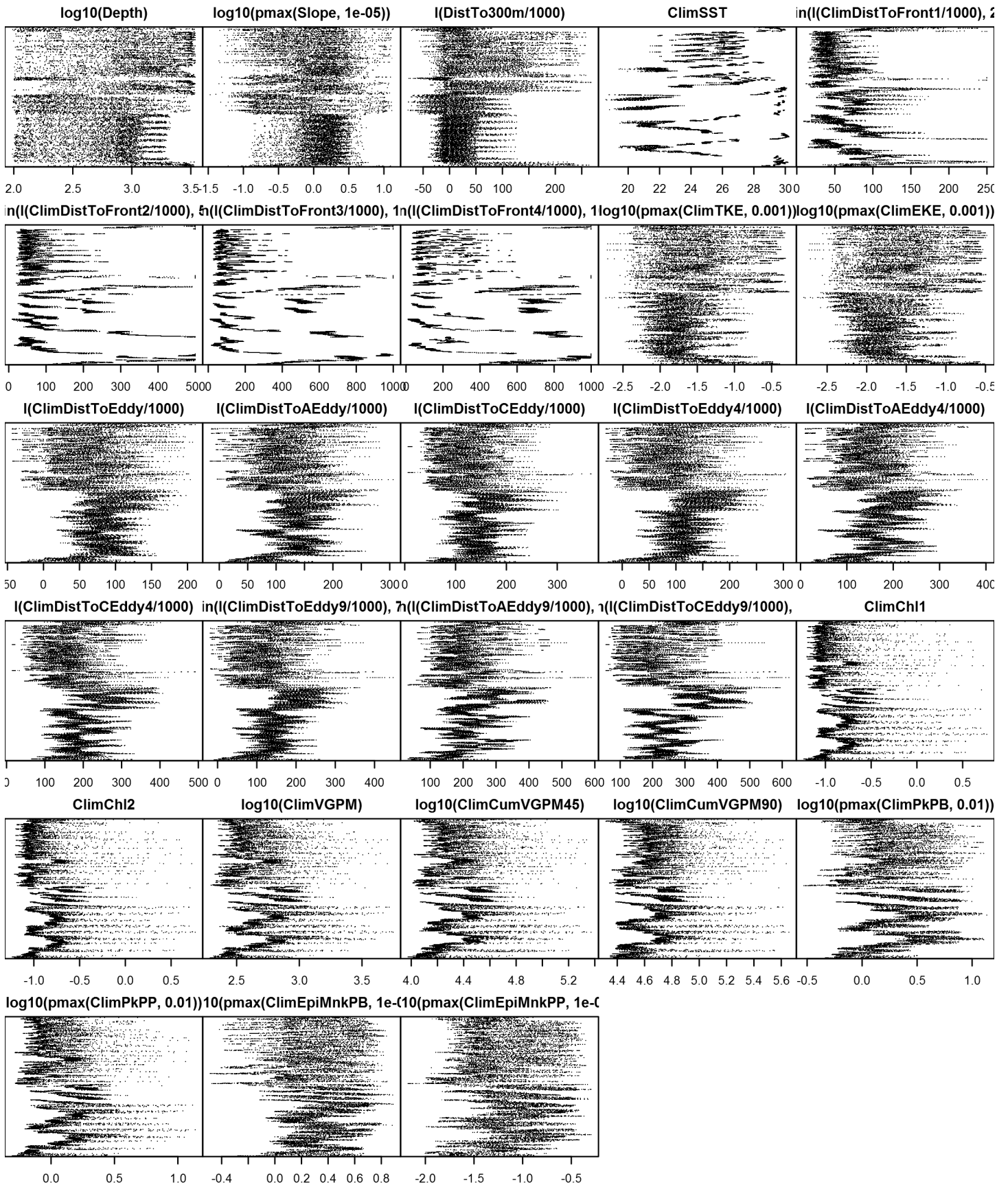


Figure 36: Dotplot for the Spinner dolphin Climatological model, Off Shelf. This plot is used to check for suspicious patterns and outliers in the data. Points are ordered vertically by transect ID, sequentially in time.

On Shelf

Density assumed to be 0 in this region.

Contemporaneous Model

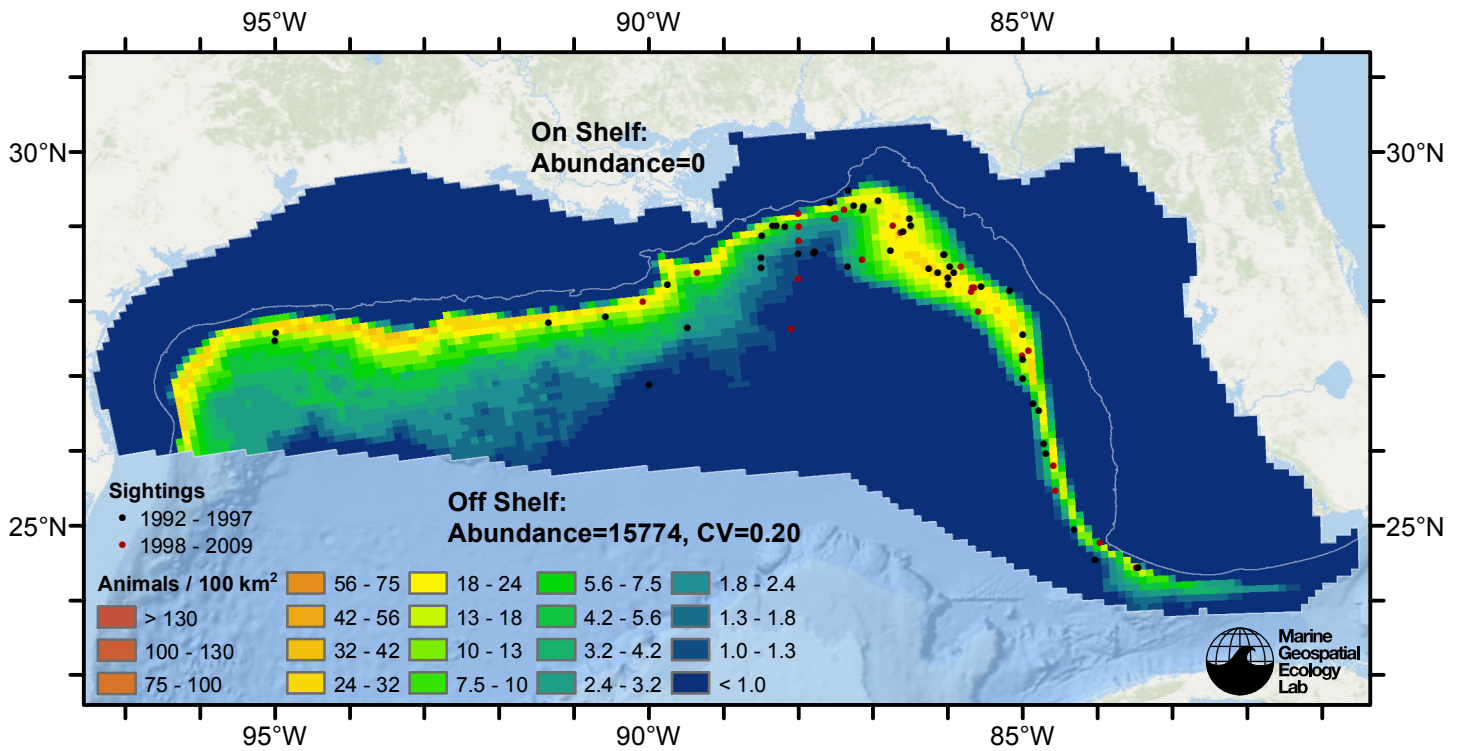


Figure 37: Spinner dolphin density predicted by the contemporaneous model that explained the most deviance. Pixels are 10x10 km. The legend gives the estimated individuals per pixel; breaks are logarithmic. Abundance for each region was computed by summing the density cells occurring in that region.

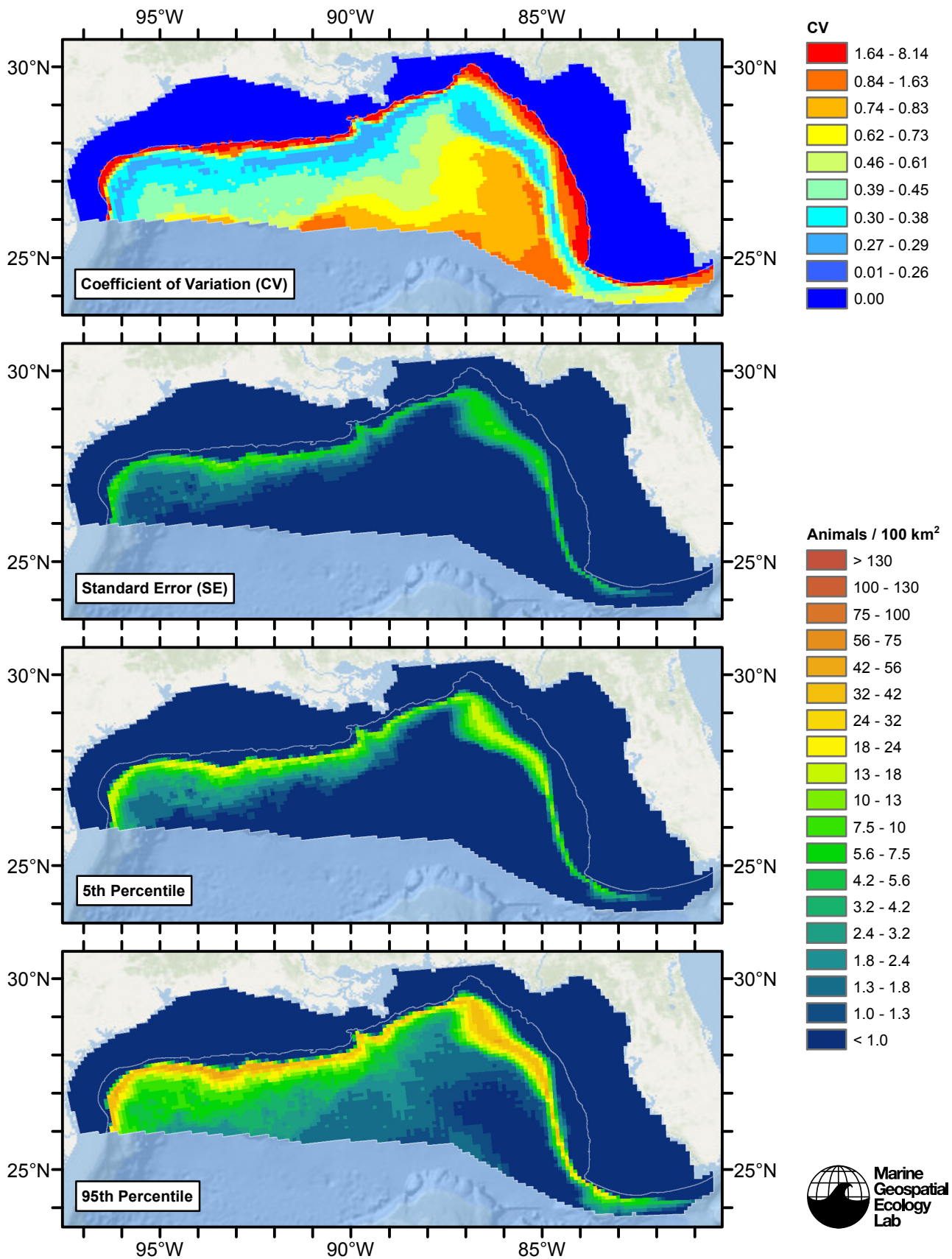


Figure 38: Estimated uncertainty for the contemporaneous model that explained the most deviance. These estimates only incorporate the statistical uncertainty estimated for the spatial model (by the R mgcv package). They do not incorporate uncertainty in the detection functions, $g(0)$ estimates, predictor variables, and so on.

Off Shelf

Statistical output

Rscript.exe: This is mgcv 1.8-3. For overview type 'help("mgcv-package")'.

Family: Tweedie(p=1.477)

Link function: log

Formula:

```
abundance ~ offset(log(area_km2)) + s(log10(Depth), bs = "ts",
  k = 5) + s(log10(pmax(TKE, 0.001)), bs = "ts", k = 5) + s(I(DistToAEddy/1000),
  bs = "ts", k = 5) + s(I(DistToCEddy/1000), bs = "ts", k = 5)
```

Parametric coefficients:

	Estimate	Std. Error	t value	Pr(> t)
(Intercept)	-4.6106	0.3674	-12.55	<2e-16 ***

Signif. codes: 0 '***' 0.001 '**' 0.01 '*' 0.05 '.' 0.1 ' ' 1

Approximate significance of smooth terms:

	edf	Ref.df	F	p-value
s(log10(Depth))	3.4902	4	10.104	4.45e-09 ***
s(log10(pmax(TKE, 0.001)))	1.0576	4	3.972	3.30e-05 ***
s(I(DistToAEddy/1000))	0.8561	4	1.320	0.01190 *
s(I(DistToCEddy/1000))	0.9479	4	2.315	0.00137 **

Signif. codes: 0 '***' 0.001 '**' 0.01 '*' 0.05 '.' 0.1 ' ' 1

R-sq.(adj) = 0.0101 Deviance explained = 32.8%

-REML = 830.46 Scale est. = 533.03 n = 12621

All predictors were significant. This is the final model.

Creating term plots.

Diagnostic output from gam.check():

Method: REML Optimizer: outer newton

full convergence after 12 iterations.

Gradient range [-0.0003633979,0.0003218697]

(score 830.4637 & scale 533.033).

Hessian positive definite, eigenvalue range [0.3522232,131.9804].

Model rank = 17 / 17

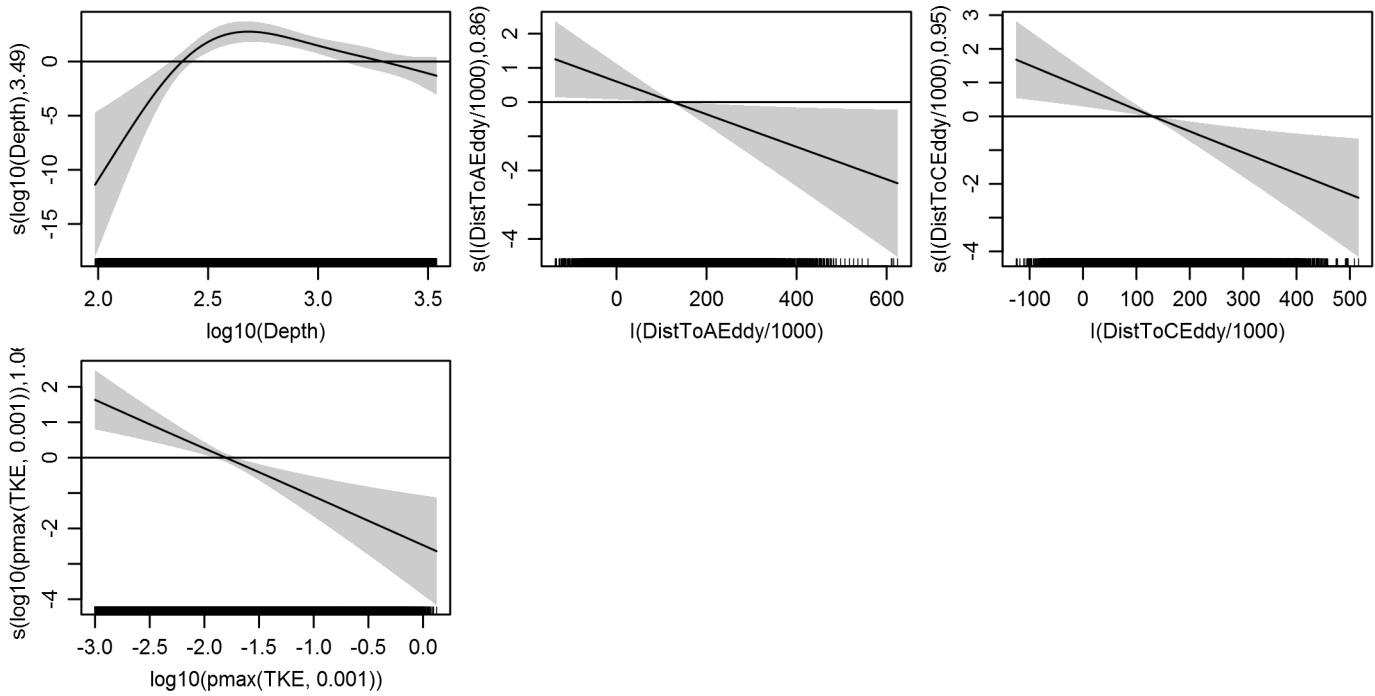
Basis dimension (k) checking results. Low p-value (k-index<1) may indicate that k is too low, especially if edf is close to k'.

	k'	edf	k-index	p-value
s(log10(Depth))	4.000	3.490	0.518	0.00
s(log10(pmax(TKE, 0.001)))	4.000	1.058	0.624	0.20
s(I(DistToAEddy/1000))	4.000	0.856	0.624	0.21
s(I(DistToCEddy/1000))	4.000	0.948	0.629	0.48

Predictors retained during the model selection procedure: Depth, TKE, DistToAEddy, DistToCEddy

Predictors dropped during the model selection procedure: Slope, DistTo300m, SST, DistToFront1

Model term plots



Diagnostic plots

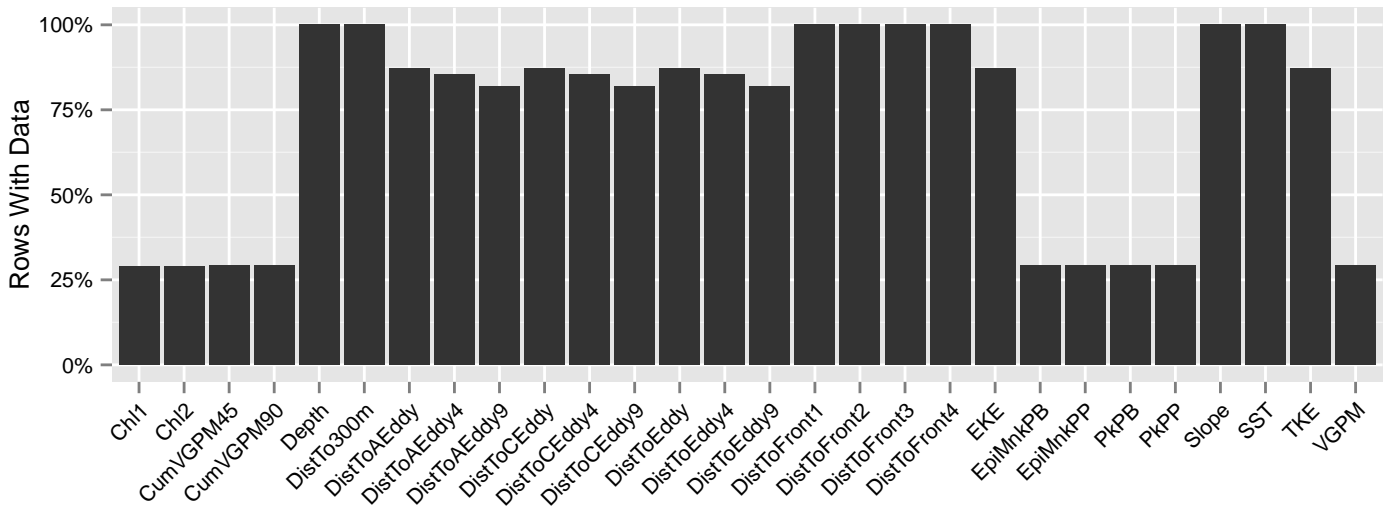


Figure 39: Segments with predictor values for the Spinner dolphin Contemporaneous model, Off Shelf. This plot is used to assess how many segments would be lost by including a given predictor in a model.

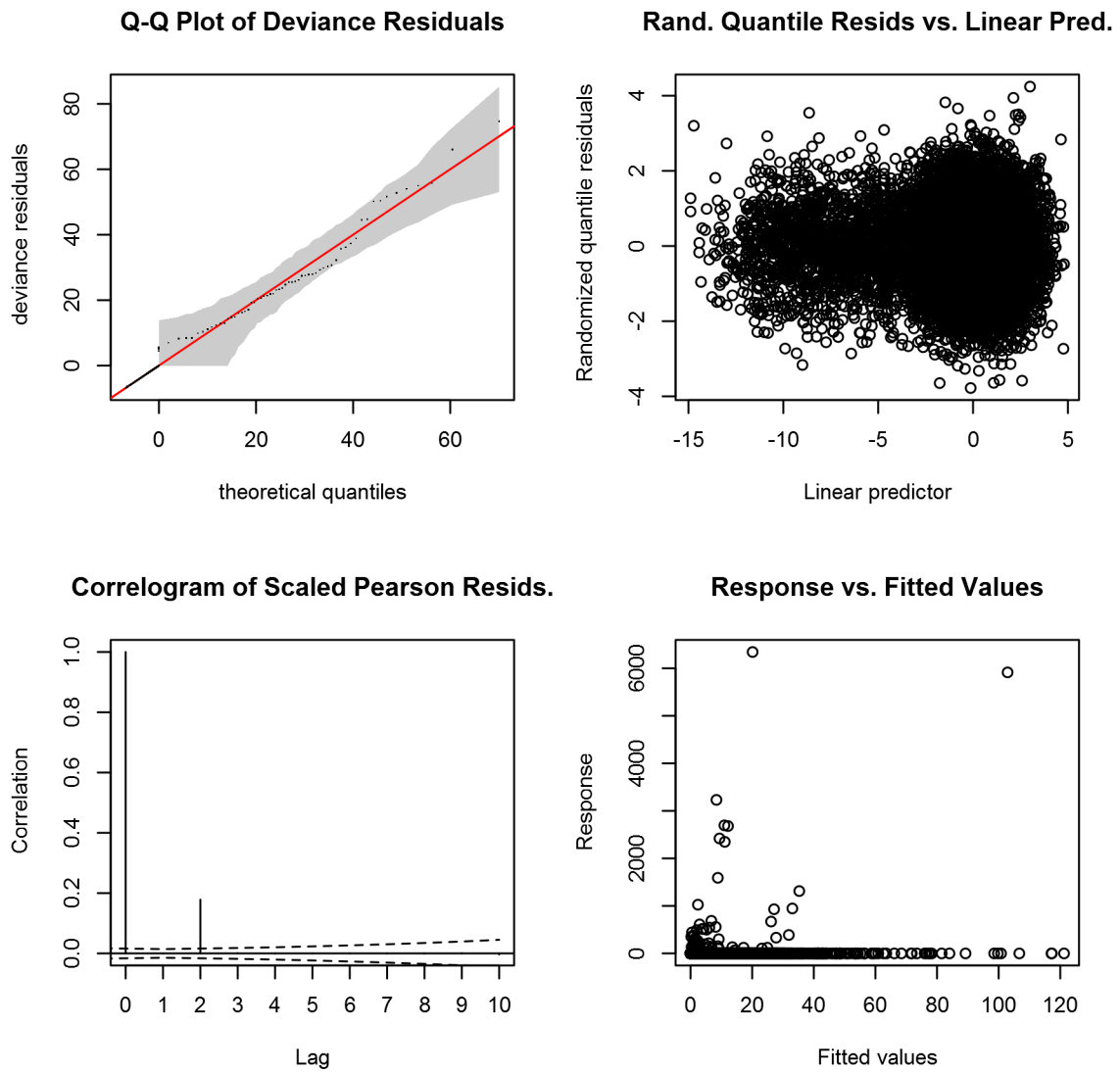


Figure 40: Statistical diagnostic plots for the Spinner dolphin Contemporaneous model, Off Shelf.

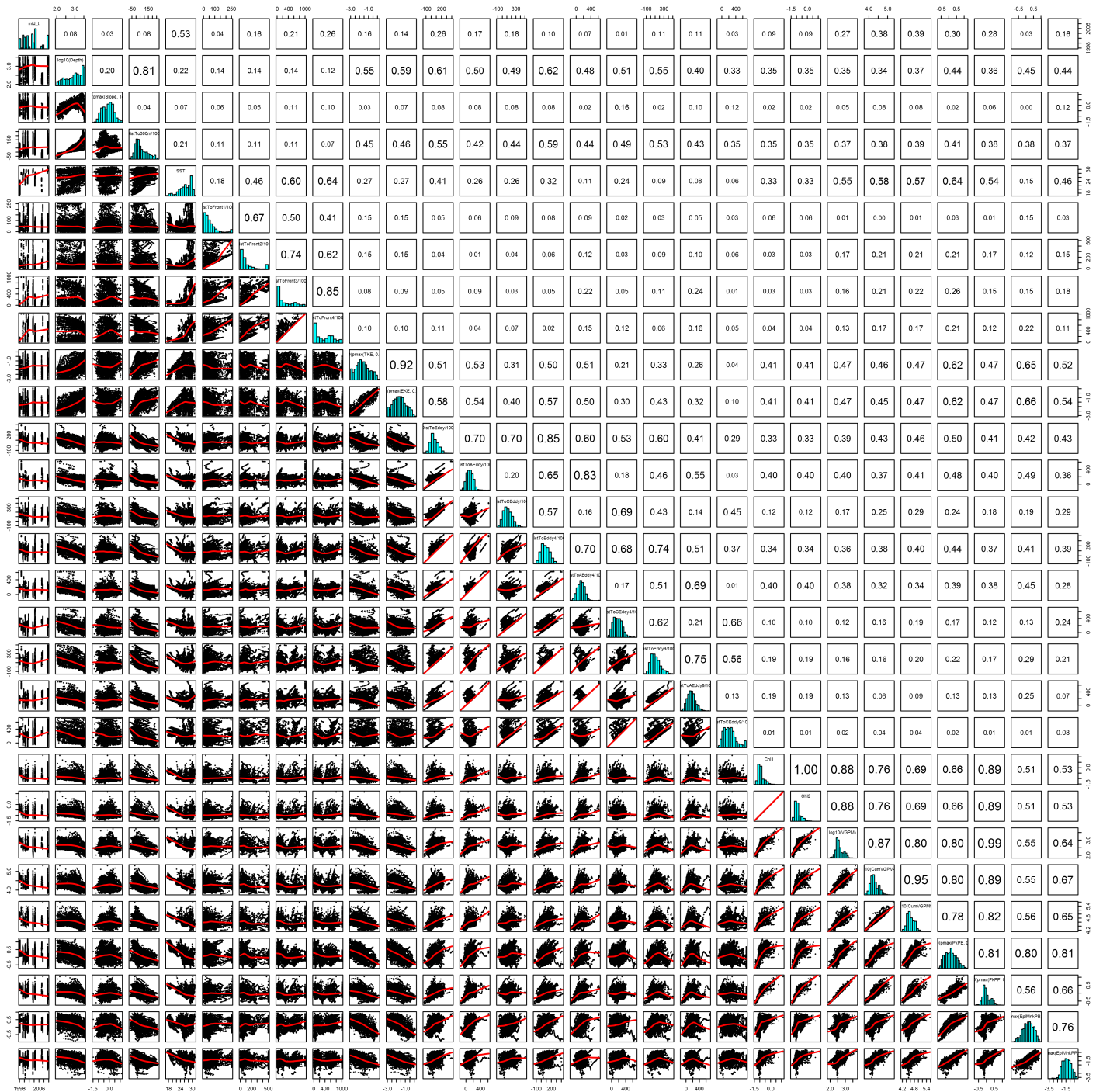


Figure 41: Scatterplot matrix for the Spinner dolphin Contemporaneous model, Off Shelf. This plot is used to inspect the distribution of predictors (via histograms along the diagonal), simple correlation between predictors (via pairwise Pearson coefficients above the diagonal), and linearity of predictor correlations (via scatterplots below the diagonal). This plot is best viewed at high magnification.

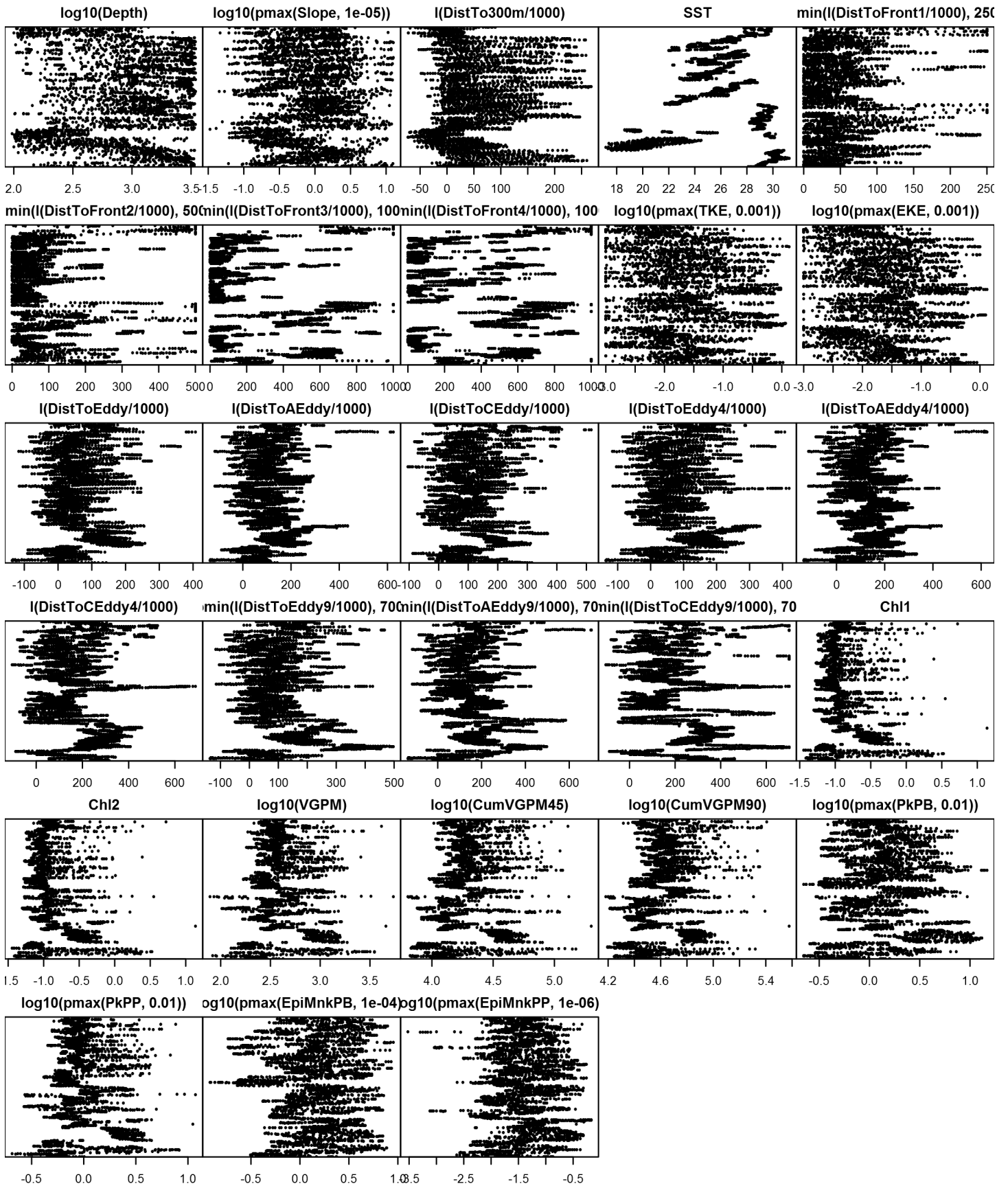


Figure 42: Dotplot for the Spinner dolphin Contemporaneous model, Off Shelf. This plot is used to check for suspicious patterns and outliers in the data. Points are ordered vertically by transect ID, sequentially in time.

On Shelf

Density assumed to be 0 in this region.

Climatological Same Segments Model

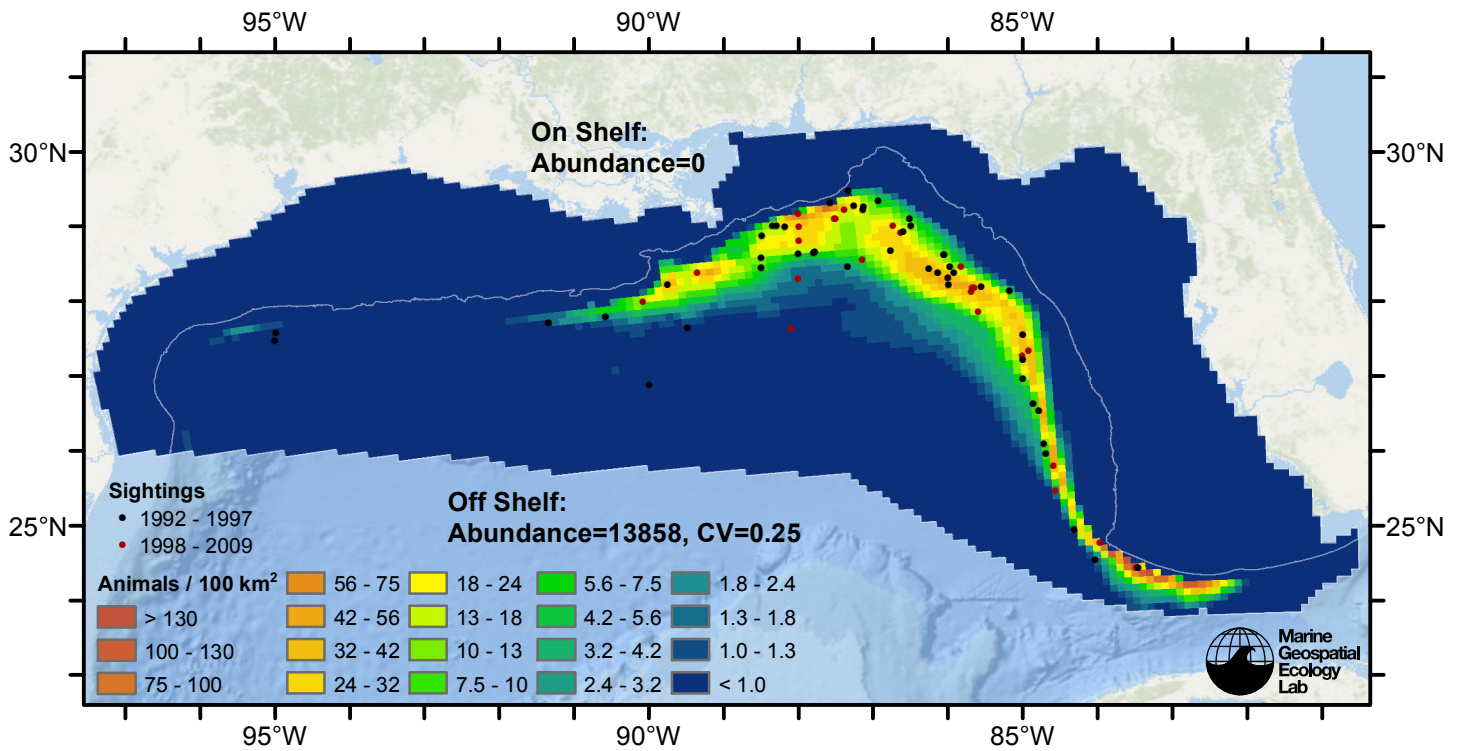


Figure 43: Spinner dolphin density predicted by the climatological same segments model that explained the most deviance. Pixels are 10x10 km. The legend gives the estimated individuals per pixel; breaks are logarithmic. Abundance for each region was computed by summing the density cells occurring in that region.

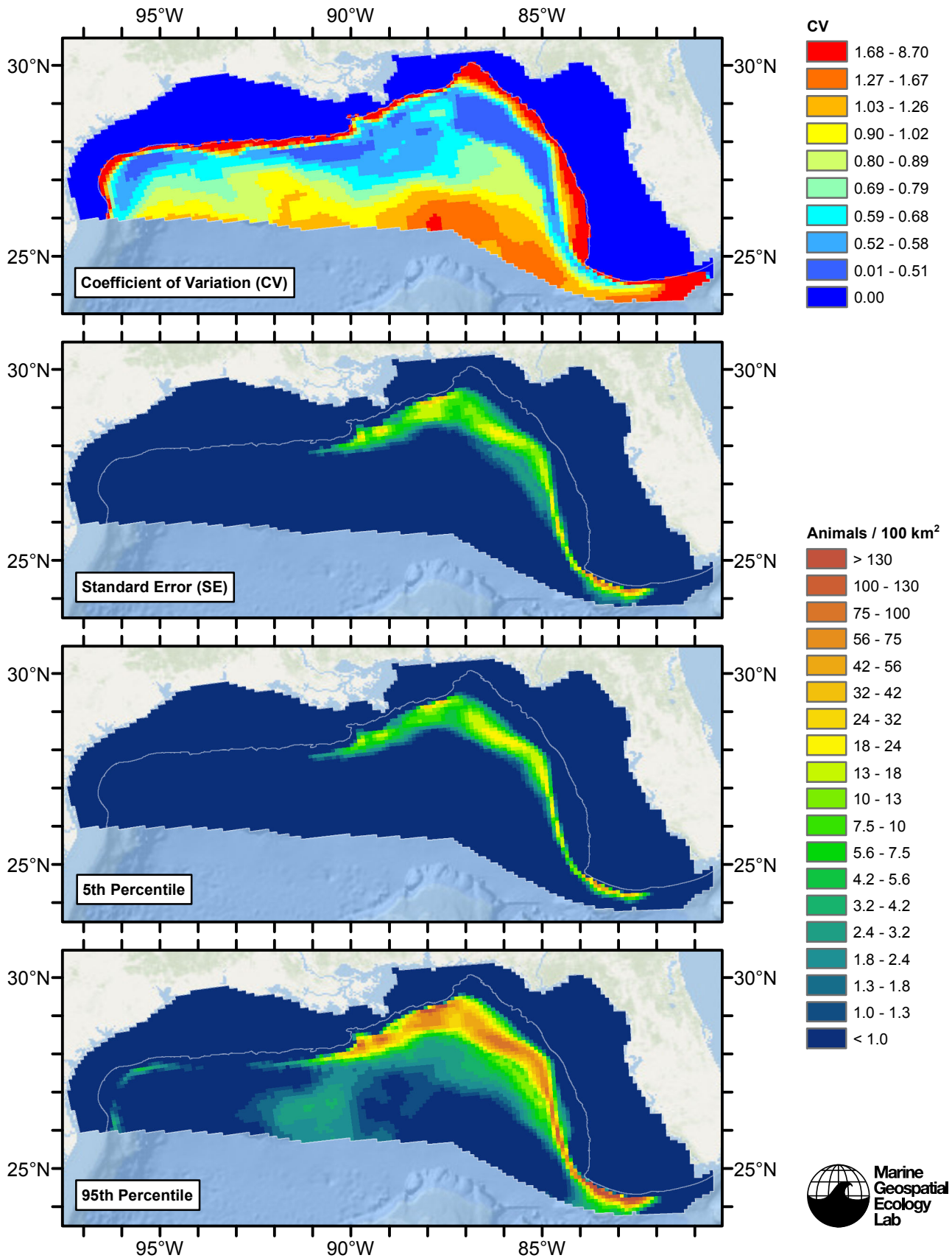


Figure 44: Estimated uncertainty for the climatological same segments model that explained the most deviance. These estimates only incorporate the statistical uncertainty estimated for the spatial model (by the R mgcv package). They do not incorporate uncertainty in the detection functions, $g(0)$ estimates, predictor variables, and so on.

Off Shelf

Statistical output

Rscript.exe: This is mgcv 1.8-3. For overview type 'help("mgcv-package")'.

Family: Tweedie(p=1.445)

Link function: log

Formula:

```
abundance ~ offset(log(area_km2)) + s(log10(Depth), bs = "ts",
  k = 5) + s(ClimSST, bs = "ts", k = 5) + s(pmin(I(ClimDistToFront1/1000),
  250), bs = "ts", k = 5) + s(log10(pmax(ClimTKE, 0.001)),
  bs = "ts", k = 5) + s(pmin(I(ClimDistToEddy9/1000), 700),
  bs = "ts", k = 5) + s(log10(ClimCumVGPM45), bs = "ts", k = 5)
```

Parametric coefficients:

```
Estimate Std. Error t value Pr(>|t|)
(Intercept) -6.4744 0.4665 -13.88 <2e-16 ***
```

Signif. codes: 0 '***' 0.001 '**' 0.01 '*' 0.05 '.' 0.1 ' ' 1

Approximate significance of smooth terms:

	edf	Ref.df	F	p-value	
s(log10(Depth))	3.507	4	7.257	1.59e-06	***
s(ClimSST)	1.075	4	7.696	9.52e-09	***
s(pmin(I(ClimDistToFront1/1000), 250))	1.017	4	6.190	1.03e-07	***
s(log10(pmax(ClimTKE, 0.001)))	3.166	4	7.204	5.73e-07	***
s(pmin(I(ClimDistToEddy9/1000), 700))	3.645	4	12.661	3.02e-11	***
s(log10(ClimCumVGPM45))	3.272	4	6.783	2.34e-06	***

Signif. codes: 0 '***' 0.001 '**' 0.01 '*' 0.05 '.' 0.1 ' ' 1

R-sq.(adj) = 0.0158 Deviance explained = 51.8%

-REML = 817.69 Scale est. = 401.91 n = 12621

All predictors were significant. This is the final model.

Creating term plots.

Diagnostic output from gam.check():

Method: REML Optimizer: outer newton

full convergence after 11 iterations.

Gradient range [-1.49847e-05,1.16596e-06]

(score 817.6896 & scale 401.9112).

Hessian positive definite, eigenvalue range [0.4706563,137.1285].

Model rank = 25 / 25

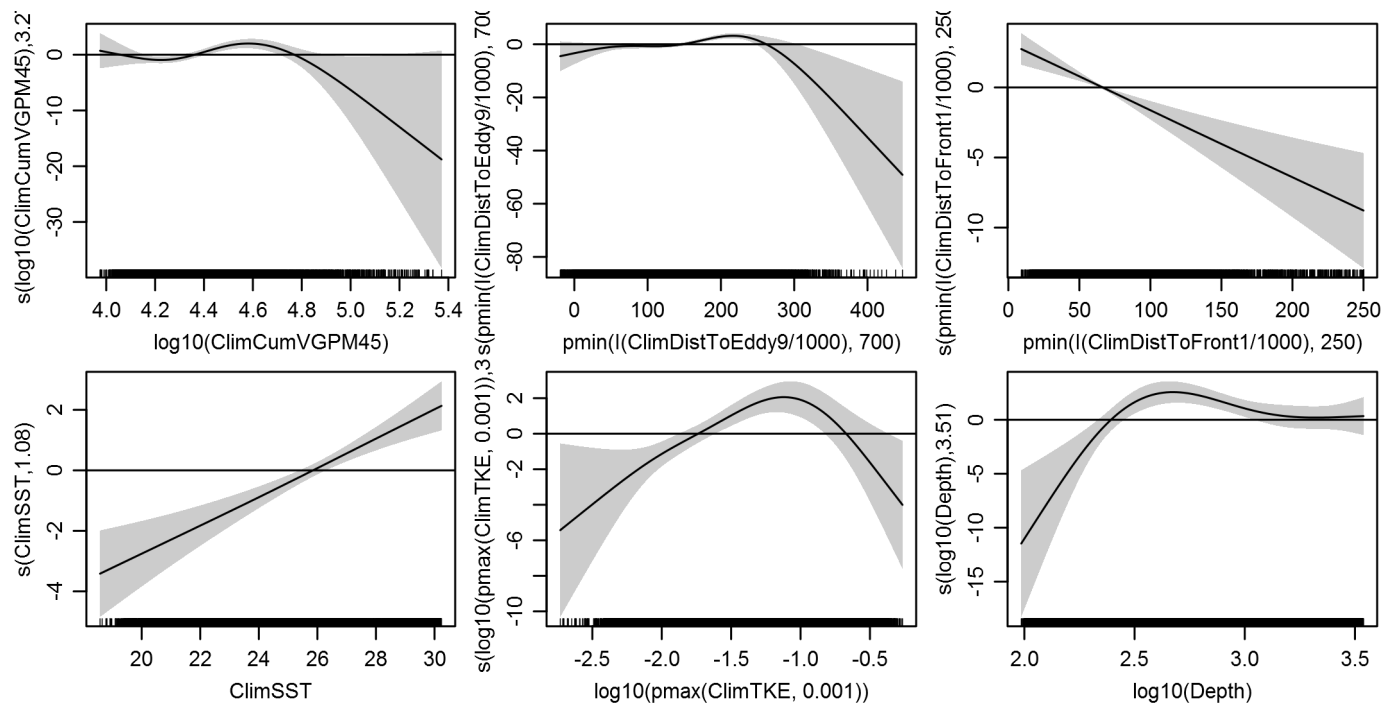
Basis dimension (k) checking results. Low p-value (k-index<1) may indicate that k is too low, especially if edf is close to k'.

	k'	edf	k-index	p-value
s(log10(Depth))	4.000	3.507	0.728	0.02
s(ClimSST)	4.000	1.075	0.752	0.02
s(pmin(I(ClimDistToFront1/1000), 250))	4.000	1.017	0.784	0.78
s(log10(pmax(ClimTKE, 0.001)))	4.000	3.166	0.777	0.36
s(pmin(I(ClimDistToEddy9/1000), 700))	4.000	3.645	0.764	0.06
s(log10(ClimCumVGPM45))	4.000	3.272	0.716	0.00

Predictors retained during the model selection procedure: Depth, ClimSST, ClimDistToFront1, ClimTKE, ClimDistToEddy9, ClimCumVGPM45

Predictors dropped during the model selection procedure: Slope, DistTo300m

Model term plots



Diagnostic plots

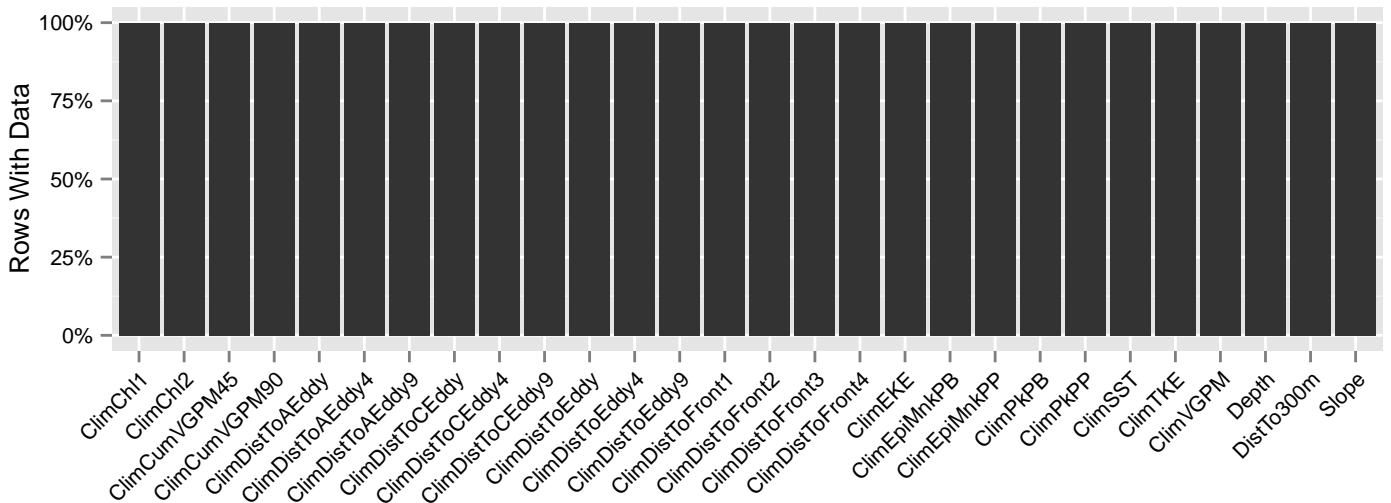


Figure 45: Segments with predictor values for the Spinner dolphin Climatological model, Off Shelf. This plot is used to assess how many segments would be lost by including a given predictor in a model.

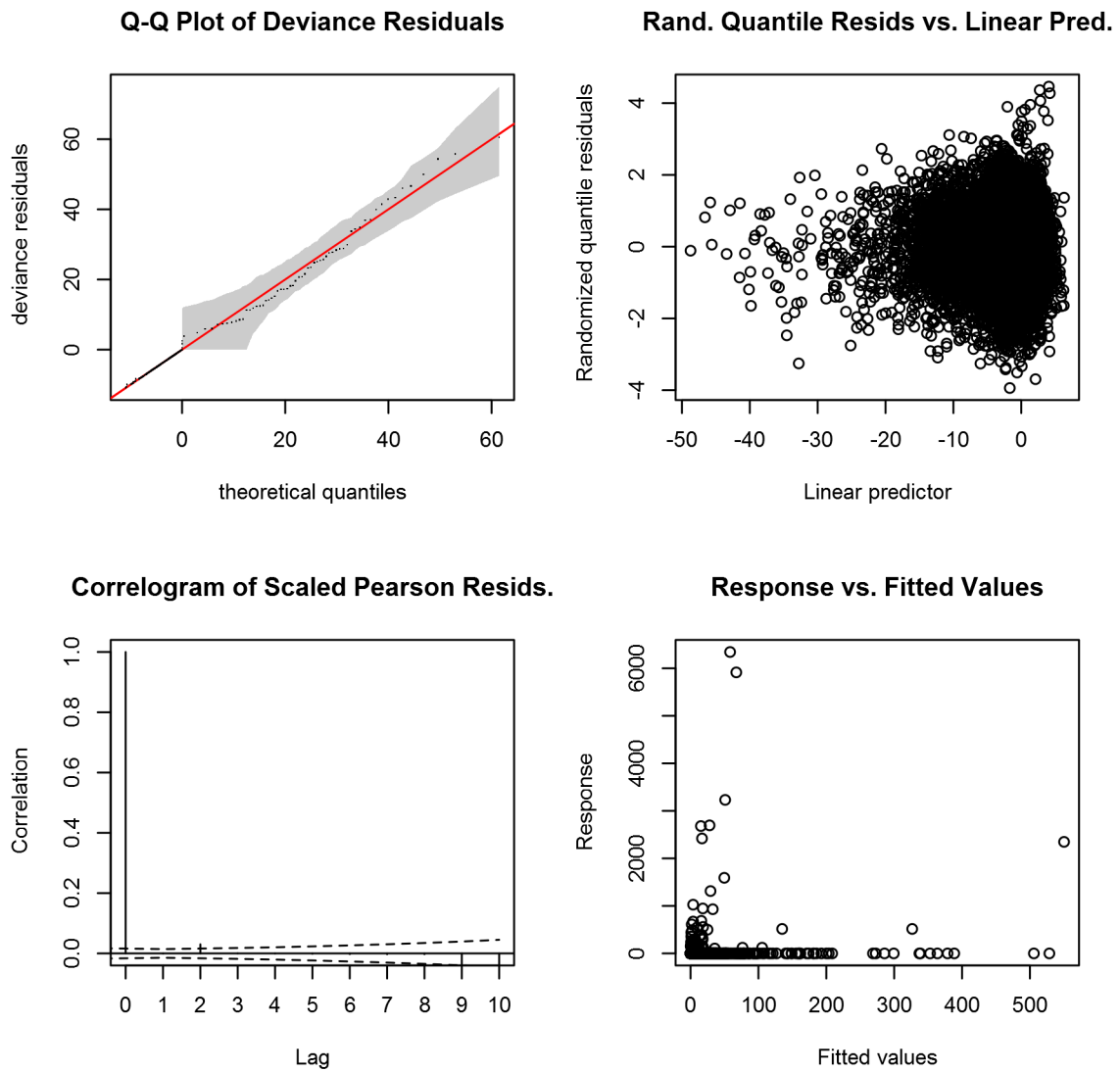


Figure 46: Statistical diagnostic plots for the Spinner dolphin Climatological model, Off Shelf.

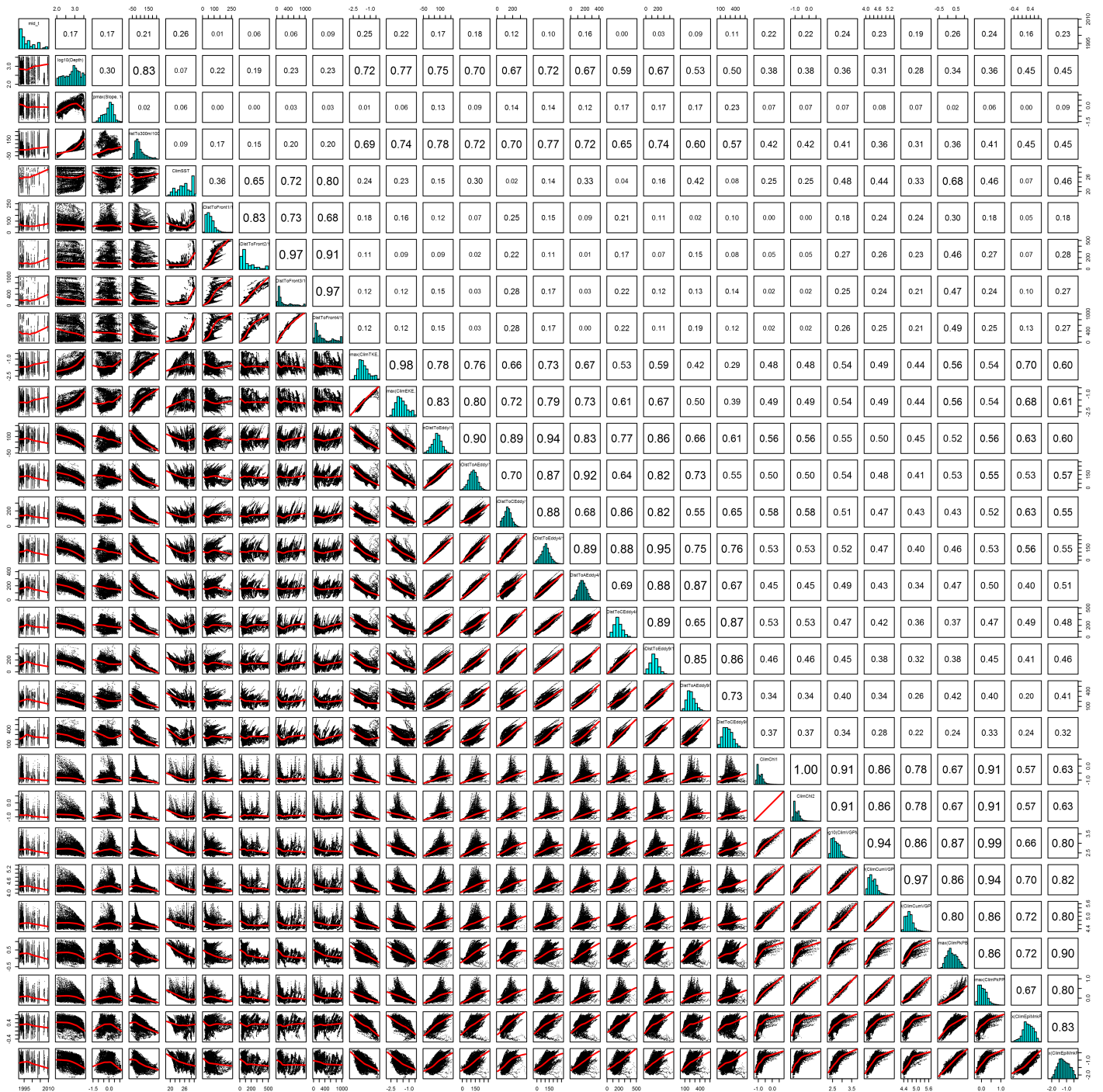


Figure 47: Scatterplot matrix for the Spinner dolphin Climatological model, Off Shelf. This plot is used to inspect the distribution of predictors (via histograms along the diagonal), simple correlation between predictors (via pairwise Pearson coefficients above the diagonal), and linearity of predictor correlations (via scatterplots below the diagonal). This plot is best viewed at high magnification.

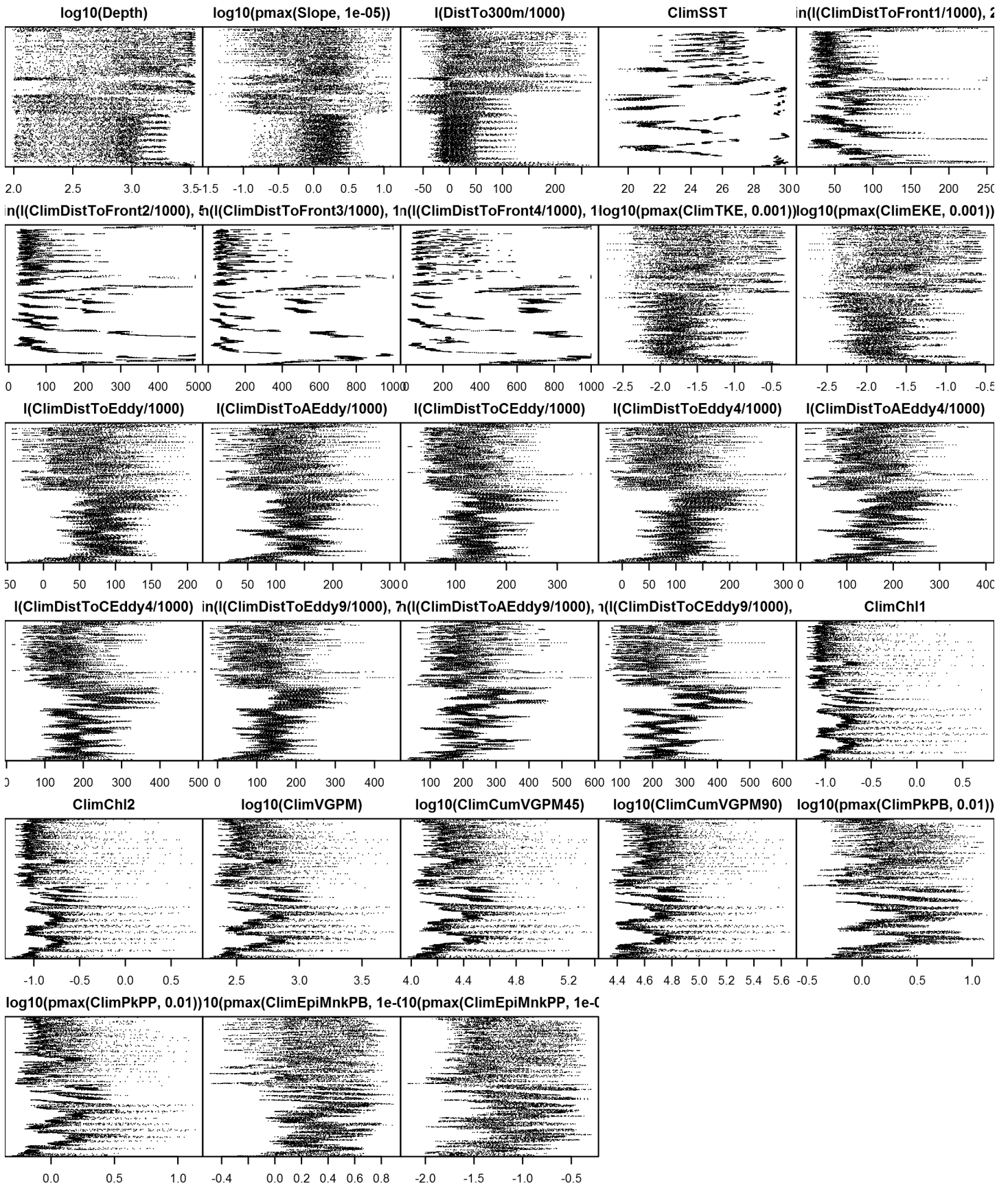


Figure 48: Dotplot for the Spinner dolphin Climatological model, Off Shelf. This plot is used to check for suspicious patterns and outliers in the data. Points are ordered vertically by transect ID, sequentially in time.

On Shelf

Density assumed to be 0 in this region.

Model Comparison

Spatial Model Performance

The table below summarizes the performance of the candidate spatial models that were tested. The first model contained only physiographic predictors. Subsequent models added additional suites of predictors of based on when they became available via remote sensing.

For each model, three versions were fitted; the % Dev Expl columns give the % deviance explained by each one. The “climatological” models were fitted to 8-day climatologies of the environmental predictors. Because the environmental predictors were always available, no segments were lost, allowing these models to consider the maximal amount of survey data. The “contemporaneous” models were fitted to day-of-sighting images of the environmental predictors; these were smoothed to reduce data loss due to clouds, but some segments still failed to retrieve environmental values and were lost. Finally, the “climatological same segments” models fitted climatological predictors to the segments retained by the contemporaneous model, so that the explanatory power of the two types of predictors could be directly compared. For each of the three models, predictors were selected independently via shrinkage smoothers; thus the three models did not necessarily utilize the same predictors.

Predictors derived from ocean currents first became available in January 1993 after the launch of the TOPEX/Poseidon satellite; productivity predictors first became available in September 1997 after the launch of the SeaWiFS sensor. Contemporaneous and climatological same segments models considering these predictors usually suffered data loss. Date Range shows the years spanned by the retained segments. The Segments column gives the number of segments retained; % Lost gives the percentage lost.

Predictors	Climatol % Dev Expl	Contemp % Dev Expl	Climatol	Segments	% Lost	Date Range
			Same Segs % Dev Expl			
Phys	25.5			14455		1992-2009
Phys+SST	34.5	25.5	34.5	14455	0.0	1992-2009
Phys+SST+Curr	46.1	32.8	45.2	12621	12.7	1993-2009
Phys+SST+Curr+Prod	52.3	30.7	51.8	12621	12.7	1993-2009

Table 20: Deviance explained by the candidate density models.

Abundance Estimates

The table below shows the estimated mean abundance (number of animals) within the study area, for the models that explained the most deviance for each model type. Mean abundance was calculated by first predicting density maps for a series of time steps, then computing the abundance for each map, and then averaging the abundances. For the climatological models, we used 8-day climatologies, resulting in 46 abundance maps. For the contemporaneous models, we used daily images, resulting in 365 predicted abundance maps per year that the prediction spanned. The Dates column gives the dates to which the estimates apply. For our models, these are the years for which both survey data and remote sensing data were available.

The Assumed $g(0)=1$ column specifies whether the abundance estimate assumed that detection was certain along the survey trackline. Studies that assumed this did not correct for availability or perception bias, and therefore underestimated abundance. The In our models column specifies whether the survey data from the study was also used in our models. If not, the study provides a completely independent estimate of abundance.

Dates	Model or study	Estimated abundance	CV	Assumed $g(0)=1$	In our models
-------	----------------	------------------------	----	---------------------	------------------

1992-2009	Climatological model*	13485	0.24	No	
1993-2009	Contemporaneous model	15774	0.20	No	
1992-2009	Climatological same segments model	13858	0.25	No	
2009	Oceanic waters, Jun-Aug (Waring et al. 2013)	11441	0.83	Yes	Yes
2003-2004	Oceanic waters, Jun-Aug (Mullin 2007)	1989	0.48	Yes	Yes
1996-2001	Oceanic waters, Apr-Jun (Mullin and Fulling 2004)	11971	0.71	Yes	Yes
1991-1994	Oceanic waters, Apr-Jun (Hansen et al. 1995)	6316	0.43	Yes	Yes

Table 21: Estimated mean abundance within the study area. We selected the model marked with * as our best estimate of the abundance and distribution of this taxon. For comparison, independent abundance estimates from NOAA technical reports and/or the scientific literature are shown. Please see the Discussion section below for our evaluation of our models compared to the other estimates. Note that our abundance estimates are averaged over the whole year, while the other studies may have estimated abundance for specific months or seasons. Our coefficients of variation (CVs) underestimate the true uncertainty in our estimates, as they only incorporated the uncertainty of the GAM stage of our models. Other sources of uncertainty include the detection functions and $g(0)$ estimates. It was not possible to incorporate these into our CVs without undertaking a computationally-prohibitive bootstrap; we hope to attempt that in a future version of our models.

Density Maps

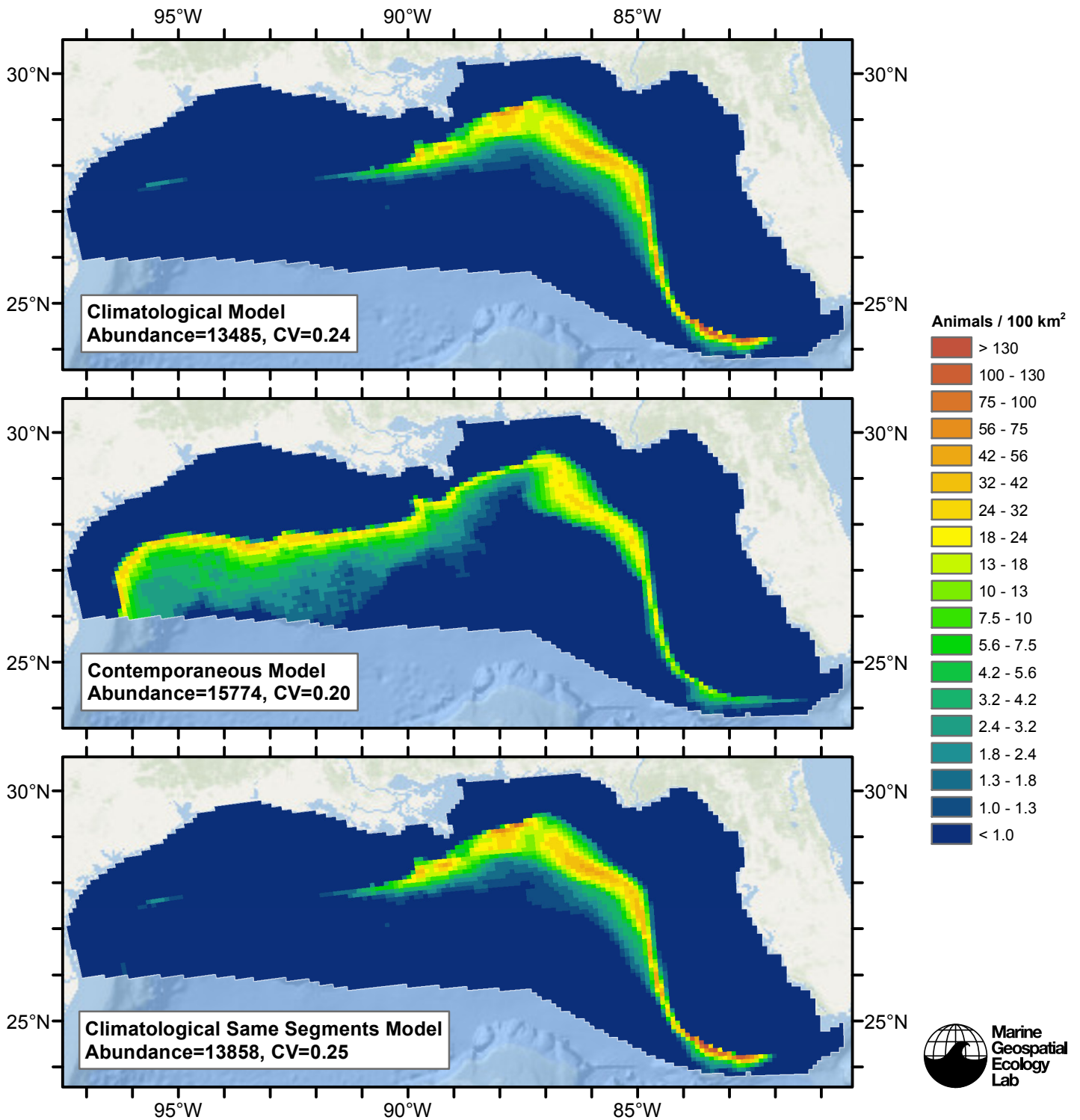


Figure 49: Spinner dolphin density and abundance predicted by the models that explained the most deviance. Regions inside the study area (white line) where the background map is visible are areas we did not model (see text).

Temporal Variability

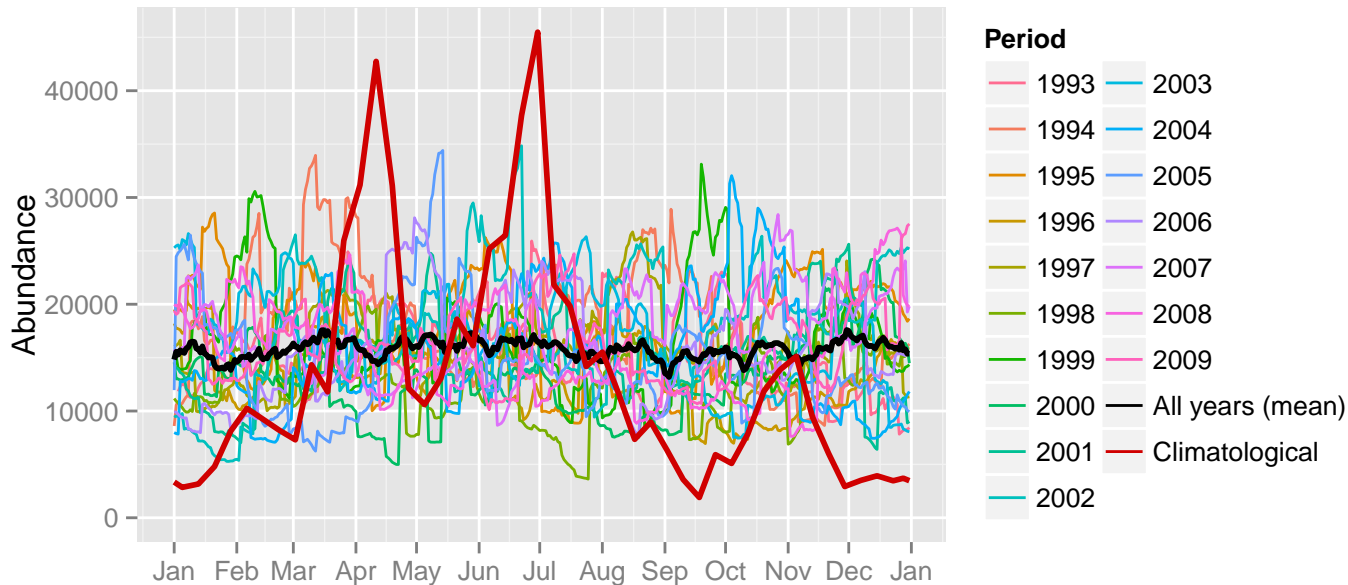


Figure 50: Comparison of Spinner dolphin abundance predicted at a daily time step for different time periods. Individual years were predicted using contemporaneous models. “All years (mean)” averages the individual years, giving the mean annual abundance of the contemporaneous model. “Climatological” was predicted using the climatological model. The results for the climatological same segments model are not shown.

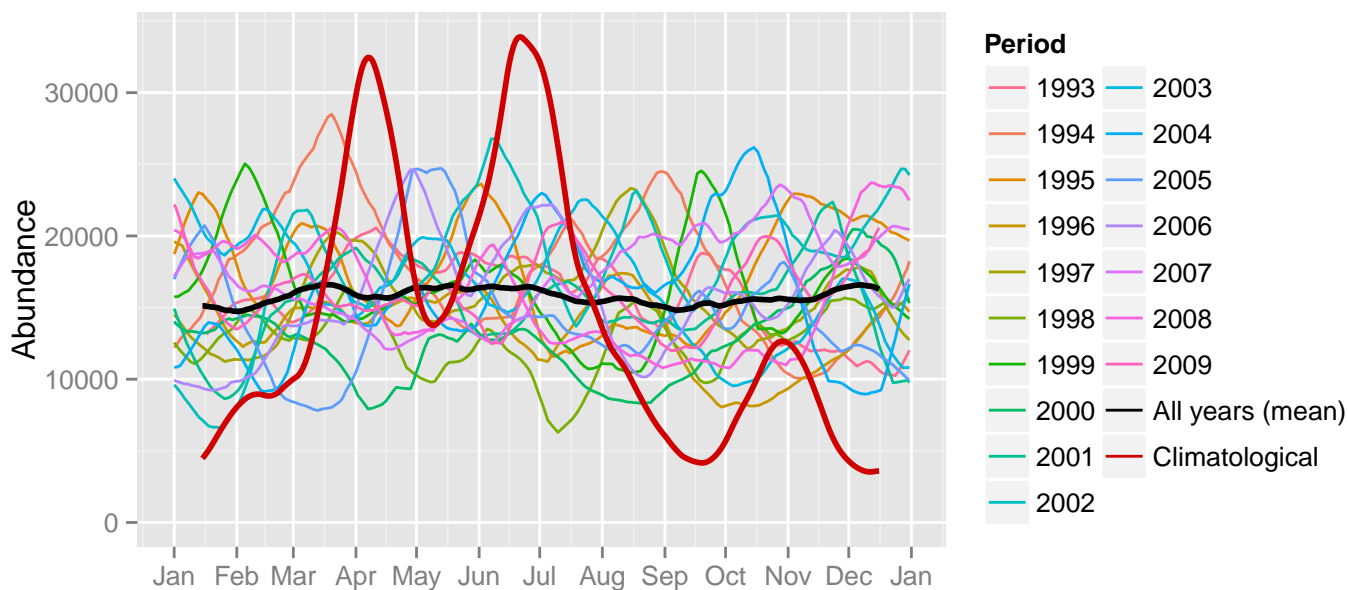
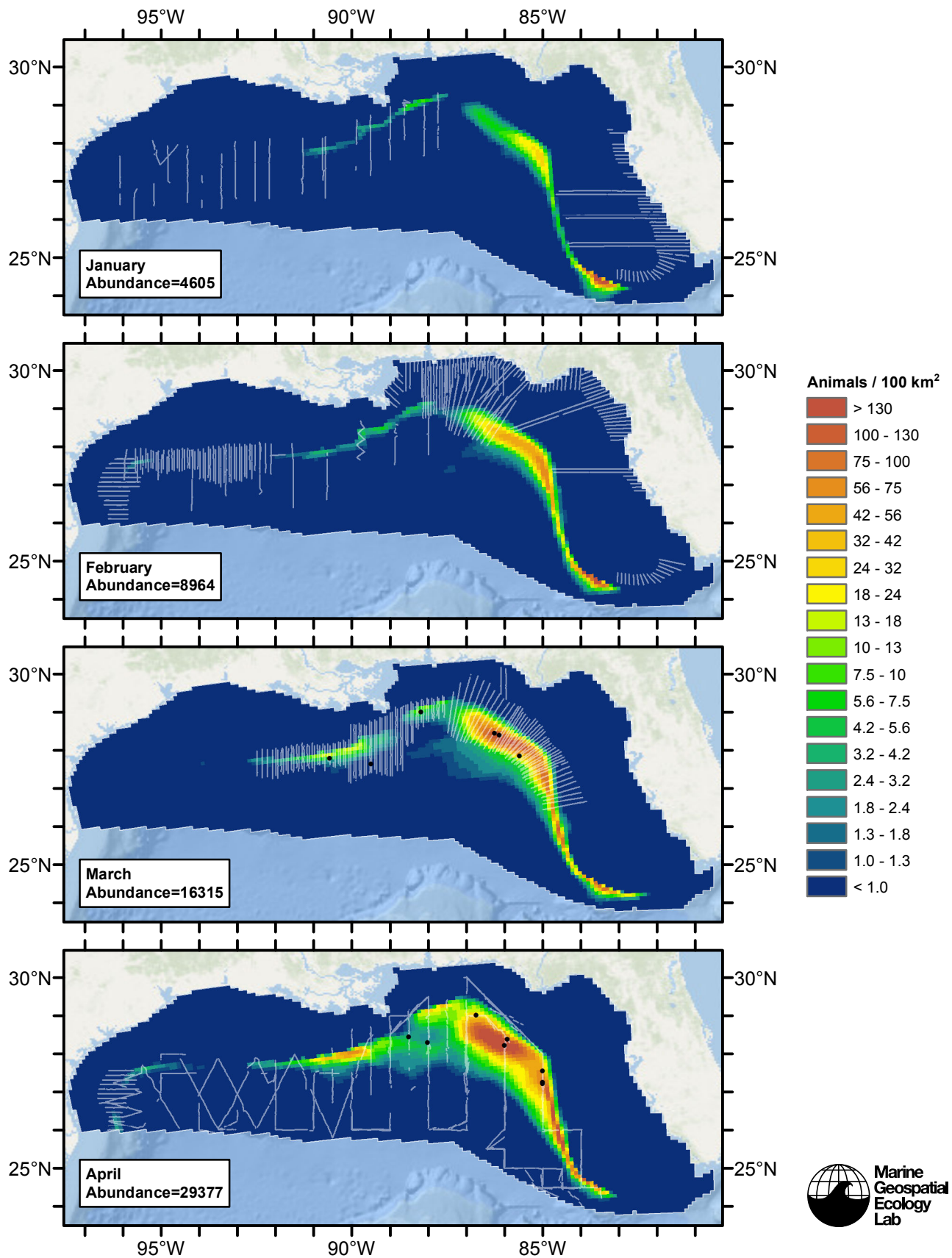
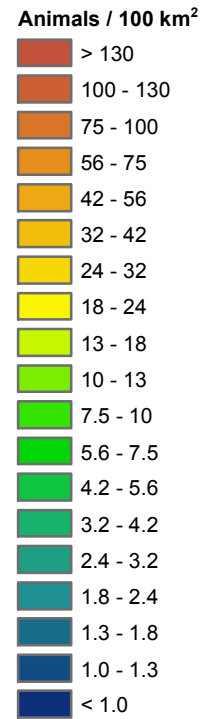
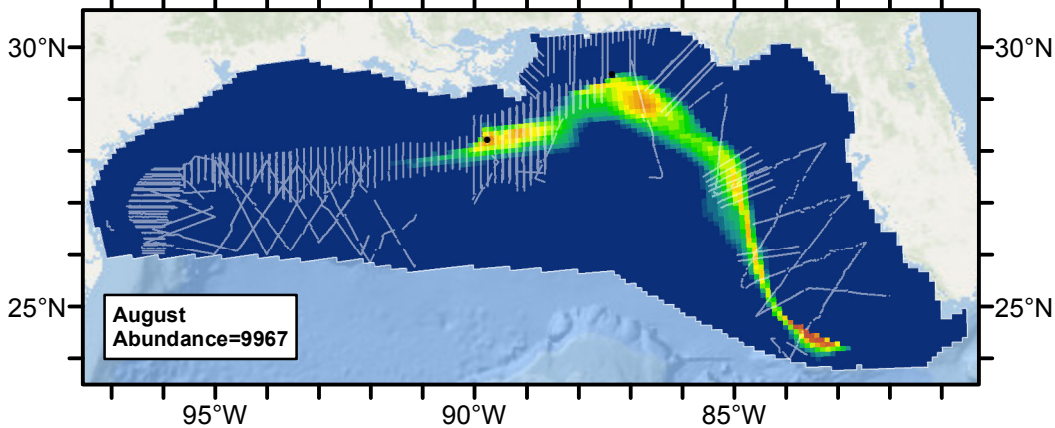
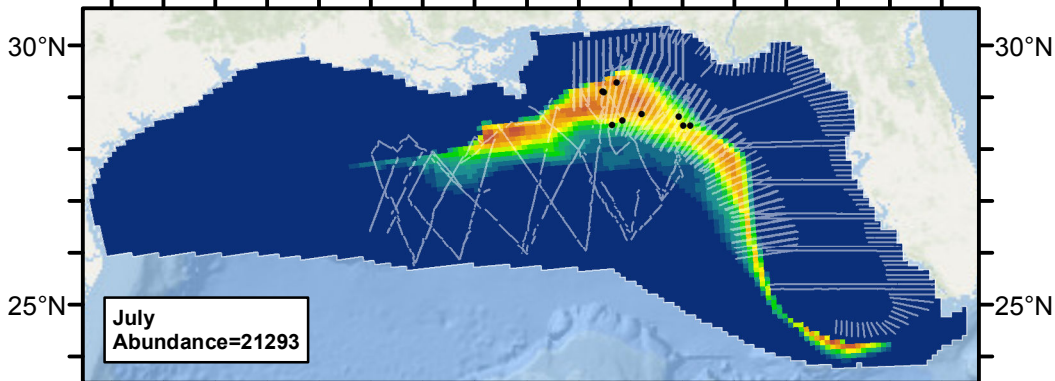
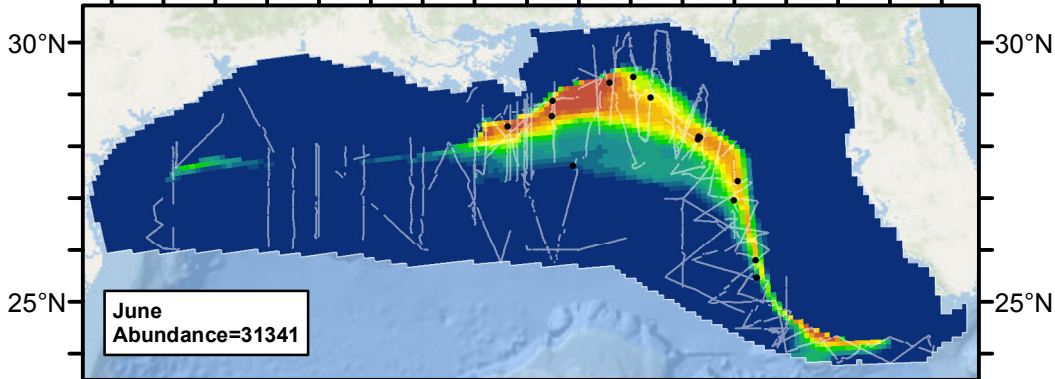
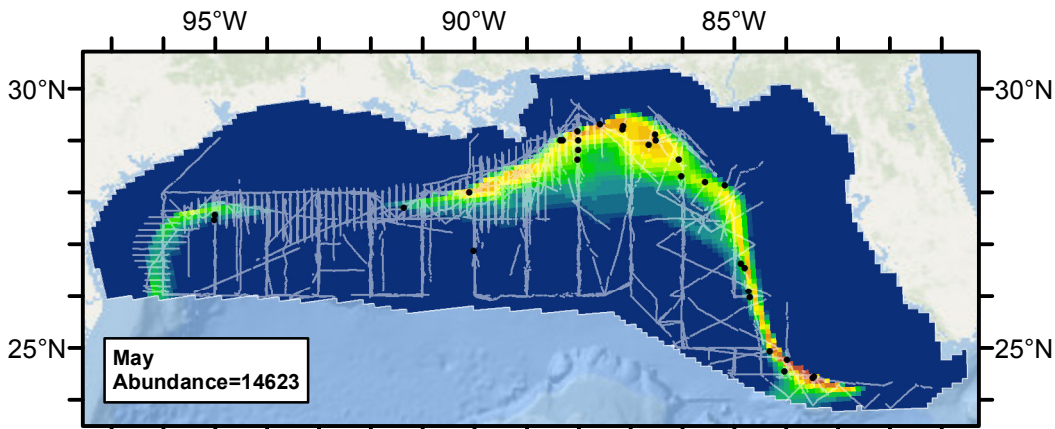
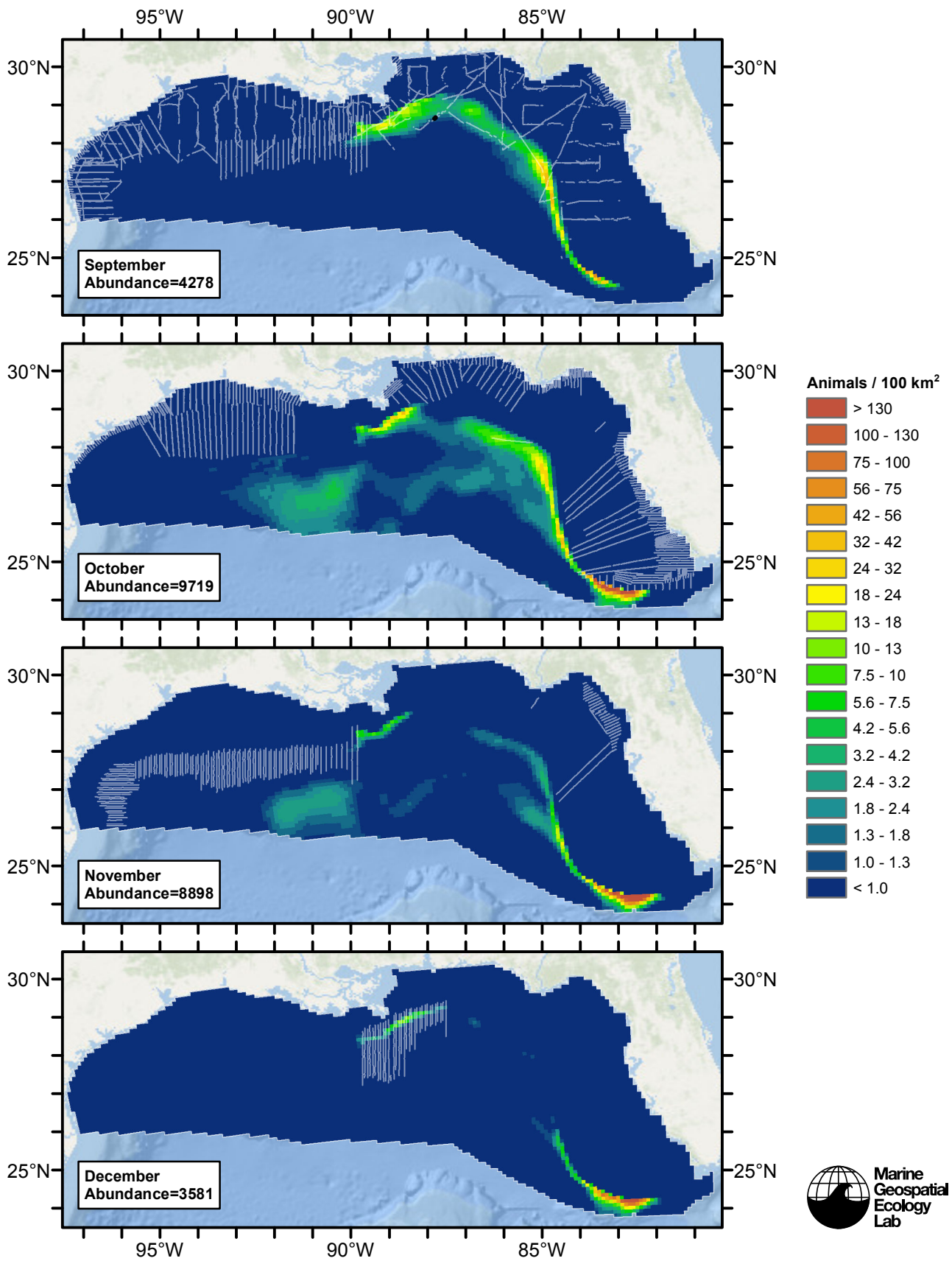


Figure 51: The same data as the preceding figure, but with a 30-day moving average applied.

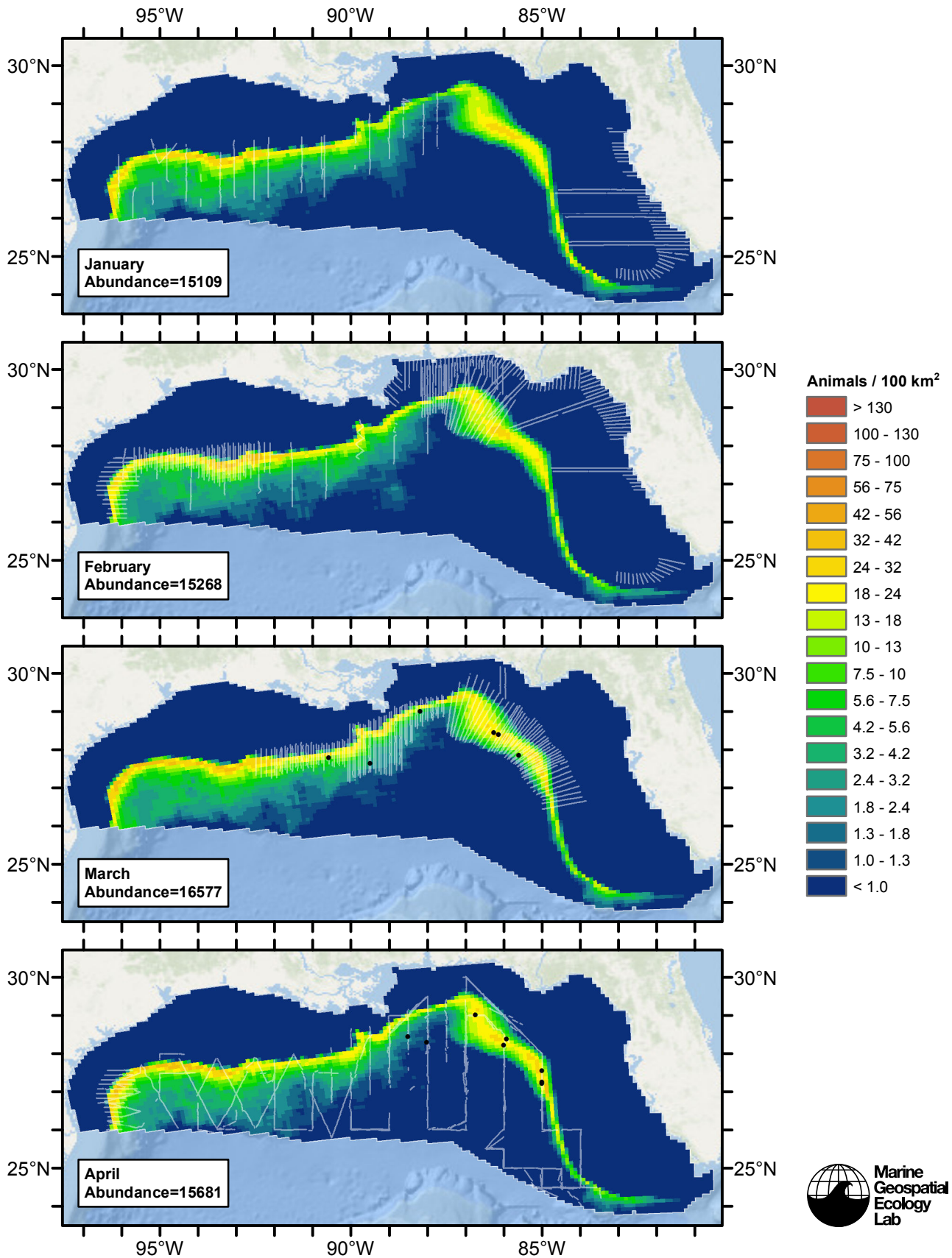
Climatological Model

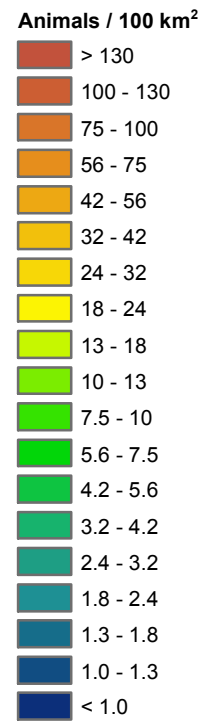
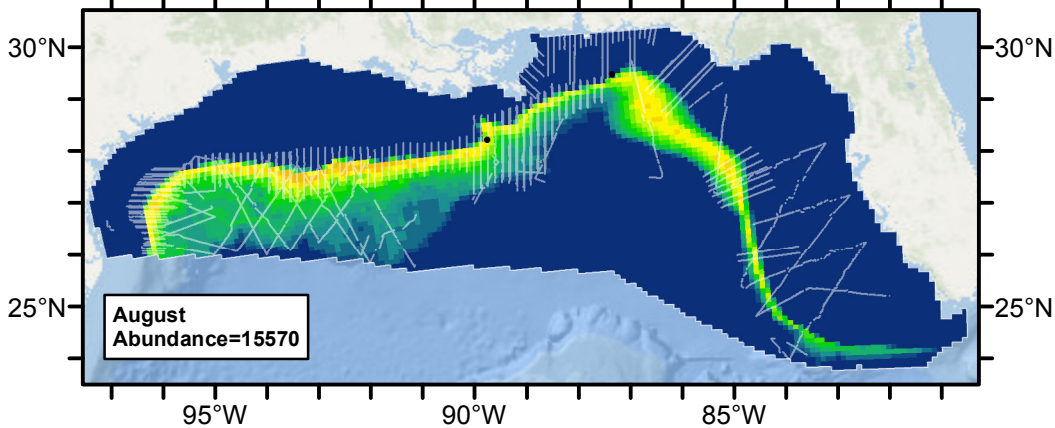
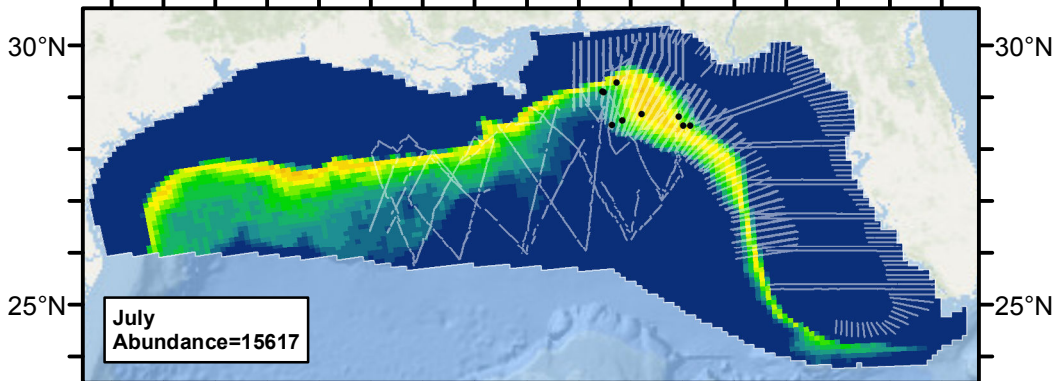
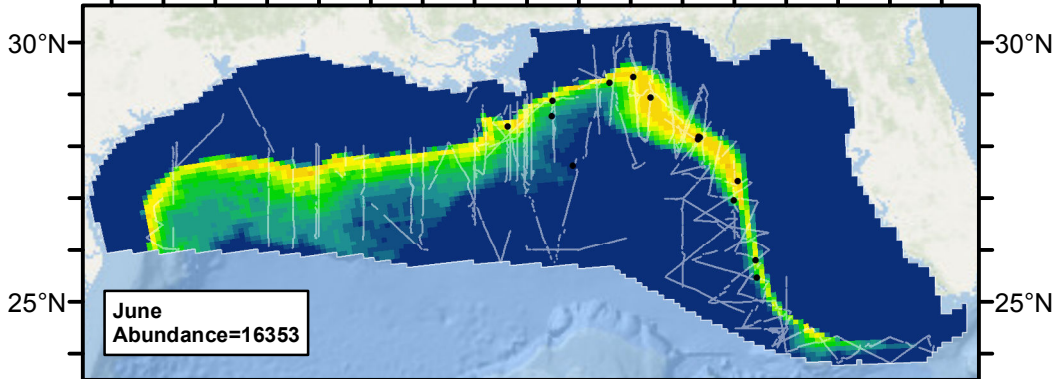
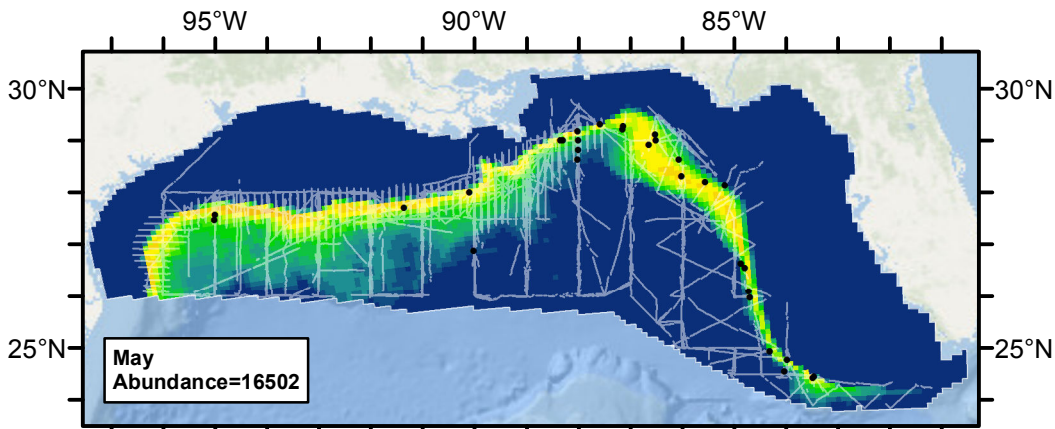


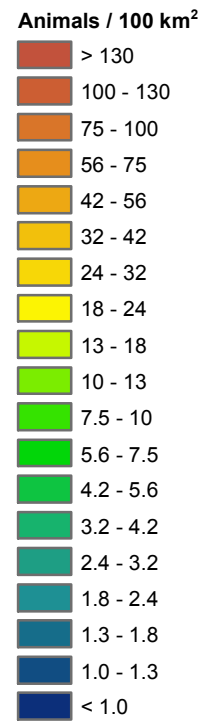
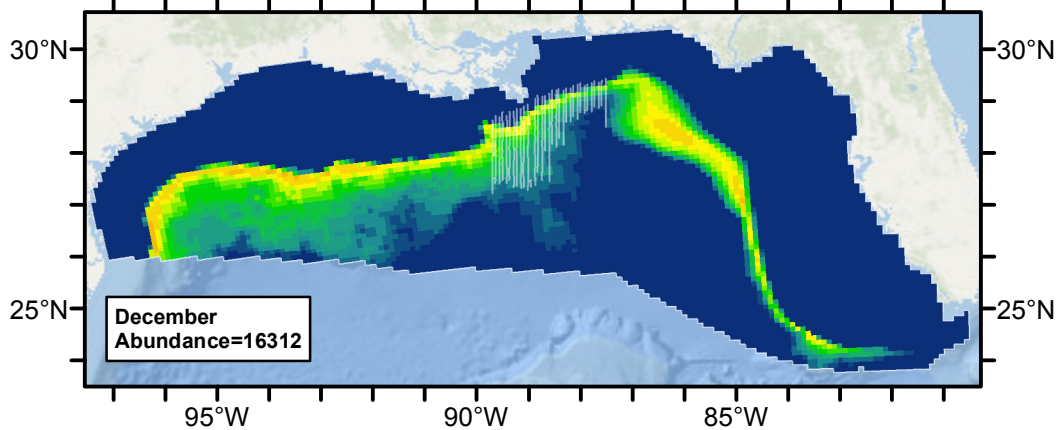
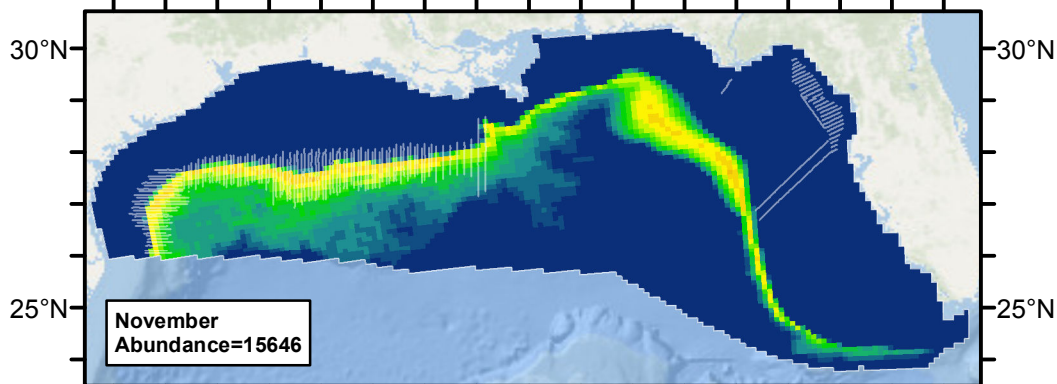
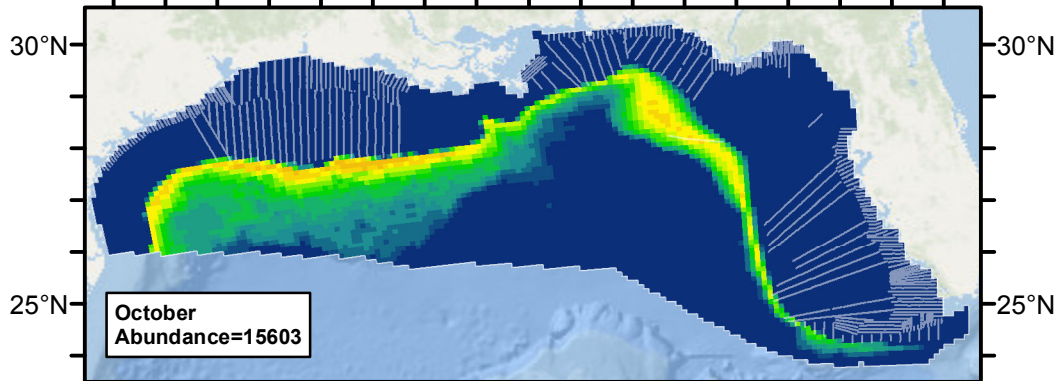
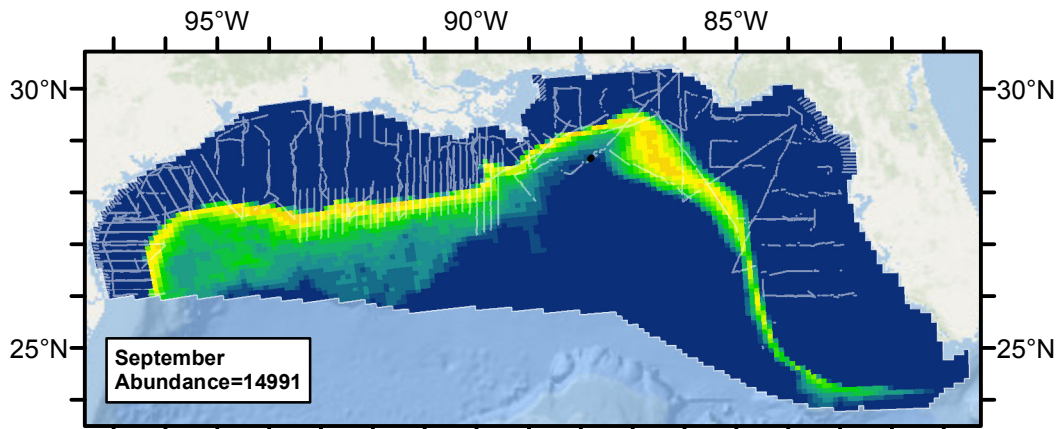




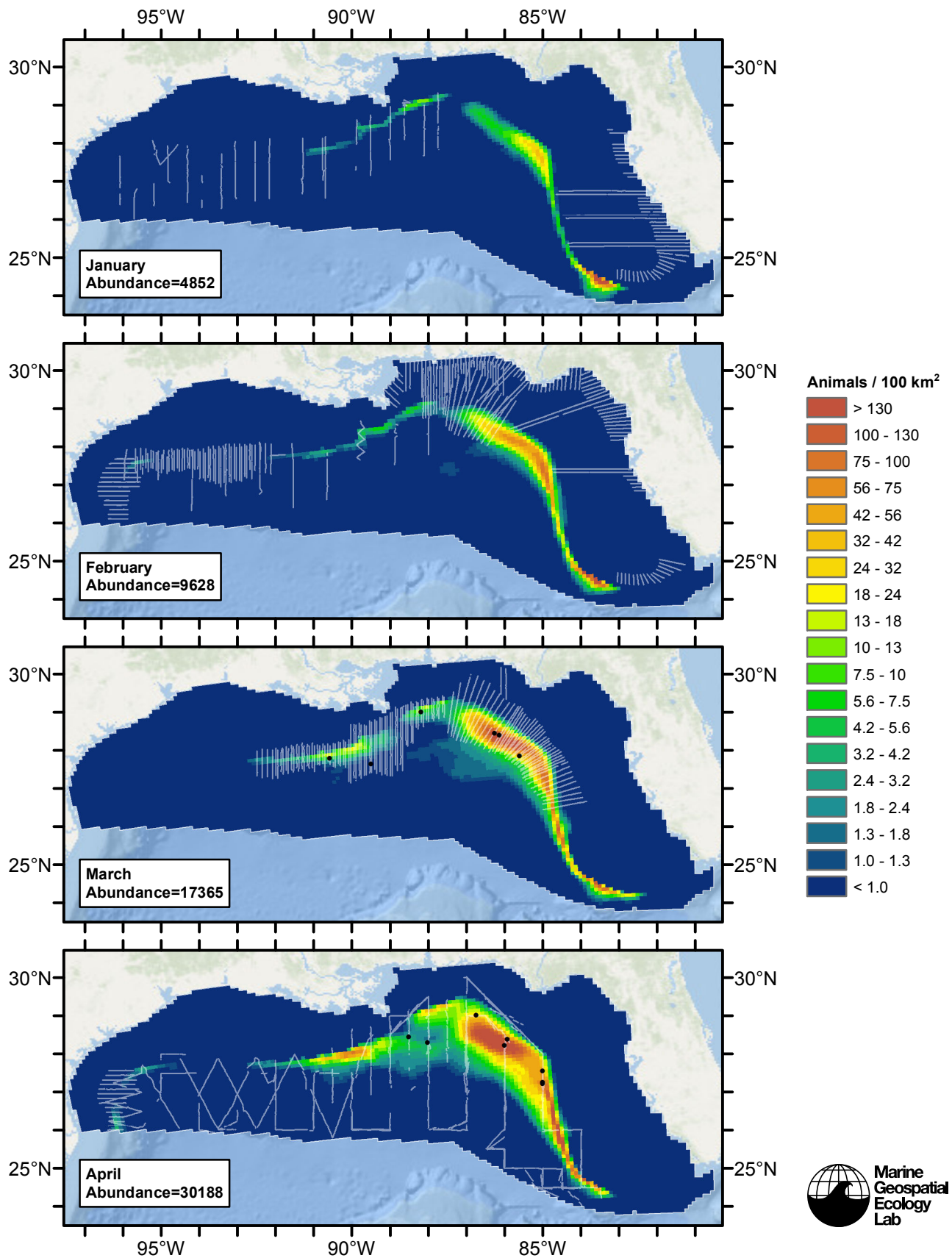
Contemporaneous Model

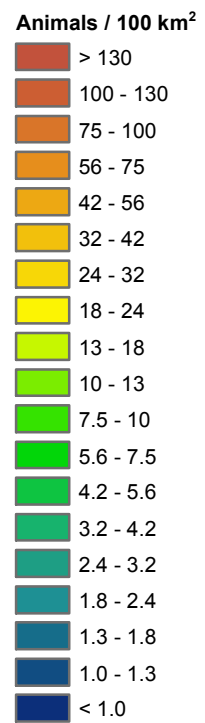
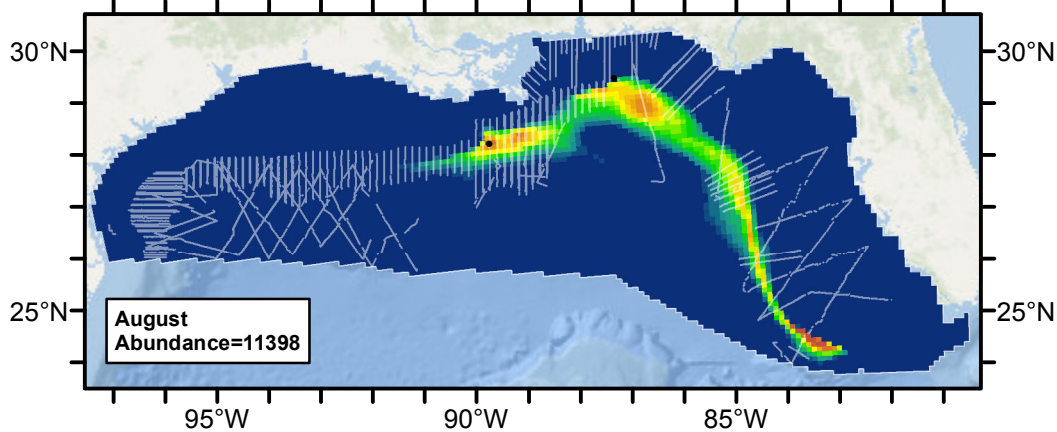
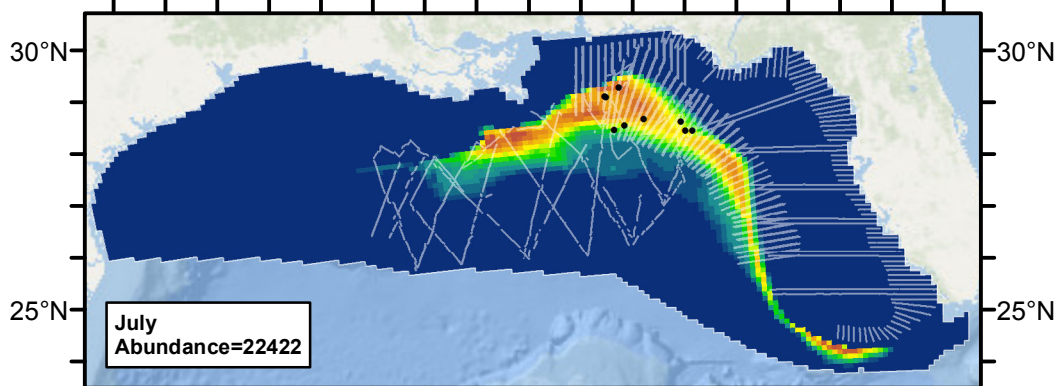
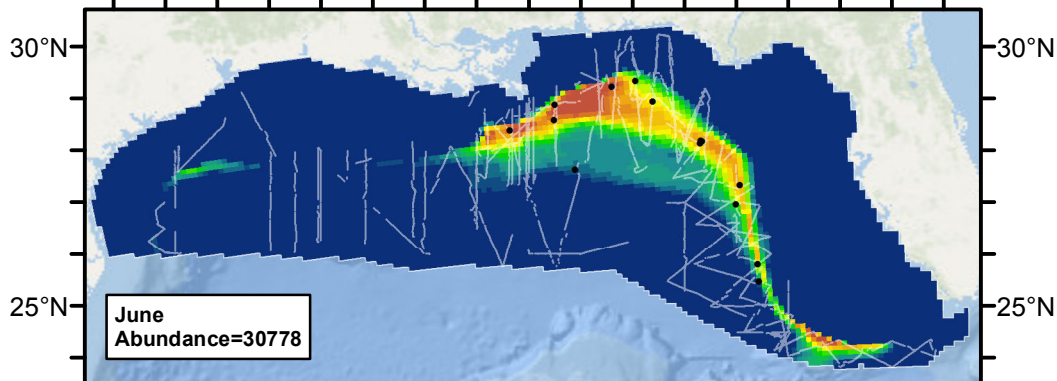
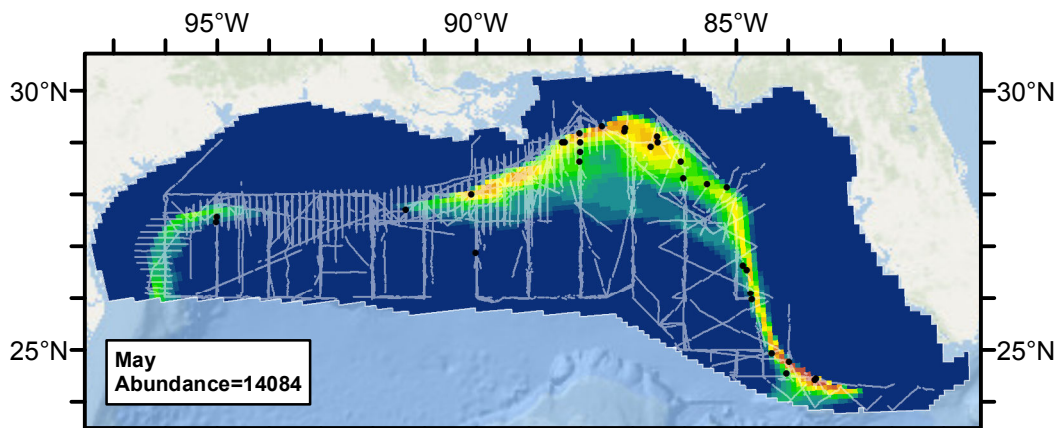


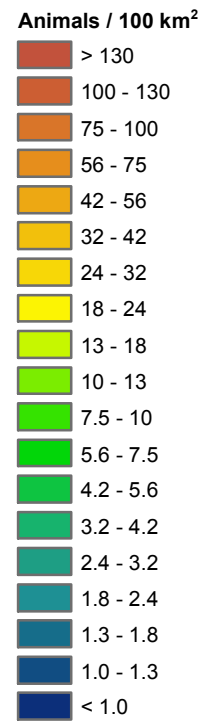
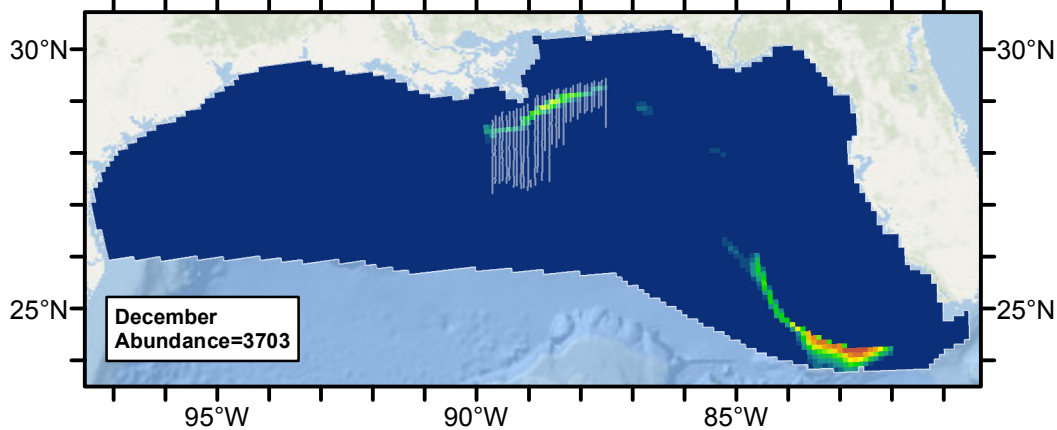
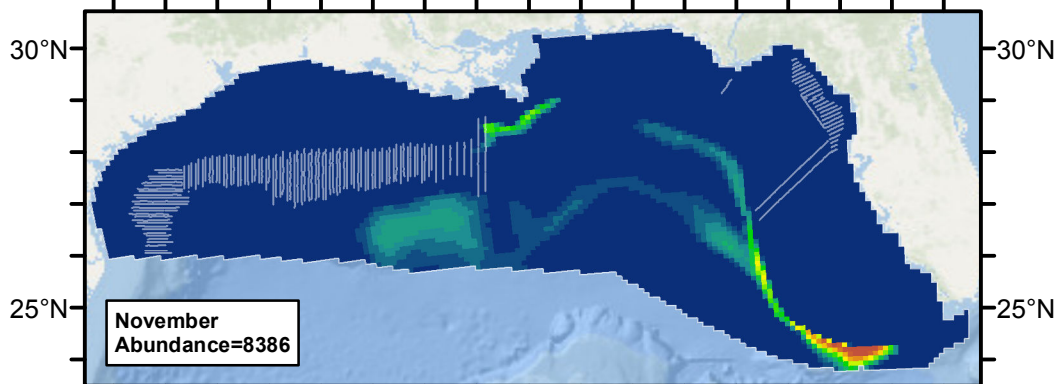
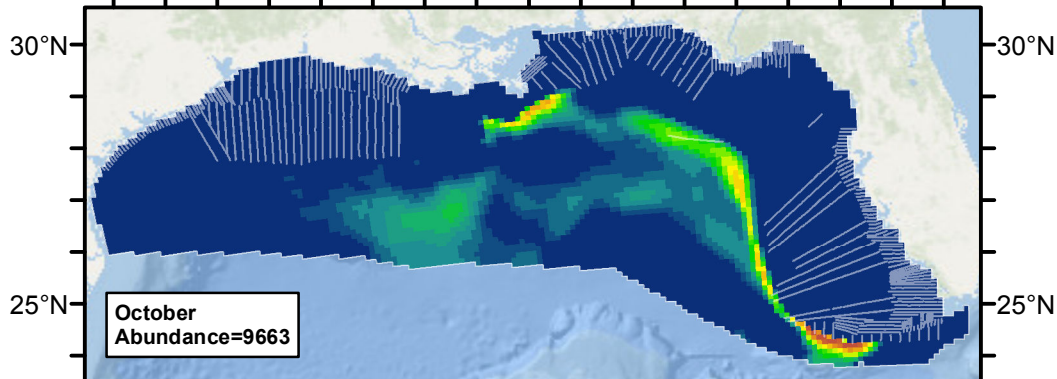
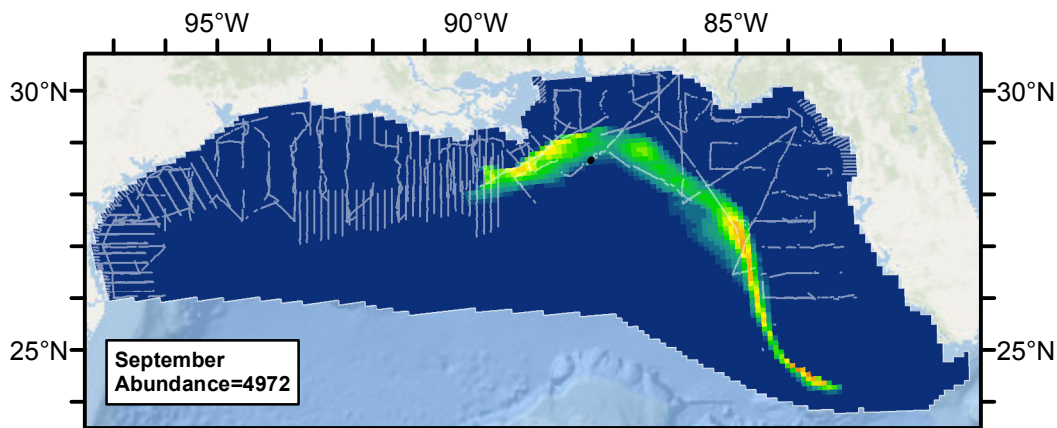




Climatological Same Segments Model







Discussion

The models that used climatological predictors explained substantially more deviance than the models that used contemporaneous predictors. The best contemporaneous model predicted substantial abundance in the the western Gulf where only two sightings occurred; the climatological models did not have this problem. On this basis of higher explained deviance and not having this mis-prediction, we selected the climatological model that was fitted to all of the segments as our best estimate of spinner dolphin distribution and abundance. We note, however that this model exhibited wide fluctuations in total abundance when predicted at the 8-day time step of the climatologies used for prediction (Fig. 50). The best contemporaneous model exhibited similar fluctuations when predicted on a year-by-year basis, so it did not necessarily perform in a more realistic way except when all years were averaged.

In any case, because the survey effort used as input to our models was biased toward spring and summer and was spatiotemporally patchy (see maps in the Temporal Variability section above), we were not confident that any of our models could produce realistic predictions at a monthly temporal resolution. This effort bias problem affected all species that we modeled in the Gulf of Mexico, and we recommend that year-round average predictions be used for all Gulf of Mexico species.

Our model predicted a total abundance that was about 18% higher than NOAA's most recent abundance estimate, although our estimate was within the confidence limits of NOAA's. We do not believe this difference is due to $g(0)$: while NOAA's estimate assumed that $g(0)=1$ and we did not, almost all of the sightings in our study were of large groups, thus we assumed $g(0)=0.970$ or 0.960 for all of the sightings (depending on which platform sighted them).

References

- Barlow J, Forney KA (2007) Abundance and density of cetaceans in the California Current ecosystem. *Fish. Bull.* 105: 509-526.
- Carretta JV, Lowry MS, Stinchcomb CE, Lynn MS, Cosgrove RE (2000) Distribution and abundance of marine mammals at San Clemente Island and surrounding offshore waters: results from aerial and ground surveys in 1998 and 1999. Administrative Report LJ-00-02, available from Southwest Fisheries Science Center, P.O. Box 271, La Jolla, CA USA 92038. 44 p.
- Hansen LJ, Mullin KD, Roden CL (1995) Estimates of cetacean abundance in the northern Gulf of Mexico from vessel surveys. Southeast Fisheries Science Center, Miami Laboratory, Contribution No. MIA-94/95-25, 9 pp.
- Hiby L (1999) The objective identification of duplicate sightings in aerial survey for porpoise. In: *Marine Mammal Survey and Assessment Methods* (Garner GW, Amstrup SC, Laake JL, Manly BFJ, McDonald LL, Robertson DG, eds.). Balkema, Rotterdam, pp. 179-189.
- Mullin KD (2007) Abundance of cetaceans in the oceanic Gulf of Mexico based on 2003-2004 ship surveys. 26 pp.
- Mullin KD, Fulling GL (2004) Abundance of cetaceans in the oceanic northern Gulf of Mexico. *Mar. Mamm. Sci.* 20(4): 787-807.
- Palka DL (2006) Summer Abundance Estimates of Cetaceans in US North Atlantic Navy Operating Areas. US Dept Commer, Northeast Fish Sci Cent Ref Doc. 06-03: 41 p.
- Waring GT, Josephson E, Maze-Foley K, Rosel PE, eds. (2013) U.S. Atlantic and Gulf of Mexico Marine Mammal Stock Assessments – 2012. NOAA Tech Memo NMFS NE 223; 419 p.
- Waring GT, Josephson E, Maze-Foley K, Rosel PE, eds. (2014) U.S. Atlantic and Gulf of Mexico Marine Mammal Stock Assessments – 2013. NOAA Tech Memo NMFS NE 228; 464 p.